A THESIS

entitled

HIGH-RESOLUTION ^{13}C AND ^{1}H NMR STUDIES OF PROTEINS AND PEPTIDES

by

Lu Yun Lian, B.Sc.(Hons.)

Submitted to the University of Warwick in fulfilment of the requirements for the award of the degree of Doctor of Philosophy

Department of Chemistry and Molecular Sciences
University of Warwick

October 1982

TABLE OF CONTENTS

LIST OF FIGURES

LIST OF TABLES

LIST OF APPENDICES

ACKNOWLEDGEMENTS

I wish to take this opportunity to express my sincere gratitude to my supervisor, Dr. Oliver W. Howarth for his constant advice and encouragement throughout the course of this work.

I would particularly like to thank Dr. Eirian H. Curzon for his help and advice. I am especially indebted to Dr. N. Borkakoti, Dr. D. S. Moss and Mr. M. Stanford of Birkbeck College, University of London, for their useful discussions and for providing the stereodrawings of ribonuclease A. My thanks also go to Dr. P. Artymiuck, Laboratory of Molecular Biophysics, University of Oxford for providing the x-ray coordinates of HEW lysozyme, to Dr. M. Delepierre, Department of Inorganic Chemistry, University of Oxford, for her constructive suggestions, and the P.C.M.U. staff for their assistance.

My very special thanks go to Michael Downes for his help in all aspects of the preparation of this thesis.

The work described here was carried out in the Department of Chemistry and Molecular Sciences, University of Warwick, between October 1979 and October 1982, the facilities of which are gratefully acknowledged. A Science and Engineering Research Council maintenance award is also acknowledged.

DECLARATION

To the best of my knowledge, the work described in this thesis is original. Parts of this work have been published in the scientific literature, with the following references:

Howarth, O. W. and Lian, L. Y. (1981)
J. C. S. Chem. Comm., 258

Howarth, O. W. and Lian, L. Y. (1982)
J. C. S. Perkin Trans. 2, 3, 249

ABSTRACT

At the magnetic field used in this research (9.4T) many individual ^{13}C resonances of protonated carbon atoms are resolved. To test the applicability of the high-resolution natural abundance ^{13}C NMR method, lysozyme and ribonuclease A are used.

The research includes the assignment of many methyl resonances and attempts to answer questions on the behaviour of these side-chains when the proteins are subjected to varying conditions of pD and temperature, and also in the presence of ligands, inhibitors and urea.

Ribonuclease A is observed to undergo conformational changes on variation of pD. The region(s) of this protein which are involved consist of many hydrophobic residues such as ile, val and met.

Many denaturation processes are effectively in slow exchange at the high magnetic field used. The individual resonances of ribonuclease A which are involved in the predenaturation transitions are identified. They are found to be of distinct types for the two denaturants. In contrast, lysozyme does not show such distinct conformational behaviour below its denaturation temperature.

At higher temperatures the main transition from the 'native' to the denatured state of both proteins is two-state. None of the unfolded states of ribonuclease A and lysozyme are random coil. Rather, the unfolded states have definable structures which have hydrophobic bondings and significant, but still restrained, internal flexibility.

The high-resolution spectra of ribonuclease A-inhibitor complexes have revealed unprecedented details of the structures of these complexes. Extensive structural changes, including the closure of the active site cleft, together with movements in the hydrophobic regions bordering the cleft, are deduced from the inhibitor-induced shift perturbations of the ^{13}C and ^{1}H NMR resonances of the protein residues.

In the assignment work, and the urea denaturation and ligand binding studies, high-resolution ^{1}H NMR is used to complement the ^{13}C NMR technique.

A theory relating ^{13}C NMR relaxation parameters to molecular motion at three levels (3-τ) is tested with gramicidin-S and glutathione dimer. The results obtained give information about the conformations and rates of internal librational motions of the two peptides. The '3-τ' model is also applied to some more-limited data on proteins. The low nuclear Overhauser effects are partially explained by this theory.

SYMBOLS AND ABBREVIATIONS

PHYSICAL PROPERTIES

Å	Angstrom
CSA	Chemical shift anisotropy
FID	Free induction decay
FT	Fourier transform
$F(t)F(t + \tau)$	Autocorrelation function of F
GB	Gaussian broadening
$\hbar$	$h/2\pi$ (h = Planck's constant)
$J(\omega)$	Spectral density function at frequency ω
LB	Line broadening
mM	Millimolar
MHz	Megahertz (10^6 cps)
MW	Molecular weight
nOe	Nuclear Overhauser effect
NMR	Nuclear magnetic resonance
O.D.	Outside diameter
pD	pH value measured with a glass electrode in D_2O solution without correction for the isotope effect (≈ 0.4 unit)
ppm	Parts per million
$\langle r \rangle$	Average distance
r.f.	Radio frequency
S/N	Signal-to-noise
T	Tesla
T_1	Longitudinal (spin-lattice) relaxation time
T_2	Transverse (spin-spin) relaxation time
X	Mean librational angle (small-angle libration)

γ	Magnetogyric ratio
Δ	Change in chemical shift
θ	Second librational angle (large-angle libration) (Chapter 7)
τ_R	Overall reorientation correlation time
τ_g, τ_S	Librational correlation times
ω	Larmor resonance frequency (in rad./sec.)

CHEMICAL SPECIES

ala	Alanine
arg	Arginine
asp	Aspartic acid
asn	Asparagine
cys	Cysteine
gln	Glutamine
glu	Glutamic acid
HEW	Hen egg white
his	Histidine
ile	Isoleucine
leu	Leucine
lys	Lysine
met	Methionine
Me_4Si	Tetramethylsilane
MeI	Methyl iodide
NAG	N-acetylglucosamine
NBS	N-bromosuccinimide
orn	Ornithine
phe	Phenylalanine

pro	Proline
RNA	Ribonucleic acid
RNAse	Ribonuclease A
ser	Serine
thr	Threonine
trp	Tryptophan
tyr	Tyrosine
val	Valine
2'CMP	Cytidine-2'-phosphate
3'CMP	Cytidine-3'-phosphate
5'CMP	Cytidine-5'-phosphate

To My Father and Mother

CHAPTER 1
INTRODUCTION TO HIGH-RESOLUTION PROTEIN NMR

1.1 INTRODUCTION

This thesis is an investigation into the behaviour in solution of medium-sized proteins (MW < 20 000) using high-resolution natural abundance carbon-13 (^{13}C) and proton (^{1}H) Nuclear Magnetic Resonance (NMR) spectroscopy.

^{1}H and ^{13}C nuclei are the two most widely used in the NMR study of proteins. The first high-resolution ^{1}H NMR spectrum of a biomolecule recorded in the literature is that of ribonuclease A as reported by Saunders, Wishnia and Kirkwood in 1957. The first natural abundance ^{13}C NMR spectrum of a protein was reported in 1970 by Allerhand, Cochran and Doddrell. Since these dates there have been considerable improvements both in instrumentation and methodology. The use of superconducting magnets to achieve high magnetic field strengths, coupled with advances in electronics and automated data-processing have made high-resolution NMR one of the most informative and versatile methods available for the study of proteins and other biological systems in solution at millimolar concentrations. There are a large number of books and reviews on the application of high-resolution NMR to biological systems (Jardetzky and Roberts, 1981; Campbell and Dobson, 1979; Allerhand, 1979). A wide variety of proteins have been studied using NMR.

Very broadly, the proteins studied can be classified into two types.

The first type consists of those having a molecular weight of less than 20 000. The most widely studied in this category are lysozyme, ribonuclease A, cytochrome c and the small trypsin inhibitor protein. Many resonances in the ^{1}H and ^{13}C NMR spectra of these proteins can be resolved and assigned at a high magnetic field strength. The possibility of monitoring individual residues in the protein means that the basic features of both the protein structure and its function in solution can be studied in detail.

The second type consists of proteins having molecular weights greater than 20 000. Here the ^{1}H and ^{13}C resonances are more difficult to resolve. However, the NMR technique can still be used if the regions of interest are restricted to particular residues. In some cases, specific residues can be labelled using chemical modifications. In many proteins the functional groups are unusual, giving rise to their peculiar properties in the NMR spectrum. Generally, the fact that the other resonances are poorly resolved in these spectra is of little consequence.

Applications requiring the use of high-resolution NMR in the elucidation of protein structure and function are numerous. Investigations can be carried out into the analysis, thermodynamics, kinetics, molecular structure and molecular motions of proteins.

1.2 HIGH-RESOLUTION ^{1}H AND ^{13}C NMR INVESTIGATIONS OF PROTEINS - ADVANTAGES AND DISADVANTAGES

For some time ^{13}C NMR has been used to complement ^{1}H NMR in the investigation of biomolecules. For example, better spectral resolution can be obtained with ^{13}C than with ^{1}H NMR and certain functional groups containing carbon atoms and with no protons attached become accessible. In addition, ^{13}C provides a more direct observation of the molecular backbone. Relaxation studies of proteins using ^{1}H NMR are difficult to interpret. Studies of ^{13}C relaxation are more straightforward especially when carbon atoms are directly bonded to protons. However, the sensitivity of ^{13}C for NMR observation at natural abundance is reduced by a factor of 6 000 compared with ^{1}H.

Advances in instrumentation have helped to overcome to some extent the major problems of resolution and sensitivity in both ^{1}H and ^{13}C NMR spectroscopy. However, it is important to bear in mind some important features of high-field ^{13}C NMR.

The greatest advantage of the high-field ^{13}C NMR technique is its improved sensitivity, and for protonated carbon resonances, the increase in resolution. This latter advantage is slight for nonprotonated aromatic carbon resonances. However, several problems occur to negate the advantages of higher sensitivity. Those encountered in using a high magnetic field for biological studies can be divided into two main categories. The first is concerned with the relaxation behaviour of large molecules in a high magnetic field, whilst the

second is related to the technical and instrumentation difficulties. Many of these problems have been discussed by Anet (1974).

1.2.1 ^{13}C Relaxation

Three parameters of ^{13}C relaxation are normally considered when describing the relaxation behaviour of carbon atoms. These are: spin-lattice relaxation time (T_1), nuclear Overhauser effect (nOe), and spin-spin relaxation time (T_2). The first two influence the intensities (and thus the signal-to-noise ratio) of the ^{13}C resonances, and the third is directly related to linewidth (and thus resolution).

At high magnetic field the relaxation behaviour of ^{13}C is dependent on the type of carbon atom (Allerhand, 1979). When dealing with proteins, the two most important relaxation mechanisms are dipole-dipole relaxation and chemical shift anisotropy (CSA) relaxation.

A protonated carbon is predominantly relaxed by a ^{13}C-^{1}H dipole-dipole mechanism. The spin-lattice relaxation time T_1 for the protonated ^{13}C becomes field-dependent if the overall isotropic molecular tumbling rate, $1/\tau_R$, is not much greater than the NMR resonance frequency. This is the case for many proteins where $\tau_R >> 10^{-10}$ s. The T_1 for these ^{13}C atoms is greater at high field than at low (Fig. 1.1). This effect is important since it reduces the S/N ratio by a considerable factor.

For protonated carbon atoms, the relaxation mechanism, for example CSA, causes negligible line-broadening even at 20T (Allerhand, 1979). Therefore, the use of a high magnetic field improves the resolution considerably by increasing the chemical shift dispersion.

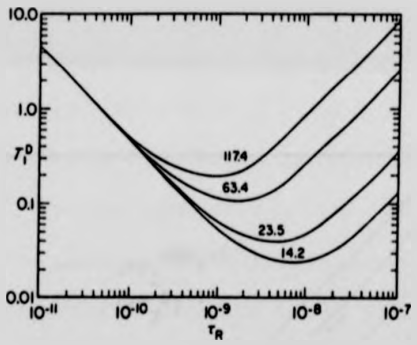

Fig. 1.1 Log-log plots of T_1 *versus* τ_R (both in seconds) for a ^{13}C spin relaxing by a dipolar interaction with a single proton 1.09 Å away, in the case of isotropic rotational reorientation and under conditions of proton-decoupling. Plots are given for various magnetic field strengths, indicated in kilogauss. Taken from Wilbur *et al.* (1976).

The mechanisms affecting the relaxation of nonprotonated and carbonyl carbon atoms differ between low and high magnetic fields. For example, for nonprotonated aromatic carbons, at high magnetic fields, one must consider both the ^{13}C-^{1}H dipolar and the CSA relaxation mechanisms. Fig. 1.2 shows the values of $(\pi T_2^{CSA})^{-1}$ and $(\pi T_2^{D})^{-1}$

computed for a nonprotonated carbon which has three hydrogen atoms two bonds away (Allerhand, 1979). [$(\pi T_2^{CSA})^{-1}$ and $(\pi T_2^{D})^{-1}$ are the contributions to the linewidth from CSA and ^{13}C-^{1}H dipolar relaxation, respectively.] It is clear that at magnetic field strengths greater than 4.2T, $(\pi T_2^{CSA})^{-1} >> (\pi T_2^{D})^{-1}$. The value of $(\pi T_2^{CSA})^{-1}$ increases approximately in proportion with the square of the magnetic field strength.

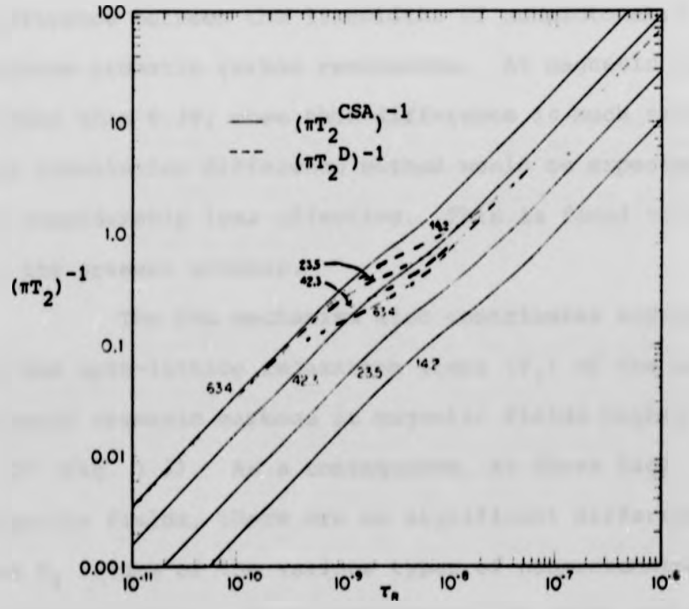

Fig. 1.2 Log-log plots of $(\pi T_2^{CSA})^{-1}$ and $(\pi T_2^{D})^{-1}$ (solid and dashed lines, respectively, both in hertz) *versus* τ_R (in seconds), in the case of isotropic rotational reorientation. Plots are given for four magnetic field strengths indicated in kilogauss. $(\pi T_2^{D})^{-1}$ was computed for a nonprotonated carbon with 3 hydrogens two bonds away (r = 2.16 Å). $(\pi T_2^{CSA})^{-1}$ was computed for a chemical shift anisotropy of 200 ppm (axially symmetric shielding tensor). Taken from Norton *et al.* (1977).

The significant contribution of the CSA relaxation mechanism to the relaxation of nonprotonated aromatic carbons means that the difference between the linewidths of methine and nonprotonated aromatic carbon resonances decreases with increasing magnetic field strength. The importance of this fact becomes apparent when the methods of resolution enhancement at high field are explored. Nonprotonated aromatic carbon resonances have in the past been readily resolved in a convolution difference spectrum. In this spectrum the broad aromatic methine carbon bands can essentially be eliminated leaving only the nonprotonated aromatic carbon resonances in the difference spectrum. This method relies on the large difference between the linewidths of nonprotonated and methine aromatic carbon resonances. At magnetic fields higher than 6.3T, when this difference is much smaller, the convolution difference method would be expected to be considerably less effective. This is found to be true in the present studies.

The CSA mechanism also contributes significantly to the spin-lattice relaxation times (T_1) of the nonprotonated aromatic carbons at magnetic fields higher than 4.2T (Fig. 1.3). As a consequence, at these high magnetic fields, there are no significant differences in the T_1 values of the various types of nonprotonated aromatic carbons. Such differences are often utilised for assigning these resonances (Oldfield *et al.*, 1975).

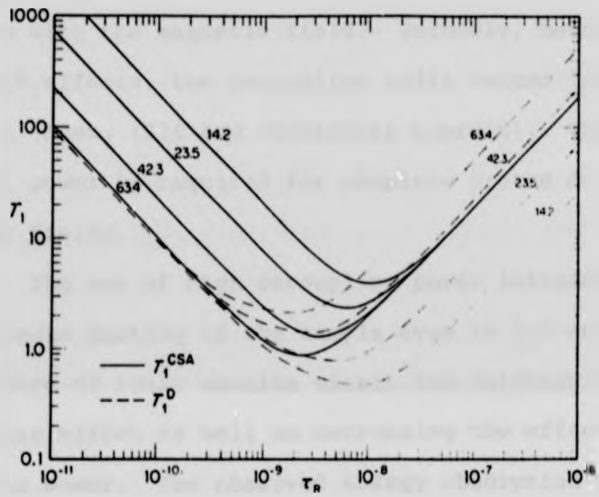

Fig. 1.3 Log-log plots of T_1^D and T_1^{CSA} (in seconds) *versus* τ_R (in seconds) for a nonprotonated aromatic carbon resonance at four magnetic field strengths (indicated in kilogauss). The meaning of solid and dashed lines is given in the legend of Fig. 1.2 Taken from Norton *et al.* (1977).

In summary, the effects of high magnetic field strengths on the relaxation of nonprotonated carbons negate the advantages of higher sensitivities. On the other hand, protonated carbon resonances which overlap severely at low fields can be resolved by large chemical shifts at higher field values.

1.2.2 Instrumentation Difficulties

The main problems encountered are related to

the use of proton decoupling. It is more difficult to achieve proton decoupling at high magnetic field strengths due to two main factors. Firstly, the spread of the proton spectrum, measured in frequency units, increases with the magnetic field. Secondly, because of skin-depth effects, the decoupling coils become less efficient (Anet, 1974 and references therein). Thus, more r.f. power is required for complete proton decoupling at higher fields.

The use of high decoupling power introduces heterogeneous heating of the sample even in D_2O solutions. The presence of ionic species within the solution increases the heating effect as well as decreasing the effective decoupling power. The observed energy absorption by the ionic species is attributed to an interaction between the oscillating electric field associated with the decoupling field and the electric dipole moments of the molecules or the ions of the electrolyte (Led and Petersen, 1978; Block *et al.*, 1980).

The heterogeneous heating effect can generally be reduced by decreasing the amount of ionic species in solution, by introducing extra cooling, and/or by gating the decoupling power.

1.3 THE ^{13}C NMR SPECTRUM OF A PROTEIN

The natural abundance ^{13}C spectrum of a protein is normally recorded under conditions of broadband proton decoupling. Under these conditions each magnetically

non-equivalent carbon atom of a protein should yield one resonance.

The folded structure of a protein when in its native conformation produces large changes in the chemical shift of similar carbons in the same type of amino acid but at different positions in the molecule. Each ^{13}C spectrum can be divided into a region of (i) carbonyl resonances, (ii) aromatic carbon resonances (this also contains the resonances of C^{ζ} of arg residues) and (iii) aliphatic carbon resonances (Table 1.1) (Fig. 1.4).

The carbonyl and carboxylate regions can be observed but very few specific assignments have been made (Allerhand, 1979, and references therein).

Detailed studies, by ^{13}C NMR, of folded proteins have almost entirely concentrated on nonprotonated aromatic carbon atoms. There are two reasons for this. Firstly, the resonances of these carbons are much sharper than those of the protonated carbons. Secondly, in proteins, there are relatively few aromatic nonprotonated carbon centres which yield resonances covering a large range of chemical shifts (106 ppm-165 ppm) (Table 1.1). These two facts permit the observation of resolved individual nonprotonated aromatic carbon resonances in a native globular protein.

The situation is different for protonated carbons. Firstly, protonated carbon resonances are broader. Secondly, there are large numbers of protonated carbons contributing to their respective spectral regions, particularly to the aliphatic regions. Thirdly, the magnetic non-equivalence caused by the folding of

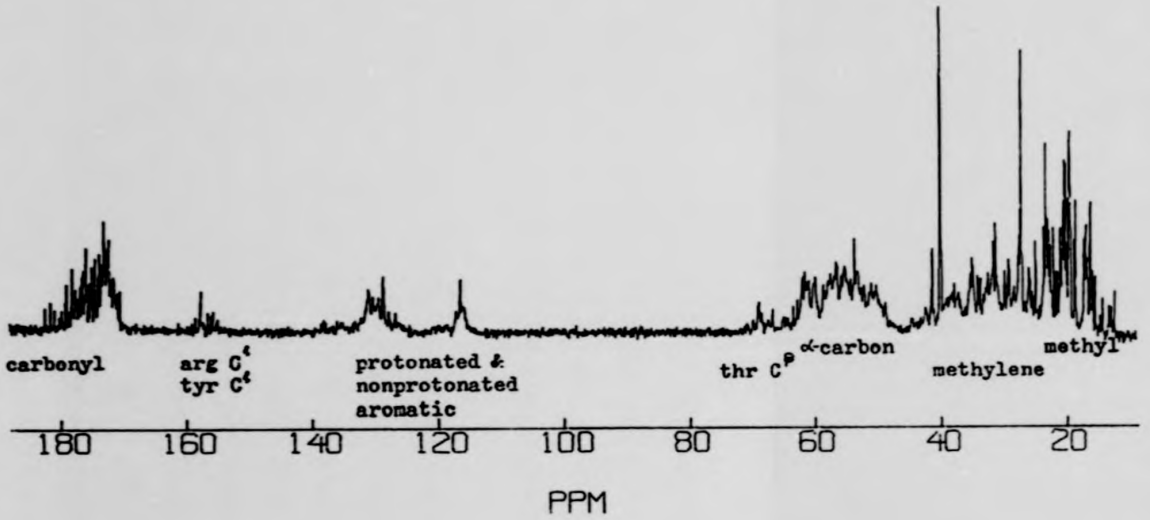

Fig. 1.4 Proton-decoupled natural abundance ^{13}C Fourier Transform NMR spectrum of Ribonuclease A (6 mM, pD 5.5, 25°C) at 100 MHz. The spectrum required 10 hours accumulation with a recycle time of 0.8 sec. The FID was processed using a Lorentz-to-Gaussian multiplication for resolution enhancement.

TABLE 1.1 ^{13}C Chemical Shift Ranges for Diamagnetic Proteins[a]

Type of ^{13}C	Approximate Shift Range (ppm)
CH_3	0-40
CH_2/CH (Aliphatic side chain)	20-40
[Ser/Thrβ-CH	60-70]
α-CH	40-70
Aromatic CH, C	105-165
Arg C^{ζ}	155-160
>C=O	165-210

[a]Table extracted from Campbell and Dobson, 1979

the protein is relatively small for side-chains which are capable of internal rotation. It is, therefore, difficult to resolve protonated carbon resonances particularly in the aliphatic carbon region of the natural abundance ^{13}C NMR spectra of proteins.

The resolution of the aliphatic carbon resonances should improve significantly with the use of high magnetic field strengths. However, even at field strengths of up to 6.34T very few aliphatic carbon resonances of HEW lysozyme are resolved. Individual ile methyl resonances of myoglobin have been resolved at 6.34T but not specifically assigned (Wittebort *et al.*, 1979). At 8.45T, many single aliphatic carbon resonances in the spectrum of bovine pancreatic trypsin inhibitor (BPTI), a small protein of molecular weight 6 000, have been observed and assigned specifically (Richarz and Wüthrich, 1978).

At 9.4T, the magnetic field used in this research, many aliphatic single carbon resonances are observed for proteins having molecular weights of up to 20 000. Even at this field, very few aliphatic carbon resonances of chymotrypsin (molecular weight 35 000) are resolved.

The resolution of single aliphatic carbon resonances has significant implications. Individual protein residues such as ile, met, val and thr can now be studied. These residues have long been considered 'silent' in the ^{13}C NMR protein spectrum because they could not be individually resolved and identified at magnetic fields below 6.34T.

1.4 THE PURPOSES OF THE PRESENT WORK

1.4.1 Introduction

The aim of the work described in this thesis is to develop the application of ^{13}C and ^{1}H NMR for the study of peptides and proteins. The work falls into two broad areas: high-resolution studies of proteins, and relaxation studies of proteins and peptides at more than one frequency.

1.4.2 High-Resolution Studies of Proteins

At the high magnetic field used in this research, many individual ^{13}C resonances of protonated

carbons, especially those away from the main peptide chain, would be expected to be resolved. To test the applicability of this high-resolution method, lysozyme and ribonuclease A are used.

Firstly, assignments of the aliphatic ^{13}C resonances of the side-chains of residues are to be made in the spectra of lysozyme and ribonuclease A. Secondly, the research attempts to answer questions on the behaviour of these and other side-chains when the proteins are subjected to varying conditions of pD and temperature; and when in the presence of ligands, inhibitors and denaturants. In the denaturation studies, using heat and urea as denaturants, it is hoped that any individual residues which are involved in predenaturation transitions may be detected. The nature of the unfolded state of the proteins will also be examined.

In the assignment work, and in the denaturation and ligand binding studies, ^{1}H NMR is to be used to complement the ^{13}C NMR technique.

Apart from the specific conclusions concerning the behaviour of lysozyme and ribonuclease A in solution, it is hoped that general conclusions may be drawn relating to other proteins and that NMR procedures may be laid down for the routine investigation of proteins, using the aliphatic ^{13}C resonances.

1.4.3 Relaxation Studies of Peptides and Proteins

A 3-τ model for molecular motion is to be

tested rigorously using gramicidin-S and glutathione dimer. The model is also to be applied to proteins. It is hoped that this model will explain the consistently low nOe observed for the resonances of small proteins.

1.5 A REVIEW OF PREVIOUS STUDIES OF LYSOZYME AND RIBONUCLEASE A

To test the applicability of the high-resolution ^{13}C NMR and ^{1}H NMR methods, the two proteins HEW lysozyme and bovine pancreatic ribonuclease A are good materials to use. In both cases, the tertiary structures have already been obtained from x-ray crystallography and many other properties are known.

1.5.1.1 The Structure and Function of HEW Lysozyme

HEW lysozyme is a globular protein of molecular weight 14 600, with 129 amino acid residues including 4 disulphide bridges, in one polypeptide chain. The protein lyses the mucopolysaccharide structure of bacteria cell walls by hydrolysing peptidoglycans at the β-1,4 linkage of N-acetylmuramic acid.

The lysozyme molecule can be described as a bridged structure. There are two lobes connected by looser strands which form the back of the substrate groove. The active site is bordered by a hydrophobic box which consists of 5 aromatic residues: tyr-20, tyr-23, trp-28, trp-108 and trp-111; and by other hydrophobic

residues, notably leu-17, ile-98 and met-105 (Blake *et al.*, 1967; Perkins *et al.*, 1977; Cassels *et al.*, 1978) (see Appendix I).

As the groove of a hinged protein is not in fixed dimensions the binding of metal ions or substrates causes the groove to close above the hinge with general internal tightening of the protein structure. This is observed as changes in ring current interactions.

1.5.1.2 High-Resolution NMR Studies of HEW Lysozyme

The first ^{1}H NMR spectrum of lysozyme was reported by McDonald and Phillips (1967). Today, at least 110 aliphatic proton resonances of the protein have been specifically assigned and studies are still being carried out, particularly by the Oxford Enzyme Group, U.K. (Delepierre, personal communication). To achieve the primary objective of assigning the ^{1}H spectrum, new techniques which are made possible by better instrumentation, are constantly being developed.

There have been extensive and detailed ^{1}H NMR studies of lysozyme in the presence of diamagnetic ligands and paramagnetic species, and on the binding of proteins. This spectroscopic method has been used to monitor the kinetics, thermodynamics, structural changes and molecular motions involved during these protein-ligand interactions (Poulsen *et al.*, 1980, and references therein).

Lysozyme is also the protein most widely used by ^{13}C NMR spectroscopists for investigating the applicability of the ^{13}C NMR method for biological studies. Of the 129

amino acid residues of this enzyme, three are tyrosines, three are phenylalanines, six are tryptophans, one is histidine and eleven are arginines. There are 28 nonprotonated aromatic carbons. By a combination of various methods, Allerhand *et al.* have specifically assigned all the resonances from these nonprotonated aromatic carbon atoms, although not on a one-to-one basis in some cases (Allerhand *et al.*, 1977). Single carbon resonances have also been reported for some carboxylate groups and a few tentative assignments given (Shindo and Cohen, 1976). The two methine aromatic carbon C^{δ}'s of each tyr residue appear to be indistinguishable, especially at higher temperatures. Each of the three resonances have been tentatively assigned to specific tyr residues. So far, no individual aliphatic carbon resonances of lysozyme have been identified in the natural abundance ^{13}C NMR spectrum.

The ^{13}C NMR characteristics of lysozyme can provide complementary or new information concerning the behaviour of the protein in solution. For example, the effect of pH on the chemical shift of the his C^{γ} resonance can not only yield the pKa value, but also reveals the predominant tautomeric state of the imidazole form of the residues (Ugurbil *et al.*, 1977). In contrast, the pH shift characteristics of the ^{1}H resonances of the his residues will not be able to furnish this information. The trp-108, trp-62 and tyr-23 residues have been chemically modified by various methods (Allerhand *et al.*, 1977). Studies of the properties of

a protein which has been chemically modified at a specific amino acid residue can be used for determining which portions in the intact protein are involved in its biological function and in the maintenance of its native conformation. The proximity of the trp-108, phe-34 and tyr-53 residues to the major metal binding site is demonstrated by the effect of paramagnetic relaxation probes on the resonances of these residues. Tempoacetamide binds to lysozyme at the ring on binding site A and in a hydrophobic pocket near trp-123, this being observed as a broadening of the C^{γ} resonances of trp-62, trp-63 and trp-123 (Allerhand *et al.*, 1977).

1.5.2.1 The Structure and Function of Ribonuclease A

Pancreatic ribonuclease A is a digestive enzyme of molecular weight 13 000. It is a single polypeptide chain with 124 residues including 4 disulphide bridges. Ribonuclease A is responsible for the breakdown of ribonucleic acid (RNA) by catalysing the cleavage of its phosphodiester linkages.

The chain itself twists backwards and forwards forming a U-shaped structure enclosing a cleft within which lie some of the residues responsible for the enzyme's activity (Carlisle *et al.*, 1974; Borkakoti, personal communication). This cleft is divided into two distinct regions (see Appendix II). At one end, towards the opening of the cleft, lie the active site residues lys-41, his-12 and his-119, together with lys-7 and lys-11 nearby. Clustered together and situated towards

the deep end of the cleft, opposite the active site residues, are many non-polar residues. These have been identified to be phe-8, val-47, val-54, ile-81, ile-106, val-108 and phe-120. Met-13 borders this region and is protected externally by leu-51.

Another interesting feature in the native structure of ribonuclease A is the presence of a distinct hydrophobic region comprising of residues 106 to 118. This 13-residue pocket is believed to be the nucleation site for the folding of ribonuclease (Matheson and Scheraga, 1978).

It must be noted that to date the exact position of the lys-41 side-chain is still only tentatively defined. In addition, the his-119 imidazole ring in the crystal structure appears to take up two equally favoured positions (Borkakoti, personal communication) (see Appendix III).

1.5.2.2 High-Resolution NMR Studies of Ribonuclease A

Ribonuclease A was the first protein to be studied using ^{1}H NMR spectroscopy (Saunders *et al.*, 1957). With the introduction of high-resolution NMR spectrometers and the advances in techniques, it has become possible to assign ten resonances in the aromatic region of the spectrum to the protons of specific amino acid residues (Lenstra *et al.*, 1979). Four other aromatic proton resonances have also been tentatively assigned. In the aliphatic region of the ^{1}H spectrum, no known attempts have been made to assign the resonances in the upfield region with the exception of an extremely tentative

identification of the met methyl resonances by Sadler *et al.*, 1974. Unlike the lysozyme structure, there are no apparent intrinsic ring current effects which can bring about the resolution of methyl resonances in ribonuclease A.

The ^{1}H assignments obtained for the resonances of the aromatic residues have been used to describe the pH-dependent conformational transition of the protein (Markley, 1975(a),(b); Markley and Finkenstadt, 1975; Lenstra *et al.*, 1979); the binding of active site inhibitors (Arus *et al.*, 1981, and references therein; Meadows *et al.*, 1969); and the thermal, urea, acid and guanidinium chloride unfolding of ribonuclease A and the residual structure after unfolding (Benz and Roberts, 1975(a),(b)).

In the ^{13}C NMR spectrum, four arginines, six tyrosines, three phenylalanines and four histidines contribute a total of 23 nonprotonated carbon resonances. These resonances are easily identified in the convolution difference spectrum. Of the 23 identified resonances, the three phe-C^{γ}, the tyr-25 C^{ζ}, the tyr-97 C^{ζ} and the four his-C^{γ} resonances have all been assigned using a combination of various methods (Santoro *et al.*, 1979; Egan *et al.*, 1978; Walters and Allerhand, 1980). Ribonuclease A contains eleven titrating carboxyl groups arising from one terminal carboxylate (val-124), five glu residues and five asp residues. Only the val-124 carboxyl carbon resonance has been assigned with confidence (Santoro *et al.*, 1979). No other resonances in the natural abundance ^{13}C NMR spectrum of ribonuclease A have so far been assigned.

identification of the met methyl resonances by Sadler *et al.*, 1974. Unlike the lysozyme structure, there are no apparent intrinsic ring current effects which can bring about the resolution of methyl resonances in ribonuclease A.

The ^{1}H assignments obtained for the resonances of the aromatic residues have been used to describe the pH-dependent conformational transition of the protein (Markley, 1975(a),(b); Markley and Finkenstadt, 1975; Lenstra *et al.*, 1979); the binding of active site inhibitors (Arus *et al.*, 1981, and references therein; Meadows *et al.*, 1969); and the thermal, urea, acid and guanidinium chloride unfolding of ribonuclease A and the residual structure after unfolding (Benz and Roberts, 1975(a),(b)).

In the ^{13}C NMR spectrum, four arginines, six tyrosines, three phenylalanines and four histidines contribute a total of 23 nonprotonated carbon resonances. These resonances are easily identified in the convolution difference spectrum. Of the 23 identified resonances, the three phe-C^{γ}, the tyr-25 C^{ζ}, the tyr-97 C^{ζ} and the four his-C^{γ} resonances have all been assigned using a combination of various methods (Santoro *et al.*, 1979; Egan *et al.*, 1978; Walters and Allerhand, 1980). Ribonuclease A contains eleven titrating carboxyl groups arising from one terminal carboxylate (val-124), five glu residues and five asp residues. Only the val-124 carboxyl carbon resonance has been assigned with confidence (Santoro *et al.*, 1979). No other resonances in the natural abundance ^{13}C NMR spectrum of ribonuclease A have so far been assigned.

The ^{13}C NMR method for the investigation of the behaviour of ribonuclease has not been very popular. The thermal unfolding of the molecule (Howarth, 1979(a)) and the nature of the unfolded state (Howarth and Lian, 1981) have now been studied in some detail using this method. Observation of the titration behaviour of carboxyl groups by Santoro *et al.* (1979), gave only a tentative description of the behaviour of one carboxylic imidazole interaction, this being that of asp-14 with his-48. From their pH titration studies of the his resonances, Walters and Allerhand (1980) showed that three of the four his residues have the abnormal $N^{\delta 1}$-H tautomeric structure. This result has important structural implications. The stabilisation of the $N^{\delta 1}$-H tautomeric state of his-12, his-48 and his-105 is probably the result of hydrogen bonding between his-12 and the hydroxyl oxygens of thr-45; of bonding between his-48 and the carboxylate oxygen of asp-14 (or the hydroxyl oxygen of thr-17); and of bonding between his-105 and the carboxylate oxygen of val-124.

CHAPTER 2

MATERIALS AND METHODS

2.1 MATERIALS

2.1.1 Proteins

Lysozyme from hen egg white (HEW) was obtained from the Sigma Chemical Co. It was grade I, three times crystallised, dialysed and lyophilised. Before using, it was dissolved in water and dialysed according to the method of Dobson (1975). The solution was lyophilised and the solid protein stored at -5°C.

Bovine pancreatic ribonuclease A was obtained from the Sigma Chemical Co. (type II-A, phosphate-free). It was dialysed against water at 5°C before use. The solution was lyophilised and the solid powder stored at -5°C.

The purity of the proteins was tested by gel electrophoresis.

2.1.2 Other Materials

D_2O (99.8%), NaOD (30% in D_2O) and DCl (20% in D_2O) were obtained from the Aldrich Chemical Co.

All other reagents were analytical grade.

2.2 PREPARATION OF SOLUTIONS FOR NMR SPECTRA

Solutions of the protein were prepared by dissolving the weighed lyophilised solids in the required volume of D_2O or salt solution.

Concentrations were obtained from the weight of dry solid.

Different pD values were obtained by the addition of small amounts of 5% DCl or 5% NaOD. The pD values were measured using a pH M-64 research digital pH meter with a glass electrode standardised in H_2O buffers. The pD values were measured at room temperature and the pD meter readings were not corrected for isotope effects. pD values of solutions were measured in small sample vials before and after running the spectra and a mean pD was taken.

For the NMR studies of lysozyme alone, 6-7 mM solutions of the protein were used. The addition of NaOD to a solution of lysozyme caused the formation of precipitates. These partially redissolved on shaking. At pD values above pD 7.0 lysozyme became less soluble and irreversible precipitation occurred.

Once the pD of the D_2O solution of lysozyme had been adjusted to the required value the solution was thermostated at 55°C for about 30 minutes. Any precipitate present at the end of this period was removed by centrifuging. This treatment was applied to remove all insoluble precipitates which may have formed with time. The pD of the resulting supernatant was checked and adjusted as

necessary.

For the NMR studies of ribonuclease A alone, 6-7 mM solutions of the protein were prepared in D_2O or in D_2O containing 0.05 M NaCl.

At a concentration of 6-7 mM, both lysozyme and ribonuclease A are unlikely to self-aggregate over a wide range of temperature and pD. Line broadening arising from the self-aggregation of the proteins and from an increase in solution viscosity was hence kept to a minimum.

2.3 ACQUISITION OF NMR SPECTRA

2.3.1 Spectrometer

All the NMR spectra reported in this thesis are fourier transform (FT) ^1H and ^{13}C spectra. Unless otherwise stated, all spectra were recorded at 400 MHz for ^1H and 100.63 MHz for ^{13}C using the S.E.R.C.'s Bruker WH400 spectrometer at the University of Warwick. The spectrometer is fitted with an Oxford Instruments superconducting magnet and is controlled by an Aspect 2000 computer. This spectrometer required 5 mm (O.D.) sample tubes for observing ^1H, and 5 mm, 10 mm and 15 mm (O.D.) sample tubes for ^{13}C. It has a deuterium field-frequency lock and is equipped with quadrature detection. Peak positions can be measured directly from the spectrometer computer using a cursor address system.

The temperature at the probehead was kept

constant by a temperature control unit and measured with a calibrated external thermocouple. A more accurate measurement of the sample temperature in the probehead was then taken using a Comark thermocouple inserted into the sample tube. The values were read directly on a digital thermometer. The temperatures quoted were accurate to within $\pm$ 0.5°C and when checked at the end of the acquisition time were found to differ by less than $\pm$ 0.5°C. During all experiments the temperature was allowed to stabilise for about 15 minutes before acquisition of the free induction decay (FID).

2.3.2 Acquisition of Broadband Proton-Decoupled ^{13}C NMR Spectra

^{13}C spectra were recorded using tubes of 10 mm O.D. The tubes were spun at 22-25 rev/sec and Teflon vortex plugs were used to prevent vortexing.

Unless otherwise stated, all the ^{13}C spectra were accumulated under conditions of noise-modulated broadband proton decoupling with the proton irradiation centred at 2.5 ppm downfield from the ^{1}H resonance of Me_4Si and at a bandwidth of 10 ppm. The value of the decoupling power used was approximately 7 Watts. For ^{13}C excitation, r.f. pulses of about 70° were used. (A pulse duration of about 32 μs is equivalent to a 90° r.f. pulse.) A recycle time of 1.0 s, and 16K of data points were used for data acquisition. For each ^{13}C spectrum about 30K to 35K transients requiring 10-12 hours were accumulated. The choice of these

acquisition parameters gave the best compromise between the time-availability and the need to obtain good S/N ratios for the resonances of the whole ^{13}C spectrum.

In the present studies, considerable attention was given to the problems arising from the use of proton decoupling. The excessive heterogeneous heating was reduced to a minimum in both D_2O and ionic samples by introducing extra cooling, using liquid nitrogen if necessary, and by gating the decoupler power. In the latter method, the decoupler was gated to operate at a high level (≈ 7.0 Watts) when the signal was acquired, but for the rest of the waiting period (recycle time) the power was reduced to a lower value (≈ 0.1 Watts), this power being sufficient to maintain the nOe (see Appendix X(a) for the microprogram used).

The decrease in effective decoupling power caused by ionic species was dependent on the concentration of the ions present (Block *et al.*, 1980, and references therein). In the present studies the maximum allowable total concentration of ions which could be present in the sample solution was found to be 100 mM. Above this concentration the decoupling power was drastically reduced, as was seen from the quality of the spectra obtained and from the high level of reflected decoupler power (as indicated on the decoupler measurement scale).

The FID was processed by a Lorentz-to-Gaussian multiplication for resolution enhancement, using GB = 0.1 and LB = -5.0 (Ferridge and Lindon, 1978). These parameters gave optimal resolution without severe

distortion of line shape. The FID was Fourier transformed over 32K points using the zero-filling technique of Farrar and Becker (1971).

Chemical shift values were referenced to external dioxane and were converted to the δ scale using $\delta_{dioxane} - \delta_{Me_4Si} = -67.4$ ppm. The chemical shift values were measured digitally. For the protein solutions referencing of the chemical shifts was done by first assuming that the chemical shifts of many resonances should not change under different conditions (except under denaturing conditions). That is, it was easy to find a large number of resonances whose relative chemical shifts had not changed. This assumption is based on a firm foundation of experimental data obtained in the present study for the proteins under different conditions. Hence, the chemical shifts of the spectrum of a 'reference sample'* were first measured as described above. The 'pattern recognition' method was then applied to the chemical shifts of the protein samples which were subjected to conditions different from the 'reference sample'. The dual display mode in the DISNMR programme facilitated the use of the 'pattern recognition' method. Both the reference spectrum and the spectrum of interest can be examined together on the screen.

---

*'Reference sample ' refers to sample of protein at a particular pD, temperature and ionic strength. Variations in conditions can take the form of changes in pD or temperature or the addition of denaturants or ligands (both paramagnetic and diamagnetic).

2.3.3 Acquisition of ^{13}C NMR Spectra using Single Proton-Frequency Decoupling

The proton decoupling coils of the multinuclei probehead of the spectrometer used in the present study are pretuned to the ^{1}H resonance frequency and can therefore be used for proton observation.

The spectrometer was set up in the same manner as for the accumulation of a routine ^{13}C spectrum using broadband proton decoupling. To acquire the ^{1}H spectrum, the acquisition parameters were adjusted to the same settings used for obtaining a routine ^{1}H spectrum. The ^{1}H FID was then obtained using the proton decoupling channel in the multinuclei probehead.

All the ^{1}H spectra were referred to Me_4Si (external reference). The resolution of the ^{1}H spectrum was not as good as that obtained using a pretuned ^{1}H probehead, but the quality was adequate for the present purposes.

From each ^{1}H spectrum recorded, the desired specific irradiation frequency was obtained. This was the single decoupling frequency setting used for acquiring the ^{13}C spectrum. A decoupling power of between 0.8-1.0 Watts was used. As an accurate proton irradiation frequency was desirable, it was best to obtain a fresh ^{1}H spectrum for each set of double resonance experiments. Some proton shifts of lysozyme and ribonuclease A are very sensitive to temperature in the pD ranges used, so it was imperative to stabilise the temperature and acquire both the ^{1}H and ^{13}C spectra at the same temperature.

The acquisition and data manipulation parameters for the single proton-frequency decoupled ^{13}C spectrum were set as described in Section 2.3.2.

2.3.4 Acquisition of ^{1}H NMR Spectra

Unless otherwise stated, all ^{1}H spectra were recorded using 5 mm O.D. tubes. For each spectrum, between 500 and 1 000 accumulations were collected over 16K data points. The FID was processed with a Lorentz-Gaussian multiplication for resolution enhancement. Typically, GB = 0.1 and LB = -10.0.

All chemical shifts are quoted downfield of external Me_4Si. The Me_4Si solution was contained in a small Wilmad precision bore NMR cell. In cases where the peaks of interest were at 0 ppm, two spectra were obtained, one with Me_4Si as the external reference and one without. Comparison of the two spectra obtained showed no difference except for the presence of the Me_4Si resonance at 0 ppm.

2.3.5 Acquisition of ^{1}H nOe Difference Spectra

Nuclear Overhauser effect (nOe) was measured using a programme that provided the direct accumulation of an nOe difference free induction decay (FID). Two FID's were accumulated under the same conditions except for the value of the presaturation frequency. One was obtained using an on-resonance presaturation frequency,

the other with an off-resonance presaturation frequency. The difference FID was obtained by taking the difference between these two FIDS. (See Appendix X(b) for the microprogram used.)

The areas of the individual resonances in the difference spectra were measured relative to the area of the saturated resonance appearing in the difference spectrum.

In the present study, an investigation of the time-development of the Overhauser effect (under the experimental conditions used) showed that, as expected, the observed effect increased as the length of the presaturation pulse was increased (Olejniczak *et al.*, 1981). Using short pulses of about 0.2 sec, only protons which are at a small distance, fixed by the geometry of the residue, from the saturated proton, showed a significant nOe. In the long-pulse experiments using a presaturation pulse length of between 0.6 and 1.0 sec, an accumulation time of 1.2 to 1.5 sec per FID and a pulse repetition time of 1.0 sec were used. Spectra with acceptable S/N ratio were obtained after about 3 000 pulses, that is, about 3 hours were required for each experiment. A very low decoupling power was used in each nOe difference experiment.

CHAPTER 3

ASSIGNMENT OF THE NMR SPECTRA OF HEW LYSOZYME AND RIBONUCLEASE A

3.1 INTRODUCTION

The characteristics of the ^{13}C NMR and ^{1}H NMR spectra of native proteins in aqueous solutions are strongly influenced by the protein tertiary structure. Therefore, detailed information can be obtained on protein conformation or on interactions which change the conformation(s) if one can resolve individual resonances, assign them to particular protein carbons (or protons), and rationalise the resonance behaviour in terms of the protein structure.

Relatively few examples of extensive identification and assignment of the ^{13}C NMR spectra of proteins are to be found in published literature (Richarz and Wüthrich, 1978, and Chapter 1 of this thesis). This is especially true for the aliphatic carbon resonances where very few of the aliphatic carbons in the native protein yield resolved single carbon resonances even at a magnetic field of 6.34T. At 9.4T, many resolved single aliphatic carbon resonances are observed for the two proteins HEW lysozyme and ribonuclease A (RNase).

The procedures involved in the assignment of the ^{1}H NMR and of the ^{13}C NMR spectra of a protein differ in many ways. It is easier, in general, to assign resonances to a specific amino acid residue (that is, a second-order assignment) in ^{1}H spectra than in ^{13}C spectra. Due to the lower sensitivity of the ^{13}C NMR method, several

strategies which can be used in ^{1}H NMR spectroscopy may not be practical using ^{13}C NMR, for example, pH titrations and the comparison of spectra taken from proteins having homologous sequences. Secondary shifts arising in ^{13}C NMR are also much more difficult to interpret than those in ^{1}H NMR. Despite these difficulties, many assignments have been made in the ^{13}C NMR spectra of small- and medium-sized proteins (Allerhand, 1979; Richarz and Wütrich, 1978).

The present research concentrates on the relatively well-resolved region between 10 ppm and 23 ppm in the ^{13}C NMR spectra of lysozyme and RNase. Many methyl carbon resonances appear in this part of the spectrum. This chapter first briefly discusses the problem of resolving individual protonated ^{13}C resonances, then the general scheme that can be used to assign the resolved resonances. The assignments of some resolved methyl resonances in the lysozyme and RNase spectra are then treated separately. Finally, the problems encountered in some of the methods of assignment are discussed.

The assignment of a ^{13}C resonance at Stage 2 below is made easier by a knowledge of the x-ray structure of the protein considered.

3.2 RESOLUTION OF RESONANCES

The linewidths of resonances can cause difficulties in the resolution of individual peaks. In addition, in large molecules, the high number of resonances, compared with the

spread of chemical shift values, causes severe overlap of resonances.

The linewidths of resonances increase under various conditions. $^{1}/T_{2}$ (and linewidth) of a resonance increases with increasing viscosity. Lower viscosity can be achieved by using lower concentrations and/or increasing the temperature. In addition, self-aggregation, which causes line broadening, may be decreased by reducing concentrations, changing pH, or by altering the salt concentration and other conditions.

Another way to overcome the linewidth problem is to manipulate the FID after acquisition. A Lorentz-Gaussian resolution enhancement is used in this research.

In addition, the overlap of resonances can be effectively reduced by increasing the spectrometer field.

3.3 SCHEME FOR THE ASSIGNMENT OF RESOLVED ^{13}C RESONANCES

Two types of chemical shift characterise the spectrum of a biomolecule such as a protein. These are the primary and secondary shifts.

The primary shift of a nucleus is determined by the electron distribution around the atom whose nuclear resonance is observed. On the other hand, secondary effects arise from through-space effects such as ring current effects, paramagnetic centre effects, electrostatic effects and the anisotropic shielding of carbonyl groups. Secondary shifts are important in biomolecules which have a secondary and tertiary structure.

When a protein is in a totally random coil configuration its spectrum closely resembles that of a mixture of its constituent amino acids. Only very small differences exist between the chemical shifts of similar carbons in the same type of amino acid but in a different position in the protein. In a folded structure however, secondary shifts perturb the spectrum and like-carbons at different positions in the protein will now have different chemical shift values.

The detailed assignment of a ^{13}C NMR spectrum, like that of a ^{1}H NMR spectrum, is carried out in two main stages:

Stage 1 The first stage is to assign an observed resonance to the specific nucleus of a type of chemical unit. This stage can be subdivided into:

(a) assignment to a type of chemical group (e.g., C=O, CH_3), and

(b) assignment of this group to a chemical unit (e.g., CH_3 of thr or of ile).

The assignment of a ^{13}C resonance to a particular type of carbon atom is relatively straightforward. The range of chemical shifts over which the resonances occur is much larger than that found in the ^{1}H NMR spectrum. Thus, the primary shifts are large compared with the secondary shifts and can be used to distinguish different types of carbon atom (Howarth and Lilley, 1978).

Stage 2 The second stage is to assign the observed

resonance to a specific nucleus in the protein molecule. This stage is subdivided into:

(a) assignment to a small region of the protein molecule, and

(b) assignment to a specific atom.

The stage 2 assignment of a ^{13}C resonance is carried out in the same manner as for a ^{1}H resonance. The methods used include chemical modification, variation of pH and the binding of paramagnetic and diamagnetic species.

In many cases the linking of a methyl resonance with a specific resonance in the ^{1}H spectrum is possible. In this situation, provided the ^{13}C spectrum is well resolved, the corresponding ^{13}C resonance can be specifically identified by low-power single proton-frequency irradiation.

3.4 ASSIGNMENT OF THE ^{1}H AND ^{13}C NMR SPECTRA OF HEW LYSOZYME

3.4.1 Materials and Methods

N-Bromosuccinimide (NBS) from the Sigma Chemical Co. was recrystallised three times from water.

Praseodymium chloride ($PrCl_3$) and lanthanum chloride ($LaCl_3$) were obtained from the Aldrich Chem. Co. Inc. and BDH Chem. Ltd. respectively. Both were used without further purification.

N-Acetylglucosamine (NAG) was purchased from

the Sigma Chemical Co., and used as supplied. $(NAG)_3$ was a generous gift of Professor K. Hamaguchi, Osaka University, Osaka, Japan.

The reaction of HEW lysozyme with iodine at pH 5.5 was carried out essentially as described by Norton and Allerhand (1976(a)). The treatment of HEW lysozyme with an equimolar amount of NBS was carried out according to the procedure of Norton and Allerhand (1976(b)).

To study the effects of Pr^{3+} and La^{3+} on HEW lysozyme their respective chloride solutions were added to the lysozyme solution in D_2O. The final concentration of lysozyme, Pr^{3+} and La^{3+} were 7.0 mM, 45.0 mM and 45.0 mM respectively.

The other materials and the methods of sample preparation and spectrum acquisition were as described in Chapter 2.

Calculations of the distances between the protons in the crystal structure were carried out using refined coordinates supplied by Artymiuck (personal communication).

3.4.2 Assignment of the ^1H NMR Spectrum of HEW Lysozyme

3.4.2.1 Results and Discussion

The resonances of the ile-98 $C(\delta)H_3$, leu-17 $C(\delta_2)H_3$, ile-98 $C(\gamma_2)H_3$ and met-105 $C(\beta)H$ groups are well-resolved and have been previously assigned. (Poulsen *et al.*, 1980, and references therein.) In the present study, the nOe results obtained from the saturation of these resonances agree well with those obtained by Poulsen *et al.*.

The saturation of each of the assigned $C(\delta)H_3$

groups of leu-17 at -0.61 ppm and -0.12 ppm gives results which differ from one another. Amongst the peaks in the difference spectra are those arising from the assigned methyl resonances of val-92 and met-12. Quantitatively, there are differences between the percentage nOe values obtained for the two val-92 methyl resonances on irradiation of each of the two methyl resonances of leu-17 (Fig. 3.1 and Table 3.1).

The aromatic proton regions of the difference spectra thus obtained are of considerable interest. When the $C(\delta_2)H_3$ group resonance of leu-17 is saturated at -0.61 ppm, nOe's are observed in the resonances of the ring protons of trp-28 [C(2)H, C(4)H, C(5)H, C(6)H and C(7)H] and of tyr-20 [C(2,6) and C(3,5)] (Fig. 3.2). However, the nOe's on the aromatic protons on saturation of the $C(\delta_1)H_3$ group resonance of leu-17 at -0.12 ppm are more difficult to detect.

The differences in the nOe values of the various peaks arising from saturation of each of the methyl group resonances of leu-17 can be explained by examination of the interproton distances in the crystal structure of lysozyme (Table 3.1).

The differences in the interproton distances between the $C(\delta_2)H_3$ group of leu-17 and each of the two methyl groups of val-92 accounts for the significant difference in the percentage nOe observed in the two val-92 methyl peaks when the $C(\delta_2)H_3$ group of leu-17 is saturated. The $C(\delta_1)H_3$ group of leu-17, on the other hand, is near to both the val-92 methyl groups. This explains the small difference in terms of percentage nOe observed for both the val-92

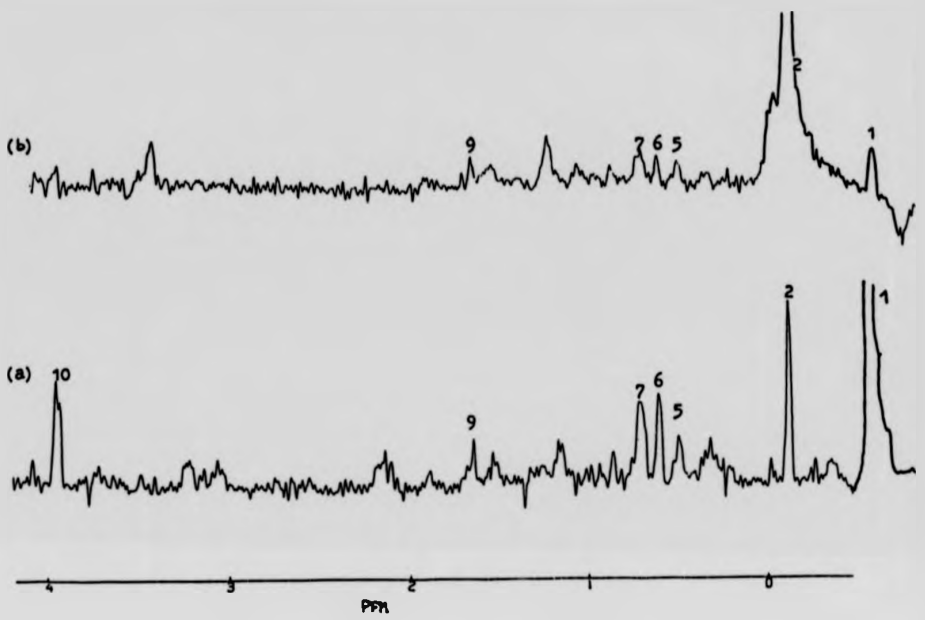

Fig. 3.1 Nuclear Overhauser difference spectra in the methyl group and methylene proton region of the ^1H NMR spectra of lysozyme (pD 4.0, 50°C) resulting from saturation of (a) the $C(\delta_2)H_3$ resonance of leu-17 at -0.61 ppm, and (b) the $C(\delta_1)H_3$ resonance of leu-17 at -0.12 ppm. Assignments are (1) leu-17 $C(\delta_2)H_3$, (2) leu-17 $C(\delta_1)H_3$, (5) val-92 $C(\gamma_2)H_3$, (6) val-92 $C(\gamma_1)H_3$, (7) leu-17 C(γ)H, (9) met-12 $C(\varepsilon)H_3$, and (10) leu-17 C(α)H. (Poulsen *et al.*, 1980).

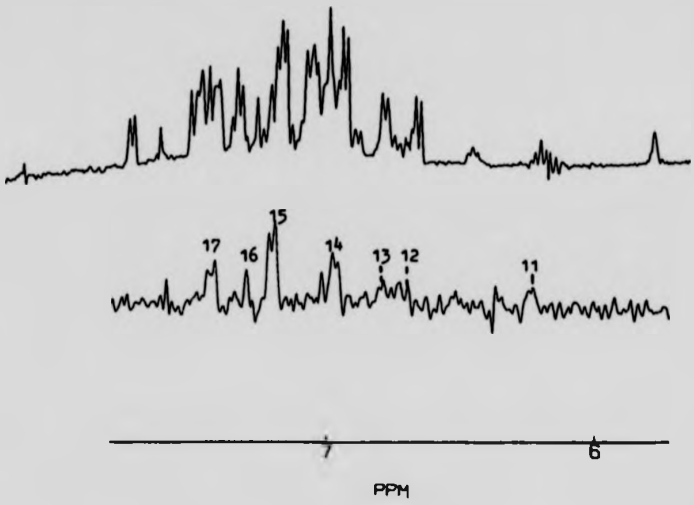

Fig. 3.2 Nuclear Overhauser difference spectrum in the aromatic proton region of the ^{1}H NMR spectrum of lysozyme (pD 4.0, 50°C) resulting from saturation of the leu-17 $C(\delta_2)H_3$ resonance at -0.61 ppm. The assignments which are known are (11) trp-28 C(5)H, (12) trp-28 C(4)H, (13) trp-28 C(6)H, (14) tyr-20 C(3,5)H, (15) tyr-20 C(2,6)H, (16) trp-28 C(2)H, and (17) trp-28 C(7)H (Poulsen *et al.*, 1980).

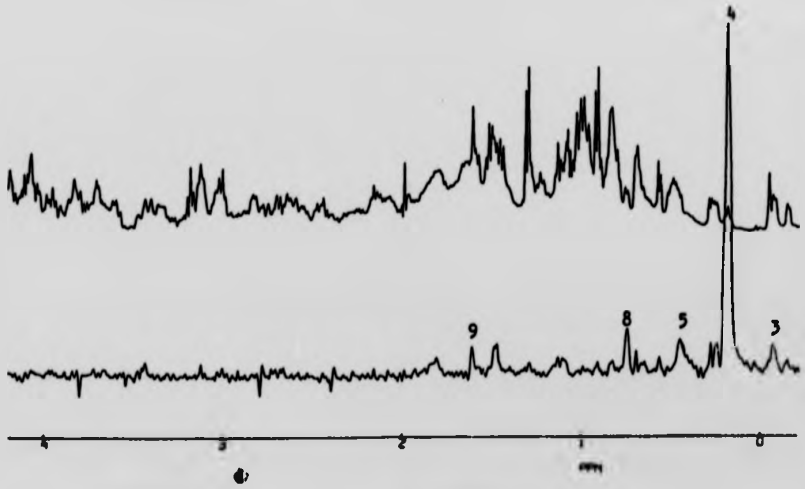

Fig. 3.3 Nuclear Overhauser difference spectrum in the methyl group and methylene proton region of the ^{1}H NMR spectrum of lysozyme (pD 4.0, 50°C) resulting from saturation of the ile-88 $C(\delta)H_3$ resonance at 0.18 ppm. The assignments are (3) leu-8 $C(\delta_1)H_3$, (5) val-92 $C(\gamma_2)H_3$, (8) ile-88 $C(\gamma_2)H_3$, and (9) met-12 $C(\varepsilon)H_3$ (Poulsen *et al.*, 1980; this work).
For comparison, the normal ^{1}H NMR spectrum of lysozyme under the same conditions is shown in the top trace.

TABLE 3.1 Interproton Distances[a] and some Nuclear Overhauser Effects[b]

Residue	Protons[c]	Leu-8 $C(\delta_1)H_3$ [3]	Val-92 $C(\gamma_2)H_3$ [5]	Val-92 $C(\gamma_1)H_3$ [6]	Ile-88 $C(\gamma_2)H_3$ [8]	Met-12 $C(\varepsilon)H_3$ [9]	Trp-28 C(5)H [11]	Trp-28 C(4)H [12]	Trp-28 C(6)H [13]	Tyr-20 C(3,5)H [14]	Tyr-20 C(2,6)H [15]	Trp-28 C(2)H [16]	Trp-28 C(7)H [17]
Leu-17	$C(\delta_2)H_3$ [1]		5.73 (0.7%)[d]	4.35 (2.4%)[d]		6.96	5.38	5.06	4.44	6.18	4.80	5.70	4.18
Leu-17	$C(\delta_1)H_3$ [2]		3.75 (3.0%)[e]	4.21 (2.9%)[e]		4.13	5.69	4.22	5.93	8.90	7.64	5.70	6.13
Ile-88	$C(\delta_1)H_3$ [4]	4.25	3.14	5.72	3.88	5.29							

[a] Values calculated from refined coordinates supplied by Artymiuck (personal communication). For methyl groups and tyr ring protons, an average distance is given. The interproton distances are given in Angstroms

[b] Values of Overhauser effects are negative and are given in percent. The numbers are in parenthesis ( )

[c] Numbers in square brackets [ ] represent the peak numbers as shown in Figs. 3.1, 3.2 and 3.3. Except for peak 8, all the assignments are taken from Poulsen *et al.* (1980)

[d] Poulsen *et al.* (1980)

[e] This work; pD 4.0, 50°C

methyl group resonances when the $C(\delta_1)H_3$ group of leu-17 is saturated.

The results observed in the aromatic proton region of the difference spectra are explained by the orientation in the crystal structure of the two methyl groups of leu-17 with respect to the trp-28 and tyr-20 aromatic rings. The $C(\delta_2)H_3$ group of leu-17 is positioned directly above the trp-28 ring, all the protons of trp-28 being less than 6.2 Å away from the leu-17 $C(\delta_2)H_3$ group (Table 3.1). In contrast, the $C(\delta_1)H_3$ group of leu-17 is not directly above the trp-28 ring and the aromatic protons of trp-28 and tyr-20 are at a greater distance from the $C(\delta_1)H_3$ group than from the $C(\delta_2)H_3$ group of leu-17 (Appendix I and Appendix IV(a)).

The $C(\delta)H_3$ group resonance of ile-88 has been previously assigned (Campbell *et al.*, 1975). At pD 5.0 this resonance appears together with the assigned methyl resonance of leu-56 and thr-51, as a broad multiplet at 0.28 ppm. At pD values below 5.0, the ile-88 $C(\delta)H_3$ group resonance is observed to shift upfield, appearing as a triplet at 0.18 ppm at pD 4.0.

Saturation of the ile-88 $C(\delta)H_3$ group resonance results in many peaks in the difference spectrum (Fig. 3.3). The most prominent peaks are the assigned resonances of the $C(\delta_1)H_3$ group of leu-8, the $C(\gamma_2)H_3$ group of val-92 and the $C(\varepsilon)H_3$ group of met-12. The other significant peak at 0.74 ppm has not been previously assigned. It is hence tentatively assigned to the $C(\gamma_2)H_3$ group resonance of ile-88*. All the peaks observed in the difference spectrum

---

*This assignment concurs with the assignment made independently by the Oxford Enzyme Group (Delepierre, personal communication).

result from methyl protons which are close to the irradiated C(δ) protons of ile-88 (Table 3.1).

The above results show a high correlation between the magnitude of the nOe and the crystallographic interproton distance. This concurs with the results previously obtained by Poulsen *et al.* (1980). These authors concluded that under their experimental conditions, Overhauser effects were very small between protons more than 5 Å apart; and large only between protons closer together than about 3 Å. The correlations obtained in the present study are significant in that they demonstrate the applicability of the nOe method to both assignment and to structural analysis.

3.4.3 Assignment of the ^{13}C NMR Spectrum of HEW Lysozyme

3.4.3.1 Results

3.4.3.1.1 Assignment of Corresponding Methyl ^{1}H and ^{13}C Resonances by Single Proton-Frequency Decoupling

A selected region of the ^{13}C NMR spectrum of lysozyme at 100.63 MHz is shown on an expanded scale in Fig. 3.4. The numbered lines are identified as methyl resonances by comparison with the spectrum of the denatured protein. In the following paragraphs, experiments are described which result in the identification of the corresponding ^{13}C and ^{1}H methyl resonances.

Fig. 3.5 shows that after suitable resolution enhancement, many methyl ^{1}H multiplets can be resolved. Ten of the sixty-one methyl groups of lysozyme are

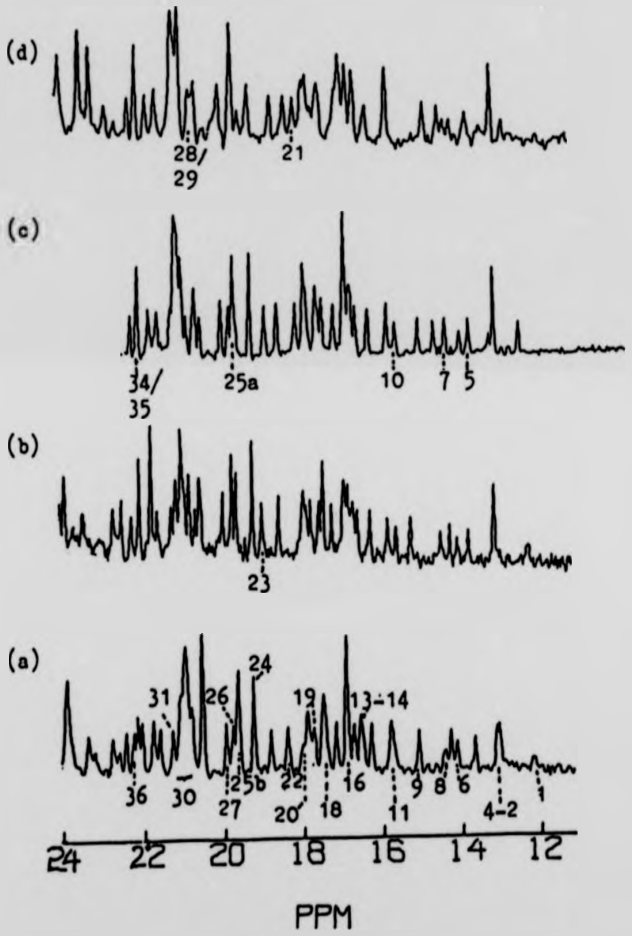

Fig. 3.4 Spectral region from 11.0 ppm to 24.0 ppm of the proton-decoupled ^{13}C NMR spectrum of lysozyme (6 mM in D_2O)
(a) free protein, pD 5.0, 50°C
(b) free protein, pD 3.2, 50°C
(c) + 100 mM NAG, pD 3.2, 45°C
(d) + 12 mM $(NAG)_3$, pD 5.0, 40°C

In this figure and in subsequent figures of lysozyme the numbers indicate the positions of individual methyl carbon resonances.

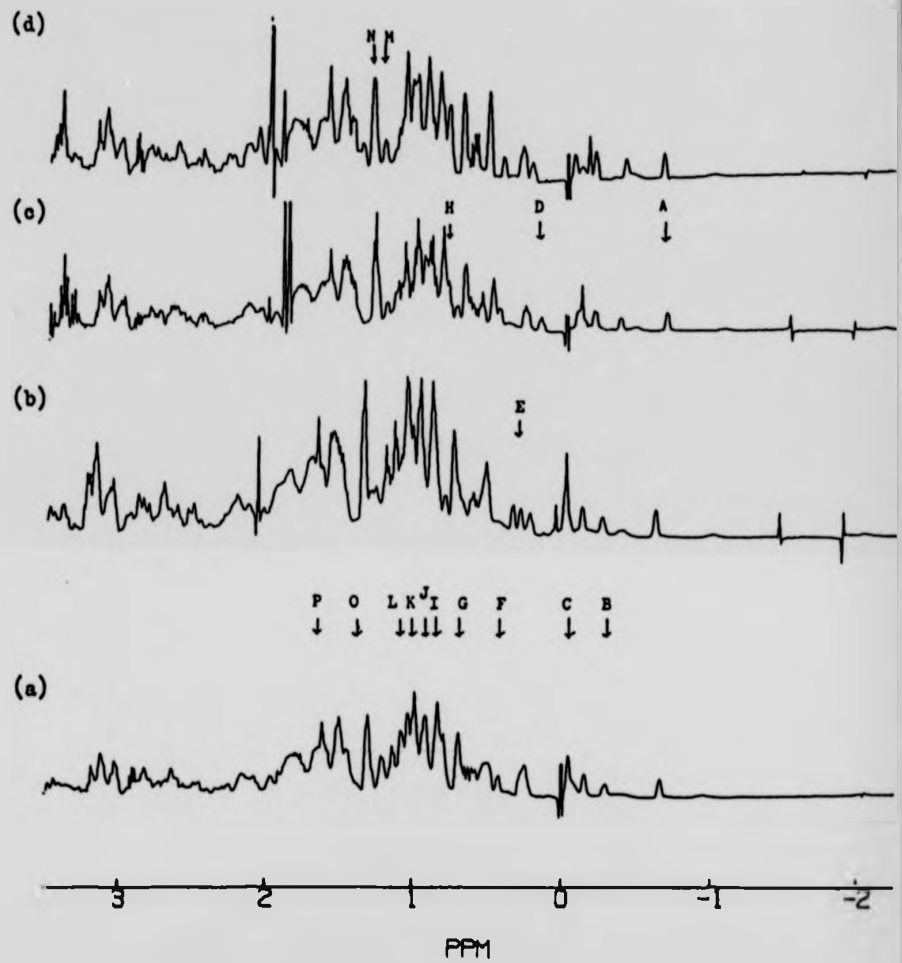

Fig. 3.5 Spectral region from -2.0 ppm to 3.5 ppm of the ^1H NMR spectrum of lysozyme (6 mM in D_2O)
(a) free protein, pD 5.0, 50°C
(b) free protein, pD 3.2, 50°C
(c) + 100 mM NAG, pD 3.2, 45°C
(d) + 12 mM $(NAG)_3$, pD 5.0, 40°C
The letters and arrows indicate the proton irradiation frequencies used in the selective decoupling experiments of Fig. 3.6.

sizeably affected by large ring current shifts. Their resonances appear as distinct well-resolved upfield shifts. The remaining methyl resonances overlap even in the spectrum obtained at the high magnetic field strength used here (9.4T). By a combination of several techniques many of these methyl resonances have been assigned to specific residues in the amino acid sequence (Poulsen *et al.*, 1980 and references therein).

The sufficiently well-separated ^{1}H methyl peaks in the 400 MHz spectrum are made use of to identify corresponding ^{13}C NMR peaks by selective ^{1}H-^{13}C heteronuclear double resonance experiments. The clearest results are obtained when the ^{13}C methyl peaks are also well resolved.

Fig. 3.6 shows the ^{13}C NMR spectra obtained using selective ^{1}H irradiation at the frequencies indicated by the arrows in Fig. 3.5. The resonance of the carbon atom attached to the irradiated protons of each methyl group is observed as a sharp single line. For the methyl ^{13}C resonances, the chemical shifts of the corresponding ^{1}H resonances, and the conditions for heteronuclear double resonance experiments, are collated in Table 3.2. The assignments of the methyl resonances of ile-98, ile-58, ile-88, leu-56 and some val residues are supported by additional evidence as indicated in Table 3.2. Some of this evidence is discussed in the following sections.

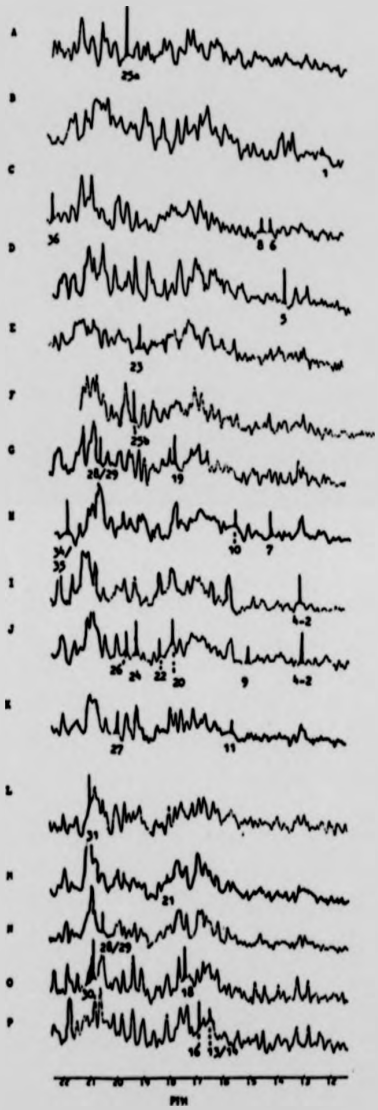

Fig. 3.6 (A-P) Same as Fig. 3.4(a-d) with selective ^{1}H irradiation at (A) -0.67 ppm, (B) -0.26 ppm, (C) -0.01 ppm, (D) 0.17 ppm, (E) 0.22 ppm, (F) 0.43 ppm, (G) 0.64 ppm, (H) 0.72 ppm, (I) 0.86 ppm, (J) 0.91 ppm, (K) 1.04 ppm, (L) 1.14 ppm, (M) 1.20 ppm, (N) 1.27 ppm, (O) 1.38 ppm, (P) 1.55 ppm. The main collapsed multiplets in the individual spectra are shadowed.

TABLE 3.2 ^{13}C NMR Chemical Shifts and Assignments of some Methyl Carbon Resonances in HEW Lysozyme[a]

	^{13}C NMR		^{1}H NMR		
Peak No.[b]	$\delta(^{13}C)$ (ppm)[c]	Resonance Assignment[d]	$\delta(^{1}H)$ (ppm)[e,f]	Sample Conditions[g]	Additional Evidence for Assignment
1	12.11	ile-98 $C^{\gamma 2}$	-0.26 (B)[j]	pD 5.0, 50°C	Differential line broadening; I_2 treatment; NAG binding
2 }	13.0-	?ile-78 $C^{\gamma 2}$	0.86 (I)[k]	pD 5.0, 50°C	
3 }	13.05	and another ile methyl group			
4	13.05	?ile-55 $C^{\gamma 2}$ or C^{δ}	0.91 (J)	pD 5.0, 50°C	Pr^{3+} binding
5	13.61	ile-88 C^{δ}	0.17 (D)[j]	pD 3.2, +NAG, 45°C	
6	14.05	ile-98 C^{δ}	-0.01 (C)[j]	pD 5.0, 50°C	Differential line broadening; I_2 treatment; NAG binding
7	14.28	ile C^{δ} or $C^{\gamma 2}$	0.72 (H)	pD 3.2, +NAG, 45°C	
8	14.37	met-105 C^{ε}	-0.01 (C)[j]	pD 5.0, 50°C	I_2 treatment; NAG binding
9	15.05	ile-58 $C^{\gamma 2}$	0.91 (J)[k]	pD 5.0, 50°C	NAG binding
10	15.73	ile-88 $C^{\gamma 2}$	0.72 (H)[l]	pD 3.2, +NAG, 45°C	pH titration (pKa = 5.7)

/11

11	15.73	ile-58 C^{δ}	1.04 (K)[k]	pD 5.0, 50°C	
12	16.08	?ile-55 $C^{\gamma 2}$ or C^{δ}	–[h]	pD 5.0, 50°C	Pr^{3+} binding
13 14	16.49	met-12 C^{ϵ}	1.55 (P)[j]	pD 5.0, 50°C	Photooxidation[i]
16	16.86	ala-95 C^{β}	1.55 (P)[j]	pD 5.0, 50°C	
18	17.43	ala-110 C^{β}	1.38 (O)[j]	pD 5.0, 50°C	
19	17.72	ala-107 C^{β}	0.64 (G)[j]	pD 5.0, 50°C	
20	17.89	?val-$C^{\gamma 1}$ or $C^{\gamma 2}$	0.91 (J)	pD 5.0, 50°C	
21	17.97	?val-99 $C^{\gamma 2}$	1.20 (M)[j]	pD 5.0, +$(NAG)_3$, 40°C	
22	18.37	?val $C^{\gamma 1}$ or $C^{\gamma 2}$	0.91 (J)	pD 5.0, 50°C	
23	18.78	leu-56 $C^{\delta 1}$	0.22 (E)[j]	pD 3.2, 50°C	Pr^{3+} binding
24	19.25	?val $C^{\gamma 1}$ or $C^{\gamma 2}$	0.91 (J)	pD 5.0, 50°C	
25(a)	19.62	leu-17 $C^{\delta 2}$	-0.67 (A)[j]	pD 3.2, +NAG, 45°C	
25(b)	19.62	val-92 $C^{\gamma 2}$	0.43 (F)[j]	pD 5.0, 50°C	
26	19.63	?val $C^{\gamma 1}$ or $C^{\gamma 2}$	0.91 (J)	pD 5.0, 50°C	
27	19.93	val-109 $C^{\gamma 1}$	1.04 (K)[j]	pD 5.0, 50°C	
28 or 29	20.53	val-99 $C^{\gamma 1}$	1.27 (N)[j]	pD 5.0, +$(NAG)_3$, 40°C	
28 or 29	20.53	val-92 $C^{\gamma 2}$	0.64 (G)[j]	pD 5.0, 50°C	

/30

30	20.94-20.96	?main thr C^{β}	1.38 (O)	pD 5.0, 50°C
31	21.00	?leu $C^{\delta 1}$ or $C^{\gamma 2}$	1.14 (L)	pD 5.0, 50°C
34 or 35	22.03	?leu $C^{\delta 1}$ or $C^{\delta 2}$	0.72 (H)	pD 3.2, +NAG, 45°C
36	22.26	leu-8 $C^{\delta 1}$	-0.01 (C)[j]	pD 5.0, 50°C

[a] The corresponding ^1H NMR chemical shifts, $\delta(^1H)$, used in the single proton-frequency decoupling experiments are also indicated

[b] Peak numbers are those shown in Fig. 3.4

[c] ^{13}C chemical shifts are relative to external Me_4Si; they were obtained under the conditions described in column 5

[d] Less definite assignments are indicated by (?)

[e] ^1H chemical shifts are relative to external Me_4Si; they were obtained under the conditions described in column 5

[f] The letters in parenthesis are those shown in Fig. 3.5

[g] These conditions were used in order to minimise overlap in the ^1H spectrum

[h] Single proton-frequency decoupling experiments did not give conclusive results

[i] Photooxidation experiments indicated a met methyl group at this chemical shift although the analysis was hampered by another methyl group resonating at this same frequency

[j] From Poulsen *et al.* (1980) and references therein

[k] From Delepierre, personal communication

[l] This work

3.4.3.1.2 Identification of the Methyl Resonances by the pD Titration Method

Some ^{13}C methyl and methylene resonances in proteins have previously been assigned by observing parallel titration characteristics in the methyl and carboxylate carbon resonances of the same amino acid residues (Richarz and Wüthrich, 1978).

The carboxylate terminal residue of lysozyme is leu-129. The carboxylate carbon resonance of this residue has been assigned in the ^{13}C spectrum based on its pKa value of 3.1 (Shindo *et al.*, 1978). Therefore, at least two leu methyl resonances would be expected to titrate with this pKa value. Inspection of the methyl resonance region of the ^{13}C spectrum reveals no obvious evidence of the parallel titration of these resonances below pD 5.0.

The leu methyl resonances appear in a region containing many overlapping peaks. It is, therefore, difficult to monitor the very small pD-dependent shift changes.

The observation of differential line broadening in resonances 1 and 6 above pD 5.0 provides the initial assignment of these resonances to the methyl groups of ile-98.

pD titration of the lysozyme-NAG complex affords the assignment of the ile-88 $C^{\gamma 2}$ resonance. This residue titrates with the same pKa value as his-15 (pKa = 5.7) (Perkins and Dwek, 1980, and references therein).

3.4.3.1.3 Identification of the Methyl Resonances by Chemical Modification

The addition of an equimolar amount of N-bromosuccinimide (NBS) to HEW lysozyme causes the selective oxidation of trp-62, yielding oxindolealanine-62-lysozyme (Norton and Allerhand, 1976(b) and references therein). A comparison of the spectra of NBS-modified and native lysozyme (Fig. 3.7) indicates very little change in the upfield methyl resonances (12.0 ppm-17.0 ppm). Resonances 2-4 are very sensitive to small variations in temperature and pH. Their shift changes in Fig. 3.7(b) are perhaps due to ionic strength- and temperature-dependent perturbations rather than to the specific modification of trp-62. This is only a possible explanation.

The specific oxidation of trp-108 occurs on treatment of lysozyme with half an equivalent of I_2 at pH 5.5 (that is, a 1:1 ratio of protein to I_2) (Norton and Allerhand, 1976(a)). The modified trp-108 residue becomes the glu-35 ester of δ-hydroxytryptophan. The expanded methyl region of the spectrum of the modified protein is shown in Fig. 3.7(c). Many upfield methyl resonances are perturbed in both chemical shift and linewidth. The methyl groups of interest, ile-98 (peaks 1 and 6) and met-105 (peak 8) are shifted downfield (Appendix I): the ile-98 $C^{\gamma 2}$ resonance by 0.09 ppm, ile-98 C^{δ} by 0.12 ppm and met-105 C^{ε} by 0.25 ppm. The ile-98 C^{δ} resonance is hidden under the broad signal at 14.38 ppm.

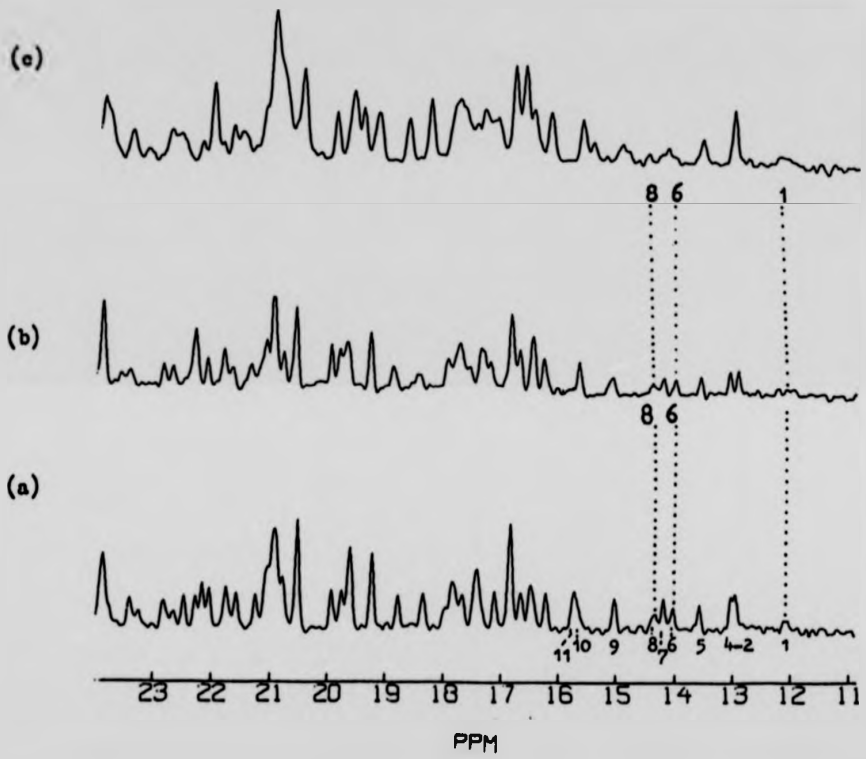

Fig. 3.7 Spectral region from 11.0 ppm to 24.0 ppm of proton-decoupled ^{13}C NMR spectrum of chemically modified lysozyme.
(a) Native protein, pD 5.2, 50°C
(b) NBS-treated protein, pD 5.4, 50°C
(c) I_2-treated protein, pD 5.4, 50°C

3.4.3.1.4 Identification of the Methyl and Aromatic Resonances by the Binding of Paramagnetic Species

The feasibility of using paramagnetic shift probes such as Pr^{3+} for assigning the ^{13}C resonances of lysozyme is explored. The shifts induced by La^{3+} are used as diamagnetic corrections in the present study. Non-specific shift changes of up to 0.05 ppm are observed. Although some of these shift perturbations cannot be used for making specific assignments, they can confirm or enhance the existing tentative assignments.

The ^{13}C resonance at 18.86 ppm (peak 23, Fig. 3.8(a)) has been tentatively assigned to leu-56 $C^{\delta 1}$ using the method described in Section 3.4.3.1.1. In the presence of Pr^{3+}, this resonance experiences an upfield shift of 0.30 ppm (Fig. 3.8(b)). This significant shift change can be attributed to a paramagnetic shift caused by the bound Pr^{3+} ion. The assignment of the leu-56 $C^{\delta 1}H_3$ resonance in the ^1H spectrum was originally made on the basis of paramagnetic shifts (Campbell *et al.*, 1975).

Peak 12 and one component of the multiplet peak 2-4 shift downfield by 0.24 ppm and 0.26 ppm respectively. Both these peaks have been attributed to ile methyl carbon centres using the method described in Section 3.4.3.1.1. The ile residue closest to the main lanthanide binding sites of lysozyme is ile-55 (Perkins *et al.*, 1981(b)) (Appendix V and Appendix VII(b)). This means that peak 12 and one component of peak 2-4 should each be tentatively assigned to the two ile-55 methyl

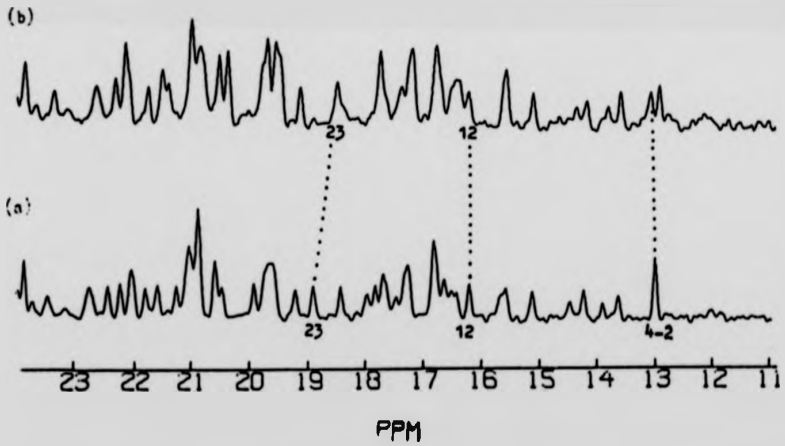

Fig. 3.8 Effect of $LaCl_3$ and $PrCl_3$ on the resonances in the spectral region from 11.0 ppm to 24.0 ppm of the proton-decoupled ^{13}C NMR spectrum of lysozyme in D_2O, pD 5.0, 40°C.
(a) + 45 mM $LaCl_3$
(b) + 45 mM $PrCl_3$

carbon atoms. Due to insufficient data, these assignments are not absolute.

In the region of the tyr C^{δ} (131.5 ppm-132.5 ppm) and tyr C^{ζ} (154.0 ppm-157.0 ppm) resonances, peaks M2 and N3 shift downfield by 0.72 ppm and 0.48 ppm respectively (Fig. 3.9(i) and Fig. 3.9(ii)). The computed distances from the bound lanthanide ion to the nonprotonated aromatic carbon atoms are available (Allerhand *et al.*, 1977) and the data for the tyr residues are shown in Table 3.3.

TABLE 3.3 Values of the sixth power of the distance (r^6) from nonprotonated tyr carbon atoms of HEW lysozyme to the bound Gd^{3+} ion[a]

Carbon Atom	r^6 (Å)
Tyr-53 C^{ζ}	4.3
Tyr-23 C^{ζ}	23.3
Tyr-20 C^{ζ}	84.2

[a]Extracted from Allerhand *et al.* (1977)

From Table 3.3, it can be seen that tyr-53 is closest to the bound lanthanide ion. Therefore, peak M2 should be assigned to the $C^{\delta 1}$ and $C^{\delta 2}$ centres of tyr-53 and peak N3 to its C^{ζ} centre. The assignment of peak M2 to the δ-carbon atoms of tyr-53 concurs with the results of Dill and Allerhand (1977).

3.4.3.1.5 Identification of the Methyl Resonances by the Binding of Diamagnetic Ligands: NAG and $(NAG)_3$

There is a general decrease in the linewidth

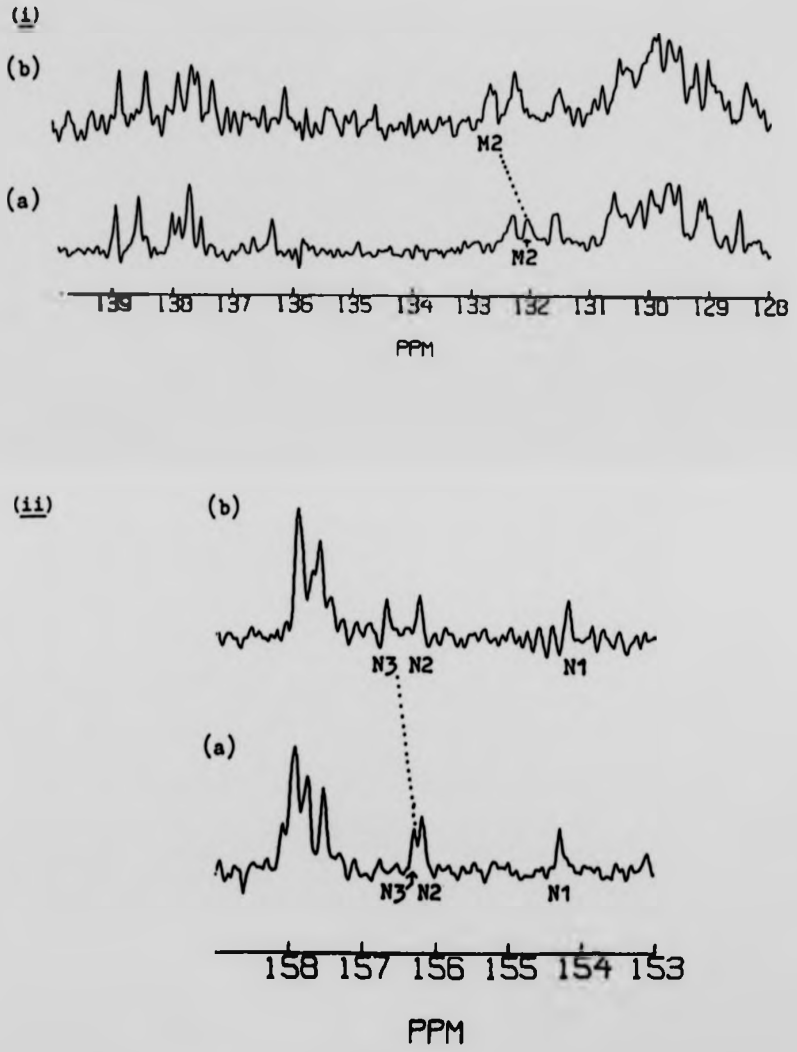

Fig. 3.9 Effect of $LaCl_3$ and $PrCl_3$ on the resonances in the proton-decoupled ^{13}C NMR spectrum of lysozyme in D_2O, pD 5.0, 40°C.
(i) 128.0 ppm to 140.0 ppm, and
(ii) 153.0 ppm to 159.0 ppm
(a) + 45 mM $LaCl_3$
(b) + 45 mM $PrCl_3$
M2, C^{δ} resonances of tyr-53; N1, tyr-23 C^{ζ};
N2, tyr-20 C^{ζ}; N3, tyr-53 C^{ζ}.

of the resolved methyl resonances when either N-acetyl-glucosamine (NAG) or the trimer, $(NAG)_3$, is added to the protein solution at pD 3.2 or pD 5.0. The difference in spin-lattice relaxation time T_1, between the free protein and the NAG-bound protein is not significant (this work). That is, the overall protein conformation (and the correlation time, τ_R) remains the same. The change in linewidth is attributed to the elimination of minor multiple conformations both at pD 3.2 and pD 5.0. Intermediate exchange between these multiple conformations would be expected to broaden the resonances in the ^{13}C spectrum.

3.4.3.1.5.1 The Lysozyme-NAG Complex Spectrum

Analyses of the methine (α-carbon) and methylene regions of the spectrum are hampered by poor resolution and the poor S/N ratio of the spectrum. From the difference-spectrum, shift changes can be seen to be present in the α-carbon region. This shows that conformational changes are present which involve the backbone carbon atoms.

In the methyl resonance region, the tentatively assigned resonances of ile-98 $C^{\gamma 2}$ (peak 1), ile-98 C^{δ}(peak 6), met-105 C^{ε} (peak 8), leu-56 $C^{\delta 1}$ (peak 23) and of two ile methyl group (peaks 7 and 9) are significantly perturbed (Fig. 3.10). The tentatively assigned ala methyl resonances are also perturbed. The val methyl resonances appear to undergo smaller shift changes when compared with the other assigned methyl resonances.

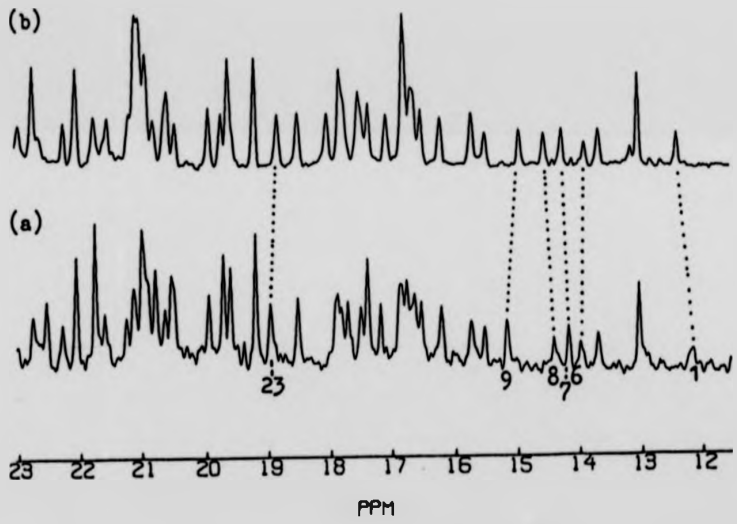

Fig. 3.10 Methyl region of the proton-decoupled ^{13}C NMR spectrum of lysozyme (6 mM in D_2O) in the presence of N-acetylglucosamine (NAG) at 45°C, pD 3.2.
(a) free protein
(b) + 100 mM NAG

3.4.3.1.5.2 The Lysozyme-$(NAG)_3$ Complex Spectrum

Fig. 3.11 shows the chemical shifts of the methyl resonances in the absence and presence of the amino sugar inhibitors NAG and $(NAG)_3$ at pD 5.0. Only the most significantly perturbed and tentatively assigned peaks are discussed here. Peaks 1 and 9 continue to shift further downfield and upfield respectively, in a steady manner when $(NAG)_3$ is added to the lysozyme solution. In contrast, peak 8 shifts downfield by 0.2 ppm in the presence of NAG and upfield by 0.08 ppm in the presence of $(NAG)_3$. Peak 23 is perturbed to a greater extent by NAG than by $(NAG)_3$.

As far as the nonprotonated aromatic signals are concerned, the results obtained here concur with those obtained by Allerhand *et al.* (1977). Both NAG and the trimer significantly perturb the C^{γ} shifts of trp-62 and trp-63, and the $C^{\epsilon 2}$ shift of trp-108. The most notable difference in effects when the two types of amino sugars are used is in the linewidth of the peak at 108.67 ppm. This peak has been assigned to the C^{γ} atoms of trp-28 and trp-111. Whilst the linewidth of the trp-123 C^{γ} resonance at 111.80 ppm is similar in both complexes, there appears to be substantial broadening in the coalesced trp-111/trp-28 C^{γ} resonance in the lysozyme-$(NAG)_3$ complex. It is difficult to ascertain precisely the contribution of each of these two groups to the broadening effect. The reason for this broadening may perhaps help to explain the perturbations seen in the aliphatic region of the spectrum.

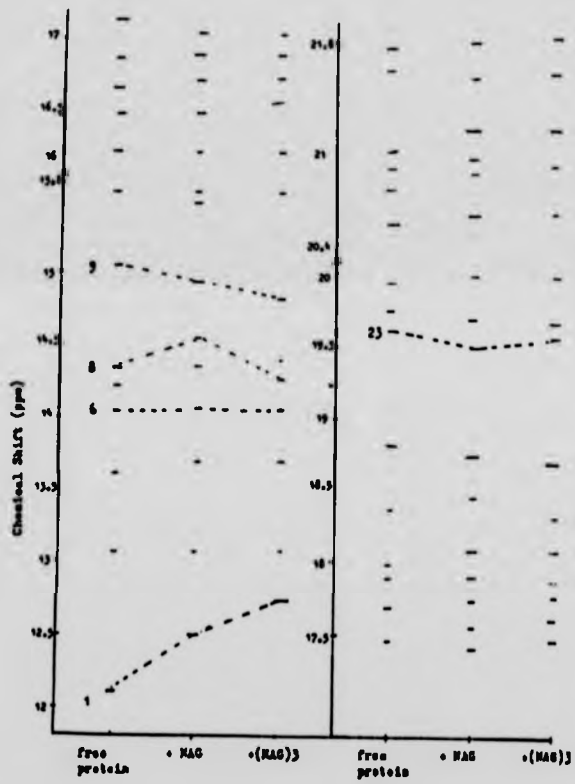

Fig. 3.11 Chemical shifts of methyl carbon resonances of lysozyme (6 mM in D_2O) in the absence and presence of either NAG (100 mM) or $(NAG)_3$ (12.5 mM), pD 5.0, 40°C.

3.4.3.2 Discussion

3.4.3.2.1 Heteronuclear Decoupling using Single Proton-Frequency Irradiation

The conditions* used in the experiments are as shown in Table 3.2. These were chosen in order to minimise the chances of coincidental overlap in the ^{1}H NMR spectra. Because of the inherently large spread of chemical shifts in the ^{13}C spectrum, changes in the conditions to resolve the ^{1}H resonances may not give rise to significant shift perturbations in the ^{13}C spectrum.

It is apparent from Table 3.2 that the identification of corresponding ^{1}H and ^{13}C resonances using heteronuclear double resonance experiments on lysozyme is mainly limited by the separation of the individual ^{1}H NMR lines. Even at the operating frequency used in these studies, many of the ^{1}H chemical shift differences are too small to establish one-to-one correspondences between the ^{1}H and ^{13}C methyl resonances.

---

*

(a) pD 5.0, 50°C: This condition was used for convenience as literature values for the shifts are quoted for this pD at 57°C. The spectra obtained showed little thermal shift perturbation between 50°C and 60°C for many of the methyl resonances.

(b) pD 3.2, 50°C: At this pD and temperature, the ^{1}H methyl resonance of ile-88 C^{δ} appears as a well-resolved triplet at 0.17 ppm. This resonance is shifted upfield from the broad overlapping signal at 0.24 ppm.
At this pD, the ^{13}C resonance of ile-98 $C^{\gamma 2}$ is sharper and more intense than at higher pD values.

(c) Complexes with NAG and $(NAG)_3$: The ^{13}C spectra of lysozyme-inhibitor complexes have improved S/N ratio compared with the free-lysozyme spectrum. The linewidths of resonances in these spectra are narrower than in the spectra of the free protein. These two characteristics are particularly advantageous for ^{13}C NMR studies where long accumulation times are normally required. This heavy usage of spectrometer time has throughout been a deterrent for the extensive use of ^{13}C NMR in protein studies.

3.4.3.2.2 pD Titration Studies

The absence of parallel pD perturbations in the carboxylate carbon and the methyl ^{13}C resonances of the same residue is one example of the limitations of using ^{13}C chemical shift changes for making specific assignments (Section 3.6.2). However, the change of spectral characteristics with pD can sometimes be used for making tentative assignments. For example, the differential line broadening of resonances 1 and 6 provided the initial assignment of these resonances to ile-98 methyl groups. In the titration experiments using the lysozyme-NAG complex, resonance 10 appears to have a pKa value of 5.7, this resonance is therefore tentatively assigned to the ile-88 $C^{\gamma 2}$ resonance (Campbell *et al.*, 1975).

The differential line broadening of the ile-98 methyl resonances observed in this study concurs with the ^{1}H NMR results obtained in previous studies (Campbell *et al.*, 1975). At higher pD values and/or lower temperatures these methyl resonances are broadened substantially. The line broadening could be attributed to the existence of different conformational forms with an intermediate exchange rate between them.

In the presence of bound NAG and $(NAG)_3$, the differential broadening of resonance 1 is reduced but not completely removed. The broadening of resonance 6 is virtually absent. The postulated restriction of conformational exchanges by the bound inhibitor does not appear to be sufficient to eliminate all broadening.

Instead, the pD dependence of the line broadening

of the ile-98 methyl resonances in the lysozyme-NAG complex strongly suggests that other types of exchange processes may also be occurring. The behaviour of a ^{13}C resonance can be affected by exchange between the protonated and deprotonated states. If the rate of this exchange is intermediate relative to the difference in the chemical shifts of the two states, a broad peak may be observed in the titrating range (Allerhand, 1979). Thus, pD-dependent chemical shifts and linewidth changes can be observed in the ^{13}C resonances of both the titrating residue (for example, carboxylic amino acid, his and tyr), and the residue in the vicinity of the perturbed group, that is, a through-space effect.

The pD-dependent line broadening of the ile-98 $C^{\gamma 2}$ resonance results from a through-space effect. As the broadening appears between pD 6 and pD 7 the titratable group involved is most likely to be glu-35 because the pKa value of this group is 6.2 (Campbell *et al.*, 1975).

In summary, the differential line broadening of the ile-98 methyl resonances arises from intermediate-rate protonation. The $C^{\gamma 2}$ atom, being nearer to the titratable site than the C^{δ} atom, has its resonance broadened to a greater extent.

3.4.3.2.3 Chemical Modification

The use of chemical modifications to assign the methyl resonances depends on the presence of ring current interactions within the protein. These interactions give rise to significant shifts in the ^{1}H spectrum of lysozyme

(Perkins and Dwek, 1980). The majority of the ring current shifts arise from trp rings. Chemical modifications of the individual aromatic groups can cause shift changes in those methyl and methylene proton resonances which are significantly influenced by these aromatic groups. In lysozyme, trp-62 does not contribute to the upfield methyl ^{1}H resonances. Trp-108 and trp-63 contribute to the ring current shifts of the ile-98 methyl groups (and of the methylene groups).

Formation of the oxindolealanine-62-lysozyme derivative does not appear to cause significant shift changes in the upfield methyl region of the ^{13}C spectrum. This confirms that the methyl resonances of ile-98 are not under the influence of trp-62.

Lysozyme treated with I_2 under the experimental conditions used here results in the specific formation of the glu-35-trp-108 ester. The extensive perturbations of the shifts and linewidths of upfield resonances illustrate the difficulties in using chemical modifications to yield specific assignments. These problems are discussed in Section 3.6. The resonances of interest, met-105 C^{ε}, ile-98 C^{δ} and ile-98 $C^{\gamma 2}$, are all perturbed (Appendix I).

The results show that shift perturbations arising from chemical modification of specific nearby residues are useful for confirming assignments made by other methods, rather than for establishing new assignments.

3.4.3.2.4 The Binding of Paramagnetic Species

In these experiments, the assignments are made by correlating the observed shift perturbations of the resolved resonances with the known nature of the lanthanide binding site(s) in lysozyme (Allerhand *et al.*, 1977). Although this method can be used for making and/or confirming assignments, proper interpretation of all the shift changes observed cannot be made for the reasons discussed in Section 3.6.

3.4.3.2.5 The Binding of Diamagnetic Ligands: NAG and $(NAG)_3$

^1H NMR studies of the binding of NAG to lysozyme have shown that there are two subsites, C and E, to which NAG can bind (Perkins *et al.*, 1981(a)). The binding constant for subsite C, however, was found to be about eight times that for subsite E when βMeNAG was used as the inhibitor. Three trp residues flank subsite C while there are no trp residues around subsite E (Appendix VII(a)). Therefore, the major conformational changes observed by ^1H NMR were attributed almost entirely to the binding at subsite C.

In addition, using ^1H NMR two types of changes are defined when either NAG or $(NAG)_3$ is bound to lysozyme (Dobson and Williams, 1975). These are:

(a) Perturbations in the chemical shifts of resolved resonances of groups near the active site cleft (trp-108, trp-62, trp-63, ile-98 and met-105).

(b) A reduction in line broadening, this being attributed to the elimination of multiple conformations.

In previous ^{13}C NMR studies, the only chemical shift changes which have been observed are those of trp-108 $C^{\varepsilon 2}$, trp-62 C^{γ} and trp-63 C^{γ} (Allerhand *et al.*, 1977).

Although in the published ^{1}H and ^{13}C NMR studies discussed above the shift changes are consistent with the modes of binding of the inhibitors, they have not been put to use to yield any specific assignments. In the present study, the resolved methyl regions of the ^{13}C spectra of lysozyme-sugar complexes are investigated in the hope of making some specific assignments.

3.4.3.2.5.1 Assignment of ile-58 $C^{\gamma 2}$ Resonance

Peaks 9 and 11 are tentatively assigned to ile-58 $C^{\gamma 2}$ and ile-58 C^{δ} respectively by the method of single proton-frequency irradiation (Section 3.4.3.1.1). These assignments are tentative as the corresponding assignments in the ^{1}H NMR spectrum have yet to be confirmed (Delepierre, personal communication). The addition of NAG (and $(NAG)_3$) causes a significant upfield shift in peak 9. Peak 11 appears to be unperturbed.

The ile-58 $C^{\gamma 2}$ atom is near to (i) the binding site C, and (ii) the hydrogen bond between the CO group of the acetamide chain and the NH proton of asp-59 (Appendix VI(a)). Perkins *et al.* (1978) in their crystallographic studies of the lysozyme-NAG complex,

have shown that part of the ile-58 residue is within 4 Å of the O(7) atom of NAG. This makes the ile-58 $C^{\gamma 2}$ atom a favourable candidate for the assignment of peak 9. The shift perturbation could be due to interactions between the ile-58 side-chain and the bound sugar residue.

3.4.3.2.5.2 The ile-98, met-105 and leu-56 Methyl Resonances

Table 3.4 shows the shift perturbations of the ile-98, met-105 and leu-56 methyl resonances on NAG binding.

Perkins and Dwek (1980) showed from their results that the methyl groups of ile-98, met-105, and leu-56 are under the influence of ring current effects from the trp rings. The ring current effects of these hetero-aromatic rings are shown in summary in Table 3.5.

TABLE 3.4 Chemical Shift Changes of Ile-98, Met-105 and Leu-56 in HEW Lysozyme Resulting from NAG Binding[a]

Resonance Assignment[b]	Δ [c]
Ile-98 C^{δ}	-0.09
Ile-98 $C^{\gamma 2}$	0.21
Met-105 C^{ϵ}	0.16
Leu-56 $C^{\delta 1}$	-0.13

[a] All solutions contained HEW lysozyme (7 mM), and NAG (100 mM); pD 3.2, 40°C

[b] This work

[c] Chemical shift changes on NAG binding: ppm, positive shifts to low field

TABLE 3.5 Calculated ^{1}H Chemical Shifts of Ile-98, Met-105 and Leu-56 Methyl Groups in HEW Lysozyme Deduced using Tetragonal Coordinates[a]

Resonance Assignment	Shift Calculated from Tetragonal Coordinates
Ile-98 $C^{\delta}H_3$	0.99 (1.10, trp-63)
Ile-98 $C^{\gamma 2}H_3$	1.34 (0.88, trp-108; 0.47, trp-63)
Met-105 $C^{\epsilon}H_3$	2.21 (0.90, trp-28; 0.80, trp-111; 0.30, trp-108; 0.15, tyr-23)
Leu-56 $C^{\delta}H_3$	0.60 (0.72, trp-108; -0.21, trp-28)

[a]From Perkins and Dwek (1980)

In solution, two anomers of NAG, the α and β anomers, normally exist in equilibrium. Using x-ray diffraction, both these anomers of NAG have been shown to bind to HEW lysozyme at site C but in two slightly different orientations, one of which corresponds to the binding of the β-anomer (termed subsite C-β) and the other of which corresponds to the binding of the α-anomer (termed subsite C-α) (Blake *et al.*, 1967; Imoto *et al.*, 1972) (Appendix VI(a)). Perkins *et al.* (1981(a)) also postulated that when β-NAG binds to subsite C-β, the trp-63 heteroaromatic ring moves by 7° towards subsite C (Appendix VI(b)). On the other hand, trp-63 was postulated not to be involved in the binding of α-NAG at subsite C-α.

At pD 3.2, the α- and β-anomers bind with equal strength (Perkins *et al.*, 1981(a)). The movement of the trp-63 residue will alter its ring current influence on the ile-98 C^{δ} methyl group. The upfield shift of the ile-98 C^{δ} resonance, as observed in this study using ^{13}C

NMR can hence, in part, be explained by this conformational change.

The ile-98 $C^{\gamma 2}$ methyl group is nearer to trp-108 than to the trp-63 aromatic ring (Appendix VI(a)). When either α- or β-NAG binds to lysozyme, the groove of the active site cleft is postulated to tighten altering the internal structure of the protein (Perkins *et al.*, 1981(a) and references therein). In the present ^{13}C NMR studies, this conformational change is seen as significant shift perturbations of both the ile-98 $C^{\gamma 2}$ and the trp-108 $C^{\epsilon 2}$ resonances. In addition, the NAG-induced shift perturbations of the met-105 C^{ϵ} and the leu-56 $C^{\delta 1}$ resonances can be explained by the movement of the trp-108 ring (Appendix VI(a)).

3.4.3.2.5.3 The Lysozyme-$(NAG)_3$ Complex Spectrum

$(NAG)_3$ binds to subsites A, B and C, all three being strong binding sites (Blake *et al.*, 1967; Dahlquist and Raftery (1968)). Dobson and Williams (1975), in ^{1}H NMR studies, concluded that the proton resonance shifts of the protein in the presence of both NAG and $(NAG)_3$ are similar. The authors showed that only one important site, subsite C, common to the binding of both types of ligand, is involved in inducing changes in the protein structure.

In the present study a comparison is made between the ^{13}C spectra of NAG- and $(NAG)_3$-lysozyme complexes. The signals observed from this type of protein-ligand mixture are exchange-averaged resonances and are

dependent on the total concentration of each species present in solution. Thus, if the only difference between the binding of NAG and of the trimer to lysozyme is the binding constant of each ligand, and if the binding constant of $(NAG)_3$ to lysozyme is higher than that of NAG, then the ligand-induced shift effect observed in the $(NAG)_3$-enzyme complex must (i) be greater than or equal to that in the NAG-enzyme complex, and (ii) be in the same direction as in the NAG-enzyme complex. In other words, a steady pattern of change in the induced shifts should be observed when shifts are plotted for the free, the NAG-bound and the $(NAG)_3$-bound lysozyme. Any departure from this characteristic strongly suggests the participation of other factors in the binding of each ligand such as: variation in the mode of binding, in molecular conformation and in the number of binding sites. In previous studies (Allerhand *et al.*, 1977) increases in the shift perturbations of the trp-62 C^{γ} and trp-63 C^{γ} resonances in the ^{13}C NMR spectrum, on changing the inhibitor from the monomer to the trimer, have been attributed to an increase in the binding constant of $(NAG)_3$ rather than to the additional occupation of subsites A and B by the trimer.

The observations made in the present study, however, show some significant differences in shift changes between the two inhibitors. A closer examination of the proposed structure of the $(NAG)_3$-lysozyme complex reveals that the trisaccharide molecule is bound to the active site cleft with its terminal residue (C) making essentially the same contacts with the enzyme as a β-NAG molecule would (Appendix VII(a) and Appendix VII(b)). The second sugar

residue B makes many nonpolar contacts with the enzyme, these contacts being as yet undefined. There is also a probable hydrogen bond from the O(6) atom of the sugar residue B to the side-chain of asp-101. Residue A appears to be linked to the enzyme by more nonpolar interactions and by a hydrogen bond between its NH group and the side-chains of asp-101 (Imoto *et al.*, 1972) (Appendix VII(b)). There have been indications from x-ray crystallography that on binding the trimer, the trp-62 ring moves to a greater extent than on binding the monomer. This movement will narrow the cleft in the region in which the sugar residue B of the trisaccharide is bound.

The anomalous shift patterns of the met-105 C^{ε} resonance and some of the val methyl resonances, observed in the present study, indicate structural differences between the lysozyme-NAG and lysozyme-$(NAG)_3$ complexes. The presence of additional conformational changes, and of hydrophobic contacts between the inhibitor and subsite B may account for the shift characteristics of these resonances.

3.4.3.2.6 General Conclusions

The results expressed here are the first set of ^{13}C chemical shift data for the methyl carbon atoms of lysozyme in which a considerable number of resolved resonances are individually assigned.

For each group of residues the dispersion of the methyl ^{13}C chemical shifts by conformation-dependent

interactions in lysozyme is approximately 2-3 ppm for the five ile $C^{\gamma 2}$'s and C^{δ}'s, 1-2 ppm for the two met C^{ε}'s, 2-3 ppm for the val $C^{\gamma 1}$'s and $C^{\gamma 2}$'s, 1 ppm for ala C^{β}'s and 0.2 ppm for the thr C^{γ}'s. The shift scatter seems to be larger for the resonances of the hydrophobic residues than for the solvent-exposed ala and thr residues. In the hydrophobic groups, most of the methyl ^{13}C resonances do not coincide with the random coil values.

Comparison of the scatter of corresponding methyl ^{1}H and ^{13}C chemical shifts in lysozyme shows that the overall spread of the ^{13}C resonances is significantly larger. The many factors which govern ^{13}C chemical shifts include electric field, bond polarisation and ring-current effects. The precise contribution of each of these factors to the methyl ^{13}C shifts of proteins is currently being investigated in many laboratories.

3.4.3.3 Summary

Table 3.2 shows the assignments of the methyl carbon resonances made in this study.

The assignment of many of the ^{13}C methyl resonances relies on the definitive assignment of the corresponding ^{1}H resonances. The low r.f. power single proton-frequency irradiation method is most reliable when the resonances of the particular residue are well resolved in both the ^{1}H and ^{13}C NMR spectra.

The initial identification of the ile-98 methyl resonances is made feasible by the differential line

broadening of these resonances. The broadenings arise from the intermediate rates of exchange between different conformations.

The use of chemical modifications to assign the ^{13}C methyl resonances is dependent on the presence of ring current interactions between the reactive aromatic residue and the respective methyl group(s).

The observed perturbations in the ^{13}C NMR spectra are consistent with the modes of binding of the inhibitors and of lanthanide ions such as praseodymium. Some specific assignments of the protonated ^{13}C resonances are made or confirmed using shift perturbations when binding these probes.

Most of the experiments carried out required a knowledge of the x-ray structures of HEW lysozyme and the lysozyme-ligand complexes.

3.5 ASSIGNMENT OF THE ^{13}C SPECTRUM OF RIBONUCLEASE A

3.5.1 Materials and Methods

Methyl iodide (reagent grade) was obtained from the BDH Chemical Co.

The materials and methods for the preparation of NMR samples and for the acquisition of the ^{13}C and ^{1}H NMR spectra of ribonuclease described in Chapter 2 were used.

The different pD values were obtained by the addition of minute amounts of 0.05 M NaOD or 0.05 M DCl. No extra salt was added to the samples so that ionic

strengths were determined by the protein and the DCl or NaOD used for the titration.

Methylation of Met-29 in Ribonuclease A with Methyl Iodide

The reaction of RNase with methyl iodide was carried out essentially as described by Jaenck and Benz (1979). 100 ml of RNase (3 mg/ml) in 0.1 M KNO_3 was placed in a 100 ml volumetric flask and the pH value adjusted to between 4 and 5 using 6 M HCl. 1 g of methyl iodide was added and the flask tightly capped. The two-phase mixture was then stirred for 24 hours at room temperature (approximately 25°C) in the dark. At the end of this period the solution was lyophilised and the unreacted methyl iodide removed under vacuum. The solute was dissolved in 50 ml of water and dialysed against frequent changes of deionised water at 5°C for 12 hours to remove the KNO_3 present. The final solution was lyophilised and the ^{13}C spectrum of the reaction product obtained in the normal way.

3.5.2 Results and Discussion

3.5.2.1 Assignment of the Met-29 C^{ε} Resonance by Chemical Modification

Fig. 3.12 shows an expanded region of the ^{13}C NMR spectra obtained from a sample of [Methyl Met-29 C^{ε}] RNase and from native RNase. The resonance (peak 3) at 13.42 ppm is assigned to the met-29 C^{ε} atom. This signal is about 1.5 ppm upfield from the met C^{ε} carbon

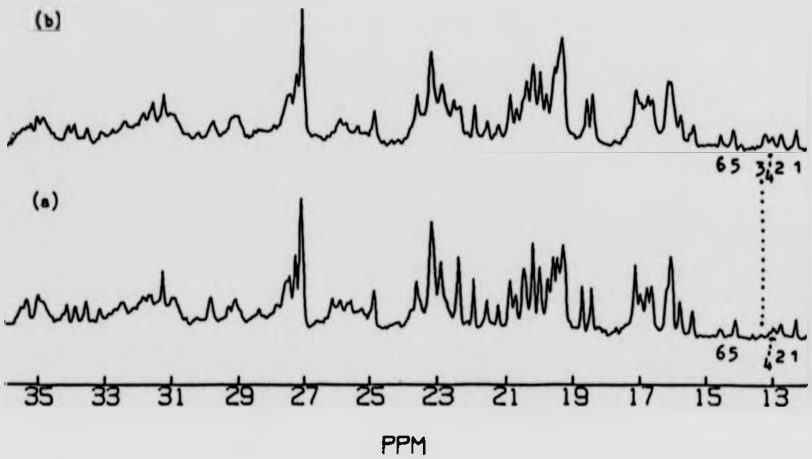

Fig. 3.12 Spectral region from 12.0 ppm to 36.0 ppm of the proton-decoupled ^{13}C NMR spectrum of native and chemically modified RNase.
(a) [Methyl Met-29 C^{ε}] RNase (5.6 mM in D_2O), pD 5.5, 25°C
(b) Native RNase (6 mM in D_2O), pD 5.5, 25°C
The numbers indicate the positions of individual methyl carbon resonances.

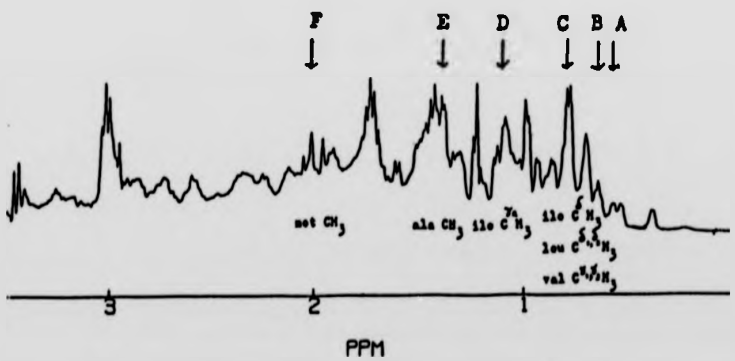

Fig. 3.13 Spectral region from 0 ppm to 3.5 ppm of ^1H NMR spectrum of RNase (6 mM in D_2O) at pD 3.2, 25°C.
The letters and arrows indicate the proton irradiation frequencies used in the selective decoupling experiments of Fig. 3.14.

in free methionine amino acid.

The broad signal further downfield (between 25.0 ppm and 26.0 ppm) is assigned to the $S^{+}(CH_3)_2$ group of the methylated protein. This signal corresponds well with the signal at 26.7 ppm which was assigned to the enriched $S^{+}(^{13}CH_3)_2$ group by Jaenck and Benz (1979). This is further supported by the evidence that the equivalent methyl groups in S-methylated methionine in the free amino acid form resonate at around 26.0 ppm (this work).

There are very few differences, in the region of the spectrum shown, between the native and the modified proteins apart from the two changes mentioned in the preceding paragraphs. Therefore, the gross conformation of the RNase molecule is essentially unchanged by the chemical modification of one particular residue in the protein.

3.5.2.2 Identification of the Corresponding Methyl ^{1}H and ^{13}C Resonances by Single Proton-Frequency Decoupling

Apart from the identification of the four met methyl resonances (Sadler *et al.*, 1974) no other methyl resonances in the ^{1}H NMR spectrum of RNase had been identified or assigned before the present work. The ^{1}H NMR spectrum contains very few well-resolved single methyl resonances even in the spectrum at 400 MHz. In the x-ray structure of native RNase, very few methyl groups are positioned so as to fall under the influence of

in free methionine amino acid.

The broad signal further downfield (between 25.0 ppm and 26.0 ppm) is assigned to the $S^{+}(CH_3)_2$ group of the methylated protein. This signal corresponds well with the signal at 26.7 ppm which was assigned to the enriched $S^{+}(^{13}CH_3)_2$ group by Jaenck and Benz (1979). This is further supported by the evidence that the equivalent methyl groups in S-methylated methionine in the free amino acid form resonate at around 26.0 ppm (this work).

There are very few differences, in the region of the spectrum shown, between the native and the modified proteins apart from the two changes mentioned in the preceding paragraphs. Therefore, the gross conformation of the RNase molecule is essentially unchanged by the chemical modification of one particular residue in the protein.

3.5.2.2 Identification of the Corresponding Methyl ^{1}H and ^{13}C Resonances by Single Proton-Frequency Decoupling

Apart from the identification of the four met methyl resonances (Sadler *et al.*, 1974) no other methyl resonances in the ^{1}H NMR spectrum of RNase had been identified or assigned before the present work. The ^{1}H NMR spectrum contains very few well-resolved single methyl resonances even in the spectrum at 400 MHz. In the x-ray structure of native RNase, very few methyl groups are positioned so as to fall under the influence of

strong ring current effects from the aromatic rings. These intrinsic ring currents, induced by the presence of a magnetic field, can produce large and relatively well-defined shifts in the ^{1}H NMR spectrum of a protein (Perkins and Dwek, 1980).

The aliphatic region of the 400 MHz ^{1}H NMR spectrum of RNase is shown in Fig. 3.13. The resonances are assigned to the chemical type of proton by comparing the ^{1}H spectrum of the native and denatured protein. Some of the ^{1}H methyl lines at 400 MHz are sufficiently well resolved to allow the corresponding ^{13}C NMR lines to be identified by selective ^{1}H-^{13}C heteronuclear double resonance experiments. The most positive identifications are made when the ^{13}C methyl resonances are also well resolved.

Fig. 3.14 (top trace) shows a selected region, from 12.0 ppm to 24.0 ppm, of the broadband proton noise-decoupled ^{13}C NMR spectrum of RNase. Fig. 3.14 (A-F) shows the ^{13}C spectra obtained using selective ^{1}H irradiation at the frequencies indicated by the arrows in Fig. 3.13. Sharp and narrow ^{13}C lines are observed for the resonances of the carbon centres attached to the protons which are irradiated. Not all the heteronuclear double resonance experiments carried out are shown in Fig. 3.14. For the ^{13}C methyl resonances, the chemical shifts of the corresponding ^{1}H resonances, and the other results which support the specific assignments made, are collated in Table 3.6. One met C^{ε} and one ile C^{γ} resonance are hidden under the major ala C^{β} resonance.

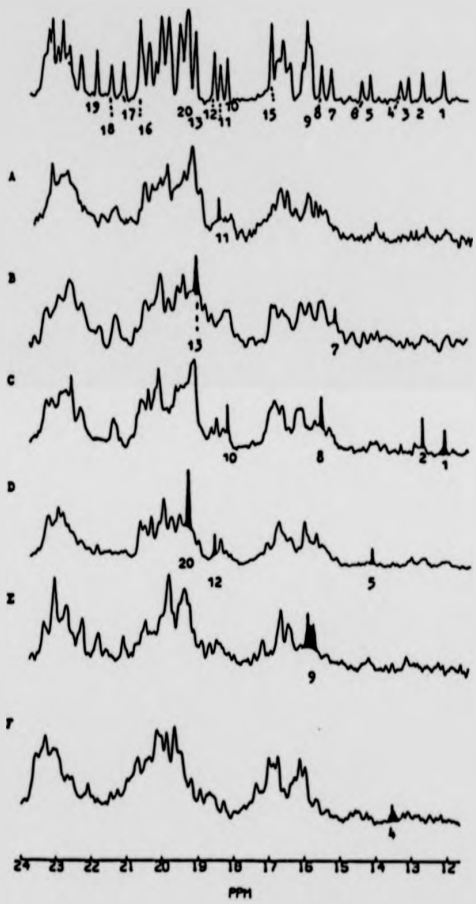

Fig. 3.14 (Top Trace) Spectral region from 12.0 ppm to 24.0 ppm of the proton-decoupled ^{13}C NMR spectrum of RNase, (6 mM in D_2O) at pD 3.2, 25°C.
The numbers indicate the positions of individual methyl carbon resonances.
(A-F) Same as top trace, with selective ^{1}H irradiation at (A) 0.57 ppm, (B) 0.63 ppm, (C) 0.75 ppm, (D) 1.02 ppm, (E) 1.38 ppm, (F) 2.0 ppm.
The main collapsed multiplets in the individual spectra are shadowed.

TABLE 3.6 ^{13}C NMR Chemical Shifts and Assignments of some Methyl Carbon Resonances in Ribonuclease A[a]

	^{13}C NMR		^{1}H NMR	
Peak No.[b]	$\delta(^{13}C)$ (ppm)[c]	Resonance Assignment	$\delta(^{1}H)$ (ppm)[d,e]	Additional Evidence for Assignment[i]
1	ile C^{δ}	12.40	0.75 (C)	
2	ile-81 C^{δ}	13.03	0.75 (C)	Cytosine inhibitor binding
3	met-29 C^{ε}	13.42	-[f]	Methyl iodide treatment; peak intensity
4	met-13 C^{ε}	13.65	2.0 (F)	pD titration; urea binding; phosphate ion binding; peak intensity
5	ile-106 $C^{\gamma 2}$	14.53	1.02 (D)	Cytosine inhibitor binding
6	met-30 C^{ε}	14.76	-[f]	Cytosine inhibitor binding; peak intensity
7	ile $C^{\gamma 2}$	15.60	0.63 (B)	
8	ile C^{δ}	15.88	0.75 (C)	
9[h]	main ala C^{β}	17.08	1.38 (E)	
10	val $C^{\gamma 1}$ (or $C^{\gamma 2}$)[g]	18.59	0.75 (C)	Cytosine inhibitor binding
11	val $C^{\gamma 1}$ (or $C^{\gamma 2}$)[g]	18.78	0.57 (A)	Cytosine inhibitor binding
12	val-47 $C^{\gamma 1}$ (or $C^{\gamma 2}$)	18.96	1.02 (D)	pD titration; urea binding; phosphate ion binding; cytosine inhibitor binding
13	val-47 $C^{\gamma 2}$ (or $C^{\gamma 1}$)	19.47	0.63 (B)	Urea binding; cytosine inhibitor binding
20	val $C^{\gamma 1}$ (or $C^{\gamma 2}$)	19.68	1.02 (D)	

/a

[a] The corresponding ^1H NMR chemical shifts, $\delta(^1H)$, used in the single proton-frequency decoupling experiments are also indicated

[b] Peak numbers are those shown in Fig. 3.14

[c] ^{13}C chemical shifts are relative to external Me_4Si; pD 3.2, 25°C

[d] ^1H chemical shifts are relative to external Me_4Si; pD 3.2, 25°C

[e] The letters in parenthesis are those shown in Fig. 3.13

[f] No single proton-frequency decoupling experiments were carried out

[g] The likely candidates include val-108 and val-118 (Chapter 6, Section 6.4.2.3)

[h] This peak number refers to a broad multiplet centred at around 17.08 ppm. One ile and one met methyl group also resonate at this frequency

[i] Methyl iodide treatment (Chapter 3, Section 3.5.2.1); pD titration (Chapter 3, Section 3.5.2.3); peak intensity (Chapter 3, Section 3.5.2.4); urea binding (Chapter 5, Section 5.4.1.2); cytosine inhibitor binding (Chapter 6, Section 6.4.2); phosphate ion binding (Chapter 6, Section 6.4.2).

The results in Fig. 3.14 and Table 3.6 show that by inspection of the ^{13}C spectrum obtained from each double resonance experiment, it is possible to identify some of the upfield methyl resonances unambiguously.

The assignments of peaks 10 and 12 are made by the examination of a series of ^{13}C spectra obtained using specific low r.f. power irradiation over a small region of the ^{1}H spectrum, that is, between 0.75 ppm and 1.02 ppm. The amino acid residues whose methyl resonances are most likely to occur between 0.75 ppm and 1.02 ppm in the ^{1}H NMR spectrum, are the val residues (Howarth and Lilley, 1978; Wütrich, 1976). Therefore, peaks 10 and 12 are tentatively attributed to the val methyl resonances.

The general assignment of the ala methyl C^{β} resonances (peak 9) is also obtained using the method described in the preceding paragraph. The important advantage here is that the main ala ^{1}H methyl resonances are at around 1.38 ppm. That is, they are well separated from the main methyl resonance regions of the other hydrophobic residues.

Thus, by visually comparing the ^{13}C spectra obtained from sequential specific ^{1}H irradiation, one may deduce the shifts of many ^{13}C methyl resonances.

3.5.2.3 Identification of the Methyl and Methylene Resonances by the pD Titration Method

As discussed in Section 3.4.3.1.2, pD titration has been used in the past to assign methyl and methylene resonances in the ^{13}C NMR spectra of proteins and peptides.

The carboxylate terminal residue of RNase is val-124. The pKa value for this terminal carboxyl carbon is 3.5 (Santoro *et al.*, 1979). At least one val methyl resonance can be expected to titrate with this pKa value. Examination of the ^{13}C NMR spectra of RNase between pD 2.8 and pD 5.0 did not reveal shift perturbation of the resolved peaks 10-12, which have been tentatively attributed to the val methyl groups. These resonances are sufficiently well separated for small shift perturbations in this low pD range to be observed. The absence of significant carboxylate-induced shifts in peaks 10-12 either suggests that peaks 10-12 do not arise from val-124 methyl groups or demonstrates that the parallel titration method is not reliable (see Section 3.6).

Fig. 3.15 shows a plot of the chemical shifts with varying pD values for resonances between 12 ppm and 20 ppm. Peaks 2, 4, 5, 6, 8, 10, 11 and 12 are those most significantly perturbed by increasing pD values. (The titration of peak 4 is determined by titration of [Methyl-Met-29 C^{ε}] RNase). The magnitudes of the shift perturbations lie between 0.2 ppm and 1.2 ppm. The pKa value of many of these resonances appears to be between 5.0 and 6.0.

The significant changes in chemical shift of the methyl carbon resonances with varying pD cannot be attributed merely to changes in the ionic strength of the protein solution. Spectra obtained at constant pD but with different concentrations of NaCl (up to 0.1 M) show very little chemical shift or linewidth change. The shifted

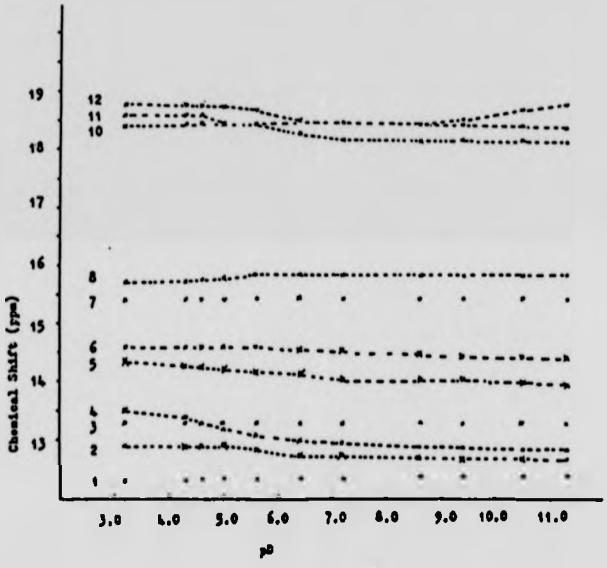

Fig. 3.15 Plot of chemical shifts of the methyl carbon resonances in the proton-decoupled ^{13}C NMR spectra of RNase as a function of pD, 25°C. The lines for peaks 2, 4, 5, 8, 10, 11 and 12 are best-fit theoretical titration curves. Except for peaks 4 and 12 a single pKa is assumed in each case.

resonances remain individually resolved throughout the pD titration range. This behaviour corresponds to a fast rather than to a slow exchange between the different conformations. The exchange rate is greater than 10^3 sec^{-1}.

The almost-linear pD-dependence of the shift of peak 4 at pD values below pD 8.0 can be attributed to the effect of small pKa transitions (Niu *et al.*, 1979). These transitions may include the titrations of asp-14 (approximate pKa = 4.33) (Santoro *et al.*, 1979), and of his-12 (pKa = 6.05) (Markley, 1975(a)) and the conformational transition (pKa = 4.0) of RNase (Benz and Roberts, 1973). Since the met-13 residue is positioned between the his-12 and asp-14 residues, peak 4 is tentatively assigned to the met-13 C^{ε} resonance.

The variations in chemical shift of the ile and met methyl resonances represented by peaks 2, 5 and 6, as shown in Fig. 3.15, cannot be a direct effect of changes in the protonation states of nearby groups. Except for the met-13 residue, neither ile nor met methyl atoms are close to titrating functional groups in the crystalline protein structure determined at pH 5.7 (Stanford, personal communication). Can variations in the chemical shifts of these ile and met methyl groups reflect conformational changes which the protein undergoes during catalytic activity? Markley (1975(a),(b)), Markley and Finkenstadt (1975) and Lenstra *et al.* (1979) have independently examined the conformational changes involved when his-12, his-119, his-48 and tyr-25 titrate, using ^1H NMR spectroscopy. From the titration characteristics of the his-48 residue,

a slow conformational transition between an acid-stable and a base-stable form with intermediate forms of the enzyme present, is believed to exist (Markley, 1975(b)). From their results, it is possible that the pD titration of RNase should give rise to conformational changes both locally and throughout the protein molecule. This conclusion is supported by x-ray crystallographic considerations.

The cleft and the active site of RNase have been defined in some detail by x-ray studies as summarised in Chapter 1 of this thesis (Carlisle *et al.*, 1974; Borkakoti *et al.*, 1982) (Appendix II(a) and Appendix II(b)). The shift changes in the ^{13}C resonances of the hydrophobic residues may be associated with the conformational changes in the active site cleft. An examination firstly of the pH effects on the protein conformation and secondly, of the postulated catalytic mechanism of RNase, suggest that it is not unreasonable to expect conformational changes in the active site cleft.

pH changes in general involve major alterations in electrostatic potential near the titratable groups. These pH changes will hence markedly alter the conformation of the enzyme including alteration to the catalytic site. This is especially true in hinged proteins like RNase in which the cleft region is not normally in fixed dimensions and in which the residues in and around the cleft region are highly mobile.

A conformational change in the active site region is probable at the pH range needed for enzymic activity. This is deduced from the proposed catalytic mechanism

of RNase which is shown below (Metzler, 1977).

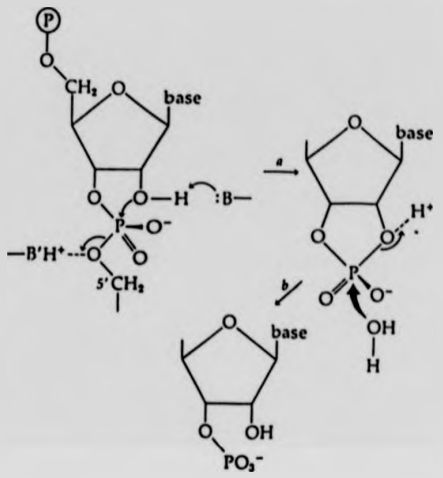

The basic his-12 group first deprotonates the 2'-hydroxyl proton and the acidic his-119 then donates a proton to the departing 5'-oxygen atom. The resulting intermediate form is a cyclic 2',3'-diphosphate which then undergoes hydrolysis by attack from the H_2O in step b to give the free 3'-nucleotide. Lys-41 is postulated to lie immediately above the two his residues, its positive charge being used to neutralise some of the negative charge on the oxygens of the phosphate group, making attack by the incoming nucleophile easier.

It is therefore clear that the his-12, his-119 and lys-41 residues must be placed in a conformation such that catalytic action can be most efficient. That is, the pH-dependence of the enzyme is regulated by a conformational change in the protein which may well include the active site

cleft. The pKa value of between 5.0 and 6.0 for the titration of the methyl resonances agrees well with the pKa range of 5.4 to 6.4 required for enzymic activity to take place. Hence, considering the location of the hydrophobic residues in relation to the active site, the pD-dependence of many of the val and ile residues can be accounted for by a conformational change in the active site.

In the ^{13}C spectrum of RNase at 100 MHz, the region from 25 ppm to 45 ppm is sufficiently well resolved to allow the pD dependence of individual groups of resonances to be observed. Two groups of resonances in this region are found to titrate in the alkaline pD range. The resonances between 27.0 ppm and 27.2 ppm and between 39.9 ppm and 40.1 ppm shift downfield at pD values higher than pD 9.0. By comparison with the chemical shifts of model peptides and amino acids (Howarth and Lilley, 1978), the resonances between 27.0 ppm-27.2 ppm are assigned to the methylene C^{δ} atoms of the ten lys residues of RNase, and those around 39.9 ppm-40.1 ppm are assigned to the methylene C^{ε} atoms of the same lys residues.

3.5.2.4 General Considerations

Before concluding this discussion on aliphatic ^{13}C methyl resonances, it is relevant to point out that the cumulative internal motions of the ile residues differ from those of the met residues as is evident from their relative peak intensities. The motion of a particular side-chain must be determined by its environment in the

protein molecule, as well as by the nature of the atoms present in the side-chain (Howarth and Lian, 1982; Wittebort *et al.*, 1979; Jones *et al.*, 1976). The replacement of a methylene group by a sulphur atom in the met side-chain provides a greater freedom of internal motion in this methyl group when compared with the ile methyl group. In addition, the rotation about the C^{α}-C^{β} bond in ile is hindered by the $C^{\gamma 2}$ methyl group. The spin-lattice relaxation time T_1 of the met methyl group will be longer than that of the ile methyl group. This will cause changes in peak intensities under conditions when saturation of the met methyl resonances is highly probable. Examples of such conditions are high temperature and short recycle time between each excitation pulse.

A comparison of the relative intensities of peaks 1 to 8 shows that the intensities of peaks 3, 4 and 6 are lower than those of peaks 1, 2, 5, 7 and 8 (Fig. 3.16). This difference in intensities is more marked at high temperatures and when short interpulse delay was used for the acquisition of the free induction delay. Peak 3 has been assigned to the met-29 C^{ε} resonance (Section 3.5.2.1). Therefore, by deduction, peaks 4 and 6 can be attributed to the met methyl resonances. Peaks 1, 2, 5 and 8 have been previously assigned to ile methyl resonances (Section 3.5.2.2).

The difference between the intensities of the met resonances is hence explained by a temperature-dependent phenomenon which affects the molecular dynamics of the two types of methyl carbon atoms.

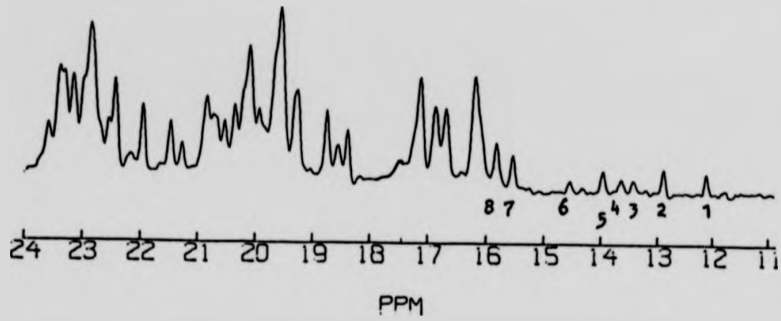

Fig. 3.16 Spectral region from 11.0 ppm to 24.0 ppm of the proton-decoupled ^{13}C NMR spectrum of native RNase (6 mM in D_2O) at pD 3.2, 44°C. The numbers indicate the positions of individual methyl carbon resonances.

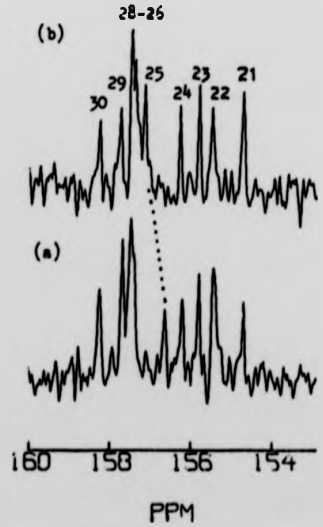

Fig. 3.17 Spectral region from 154.0 ppm to 160.0 ppm (tyr C^{ζ} and arg C^{ζ} resonances) of the proton-decoupled ^{13}C NMR spectrum of native and chemically modified RNase. The numbers in the top trace (b) indicate the positions of individual tyr C^{ζ} and arg C^{ζ} resonances.
(a) [Methyl Met-29 C^{ε}] RNase (5.6 mM in D_2O), pD 5.5, 25°C
(b) Native RNase (6 mM in D_2O), pD 3.2, 25°C.

3.5.2.5 Assignment of the Tyr C^{ζ} Resonances

The region between 154.0 ppm and 160.0 ppm contains the resonances of the C^{ζ} atoms of the four arg and six tyr residues (Fig. 3.17(b)). Peaks 21 to 25 and peak 30 are attributed to the tyr C^{ζ} atoms.

The assignment of peak 25 to tyr 25 C^{ζ} has been deduced from its pKa value of 5.9, a value lower than that of the other five tyr residues (Santoro *et al.*, 1979). In the present study, the treatment of RNase with methyl iodide causes an upfield shift of 0.45 ppm in peak 25 (at pD 3.2, 25°C) (Fig. 3.17(a)). An examination of the crystal structure of RNase reveals that the tyr-25 C^{ζ} centre is 4.34 Å away from the sulphur centre of met-29. The conversion of met-29 into methyl met-29 by methyl iodide alters the bulkiness of this amino acid side-chain and the oxidation state of its sulphur centre. Hence, its perturbation of the magnetic environment of the tyr-25 C^{ζ} atom is not surprising. The ^{1}H NMR spectrum has also revealed a shift change of the previously assigned tyr-25 C^{ε} resonance (Fig. 3.18(b)).

Peak 30 has been assigned to tyr-97 C^{ζ} on the basis of its high pKa value (Egan *et al.*, 1978). Attempts to obtain a more exact value of this pKa value in the present study failed because RNase was found to be very susceptible to alkaline denaturation (at pD > 12.0) even at low temperatures.

Peaks 21 and 24 have not previously been assigned to specific tyr residues. An attempt is made to assign

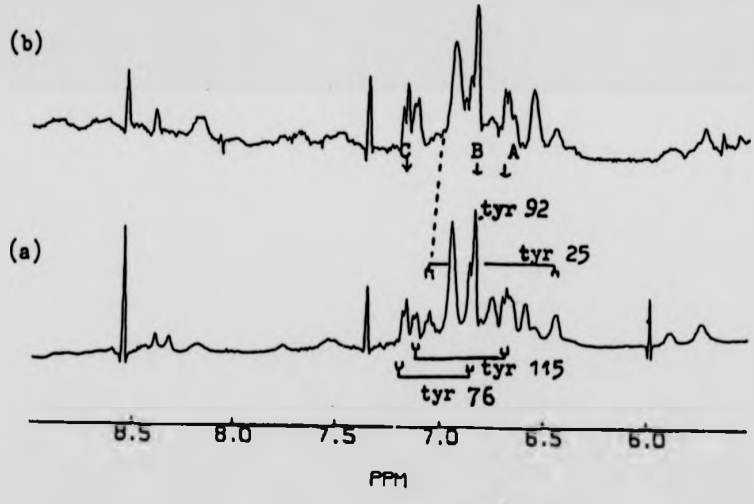

Fig. 3.18 Region of aromatic protons in the ^{1}H NMR spectrum of RNase.
(a) Native RNase (6 mM in D_2O), pD 3.2, 25°C
(b) [Methyl Met-29 C^{ε}] RNase, 5.6 mM in D_2O, pD 3.2, 25°C.
The letters and arrows in (a) indicate the proton irradiation frequencies used in the selective decoupling experiments of Fig. 3.19.

them here. Peak 22 shifts upfield slightly on increasing the temperature from 18.0°C to 25.0°C at pD 3.2. Thereafter, the chemical shift of this resonance remains constant with further increase in temperature. Its chemical shift above 25.0°C corresponds closely with the tyr C^{ζ} resonances of the unfolded protein. Peak 22 must arise from a tyr residue which normalises early in the thermal unfolding process. Above 25.0°C, this residue becomes exposed to the solvent and is not involved in any further known interactions in the protein. Tyr-92 is such a residue. Hence, peak 22 is assigned to tyr-92. This assignment is further supported by the results obtained in the specific proton irradiation experiments described in the next paragraph.

The specific assignments of the C^{δ} and C^{ε} protons of tyr-25, tyr-76, tyr-92 and tyr-115 are known (Lenstra, 1979) (Fig. 3.18). Using low r.f. power single proton-frequency irradiation at the H^{δ} and H^{ε} resonances of the tyr residues, assignments of the corresponding tyr C^{ζ} resonances in the ^{13}C NMR spectrum can be obtained. The resonance of the C^{ζ} centre of the residue whose H^{ε} and/or H^{δ} atom(s) are irradiated appears as a sharp peak (Fig. 3.19). The residual long range couplings between the other tyr C^{ζ} centres and their corresponding ring protons are sufficient to broaden these tyr C^{ζ} resonances. The results obtained from the single proton-frequency decoupling experiments are shown in Table 3.7, together with the assignments of the other tyr C^{ζ} resonances.

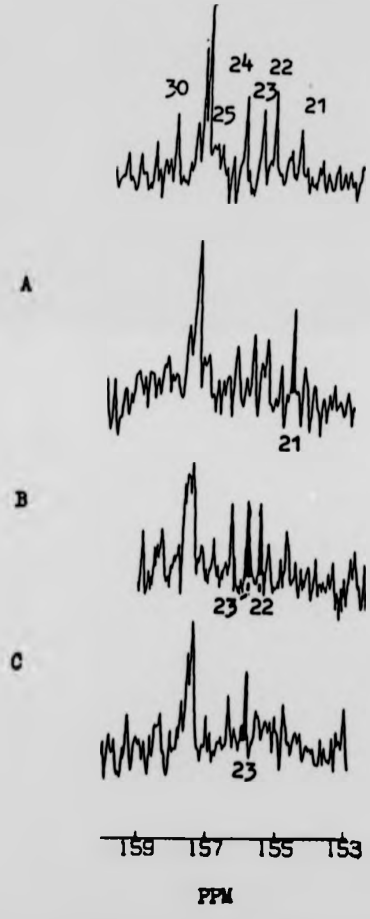

Fig. 3.19 (Top Trace) Spectral region from 153.0 ppm to 160.0 ppm of the proton-decoupled ^{13}C NMR spectrum of RNase (6 mM in D_2O) at pD 3.2, 25°C.
The numbers indicate the positions of individual tyr C^{ζ} resonances.
(A-C) Same as top trace, with selective ^{1}H irradiation at (A) 6.73 ppm, (B) 6.90 ppm, (C) 7.22 ppm (Fig. 3.18(a)).
The main collapsed multiplets in the individual spectra are shadowed.

TABLE 3.7 Summary of the Assignments of Tyr C^{ζ} Resonances in Ribonuclease A

Resonance[c]	^{13}C Spectrum: Chemical Shift δ ppm[a]	^{13}C Spectrum: Resonance Assignment	^{1}H Spectrum: Chemical Shift δ ppm[b]	^{1}H Spectrum: Resonance Assignment[d,e]	Reference or Evidence for Assignment of ^{13}C Resonance
21	154.74	tyr-115	6.73	tyr-115 H^{ε} (A)	
22	155.50	tyr-92	6.90	tyr-92 H^{δ}, H^{ε} (B)	
23	155.80	tyr-76	6.90	tyr-76 H^{ε} (B)	
	155.80		7.22	tyr-76 H^{δ} (C)	
24	156.29	tyr-73			
25	157.16	tyr-25			MeI treatment[f] Santoro *et al.* (1979)
30	158.26	tyr-97			Egan *et al.* (1978)

[a] ^{13}C chemical shifts are relative to external Me_4Si, pD 3.2, 25°C

[b] ^{1}H chemical shifts are relative to external Me_4Si, pD 3.2, 25°C

[c] See Fig. 3.19

[d] From Lenstra *et al.* (1979)

[e] The letters in parenthesis are those shown in Fig. 3.18(a)

[f] This work

3.5.3 Summary

Assignments of many methyl and tyr C^{ε} resonances are made using low r.f. power single proton-frequency decoupling. In this study, chemical modification of the met-29 side-chain affords the specific assignment of its C^{ε} resonance in the ^{13}C NMR spectrum. All these assignments are summarised in Table 3.6 and Table 3.7.

The pD-dependent chemical shifts of the methyl resonances of the ile, met and val residues are attributed to a pD-induced structural change in the active site. The results obtained in this study further explain the observation that the pD-dependent activity of RNase is regulated by a conformational change in the protein's structure. This conformational change orientates the active site residues, his-12, his-119 and lys-41 in order to achieve optimal catalytic activity.

3.6 THE USE OF CHEMICAL SHIFT PERTURBATIONS IN MAKING ASSIGNMENTS OF ^{13}C RESONANCES - PROBLEMS

3.6.1 The Use of Shift Probes in Assignments

Shift perturbations caused by the binding of diamagnetic ligands, protons and paramagnetic species have been extensively used to obtain assignments in the ^{1}H NMR spectra of proteins. In ^{13}C NMR spectroscopy, apart from the examples cited by Campbell and Dobson (1979) and Allerhand (1979), chemical shift changes caused by different ligands and paramagnetic species have not played

3.5.3 Summary

Assignments of many methyl and tyr C^{ζ} resonances are made using low r.f. power single proton-frequency decoupling. In this study, chemical modification of the met-29 side-chain affords the specific assignment of its C^{ϵ} resonance in the ^{13}C NMR spectrum. All these assignments are summarised in Table 3.6 and Table 3.7.

The pD-dependent chemical shifts of the methyl resonances of the ile, met and val residues are attributed to a pD-induced structural change in the active site. The results obtained in this study further explain the observation that the pD-dependent activity of RNase is regulated by a conformational change in the protein's structure. This conformational change orientates the active site residues, his-12, his-119 and lys-41 in order to achieve optimal catalytic activity.

3.6 THE USE OF CHEMICAL SHIFT PERTURBATIONS IN MAKING ASSIGNMENTS OF ^{13}C RESONANCES - PROBLEMS

3.6.1 The Use of Shift Probes in Assignments

Shift perturbations caused by the binding of diamagnetic ligands, protons and paramagnetic species have been extensively used to obtain assignments in the ^{1}H NMR spectra of proteins. In ^{13}C NMR spectroscopy, apart from the examples cited by Campbell and Dobson (1979) and Allerhand (1979), chemical shift changes caused by different ligands and paramagnetic species have not played

useful roles in the assignment of the nonprotonated ^{13}C resonances in a protein spectrum. The problems encountered in using chemical shift probes for making specific assignments are discussed below.

1. One-to-one interrelationships between the resonances of protein-ligand complexes and those of the free protein are difficult to establish and are not always obvious by inspection. There are three main reasons for this. Firstly, changes upon ligand binding may not be specific. Perturbed resonances do not necessarily arise from groups near to the binding site in the protein since the effects of binding, such as conformational changes, can be transmitted through proteins (see below). Secondly, if the exchange between the free protein and its complex is slow, broad and complicated overlapping peaks result in the spectra of these mixtures. In the case of fast exchange, shift-averaged ^{13}C resonances are encountered. Thirdly, the binding constant of the ligand to the protein may not be high enough to yield completely bound protein species even when a large excess of ligand is added. In the case of ^{13}C NMR, there are upper limits to the amount of ionic ligand which can be used. (The problems arising from the use of ionic ligands and salts are discussed in Chapter 2, Section 2.3.2).

2. Not all the chemical shifts of the carbon atoms close to the ligand can be guaranteed to be perturbed by the ligand (Allerhand, 1979). In principle, the ^{1}H and ^{13}C paramagnetic shifts should be identical in magnitude after allowance for the geometrical factor $(3\cos^2\theta-1)r^{-3}$ (Briggs, 1971). However, small induced shifts in the

^{13}C spectrum are difficult to measure because they will not be much larger than shifts arising from minor conformational and pKa changes.

3. The changes in the localised structure of a macromolecule caused by the binding of ligands or the ionisation of groups will most significantly alter the secondary shifts of resonances of nuclei in the immediate vicinity of the participating residues, that is, direct through-space chemical shift perturbations. In addition, conformational adjustments may also extend throughout considerable regions of the protein molecule. The results of Walters and Allerhand (1980) reveal an important point: namely that local conformational changes resulting from the ionisation of side-chains can cause through-space shift perturbations which are larger than through-bond ones.

The conformational perturbations, brought about by changes in pD, can sometimes be minimised by the addition of an inhibitor. For example, the binding of a saccharide inhibitor to lysozyme is known to restrict conformational fluctuations within the range pD 3.0 to pD 7.5. If the pKa values of the titratable groups are not changed by the presence of the inhibitor, it is possible to study the titration behaviour of nearby nontitratable groups on the assumption that no further significant conformational changes are possible.

The three sets of problems discussed above are present because the spectral shift perturbations in a ^{13}C NMR spectrum can in part be due to complex changes in the structure of the protein and it is not possible to interpret the spectral changes quantitatively. However, if the nature of the binding site(s) is (are) known in some detail, useful information can be obtained from the shift perturbations.

3.6.2 The Use of Terminal Carboxylate Group Titration

In free amino acids, pH-induced chemical shift changes are observed in the side-chain methyl groups. These shift changes are predominantly a result of spatial rather than inductive effects (Deslauriers and Smith, 1976). The group which is spatially close to both the COO^- and NH_3^+ groups is the one which is most sensitive to pH.

Many medium-sized proteins have non-polar amino acid residues such as val and leu as the terminal carboxylate group. In principle, therefore, the titration of the COO^- group of these residues may perturb the shifts of the corresponding methyl resonances. However, because ^{13}C chemical shifts in a protein are governed by many factors such as electric fields, bond polarisation and steric compression, the pH-induced perturbations of the methyl groups of terminal carboxylate residues may not be observed.

CHAPTER 4

THE THERMAL UNFOLDING OF RIBONUCLEASE A AND HEW LYSOZYME

4.1 INTRODUCTION

The denaturation of ribonuclease A (RNase) and HEW lysozyme by heat, urea, guanidinium chloride and acid has been studied extensively using a variety of physical techniques (Lapanje, 1978, and references therein). Despite the vast amount of data so far accumulated there is still no agreement as to (i) whether intermediate states exist between the native and denatured forms, and (ii) whether the heat-denatured form is completely unfolded.

The existence of identifiable intermediate states in the thermal unfolding of RNase has been suggested by many workers (Burgess and Scheraga, 1975; Benz and Roberts, 1975(a); Matheson and Scheraga, 1979(a)). From their ^{1}H NMR studies, Benz and Roberts concluded that below pD 5.0, an early unfolding process occurs, involving the C-terminal and N-terminal residues. These early unfoldings have not been observed at pD values greater than 5.0 (Lenstra *et al.*, 1979).

^{13}C NMR results at pH 3.2 (Howarth, 1979(a)) showed that at temperatures below the main transition temperature, some regions of RNase, perhaps including residues 17-24, and including not more than one his,

one glu, one phe and one met residue, unfold together. This initial unfolding was shown to destabilise the rest of the molecule which then unfolds cooperatively at the main transition temperature to give a loose structure.

Unlike RNase, no stepwise unfolding of the segments of lysozyme has been suggested in any of the studies carried out so far. The existence of three states during the heat denaturation of lysozyme at pH 2.8 has been deduced from ^{1}H NMR studies of the arg NH_2 protons by Bradbury and Norton (1974). These three states are (i) a truly native structure below 20°C, (ii) a loosened structure between 45°C and 53°C, and (iii) an unfolded structure above 75°C. The loosened state (ii) is conceivable because protein molecules tend to undergo thermal expansion below the main transition temperature (Nagayama, 1981).

The temperature-dependent conformational transition of lysozyme occurs between 20°C and 30°C at pD 4.75. This was detected using ^{13}C NMR spectroscopy at 25.2 MHz (Cozzone *et al.*, 1975). Subsites D and E have been suggested as the primary locus for these structural change(s). The molecular form on each side of the transition temperature range (20°C-30°C) is related to the A(tetragonal) and B(orthorhombic) crystal forms of lysozyme.

High-resolution ^{13}C NMR can, in principle, distinguish between the different states of a protein at various temperatures (Howarth, 1979(a)). This method relies on the ability to resolve as many individual ^{13}C resonances as possible. Any localised conformational

changes can be inferred from the selective changes in the chemical shifts and from the relaxation data of both single carbon lines and groups of lines. Jardetzky and Roberts (1981), in a recent review, have outlined a number of criteria which must be satisfied before the high-resolution NMR technique can be used to detect the existence of intermediates in this unfolding process.

In this chapter, the thermal effects on RNase and on lysozyme at temperatures below their main transition temperatures are considered. Individual hydrophobic residues which are generally 'silent' to other spectroscopic techniques are studied, together with the aromatic and polar residues. The denatured state of both the proteins is then discussed in some detail.

4.2 RIBONUCLEASE A: PREDENATURATIONAL TRANSITIONS

4.2.1 Results

In the ^{13}C NMR spectrum of RNase, the specifically assigned tyr C^{ξ}, arg C^{ξ}, and phe C^{γ} resonances are useful monitors of the thermal unfolding process. The resolved methyl resonances have not, as yet, all been assigned to a specific amino acid residue. However, some of these unassigned resonances can still provide useful supplementary information. Analysis of the predenaturational perturbations of the thr C^{β} resonances is hampered by the severe overlap of resonances.

At pD 3.2 the main structural transition occurs

at approximately 46°C-48°C and the major changes in the NMR spectrum correspondingly occur at this temperature. However, some rather significant changes also occur at temperatures well below this transition temperature.

The behaviour of some of the resolved resonances in the aliphatic region of the spectrum between 10.0 ppm and 22.0 ppm during thermal unfolding is shown in Fig. 4.1. As the temperature is increased, there are progressive shift changes in many of the methyl resonances. The most significant changes seem to occur between 25°C and 35°C. These shift changes cannot be discounted as non-specific thermal shifts because (i) they are not observed in all the resolved resonances, and (ii) the magnitude of the shift changes varies between the resolved resonances.

The assigned ile $C^{\gamma 2}$ resonance (peak 5) seems to display a continuous upfield shift between 18°C and 38°C. Thereafter, the shift remains unperturbed up to 44°C (Fig. 4.1). The assigned ile C^{δ} resonance (peak 1) undergoes an upfield shift of 0.18 ppm between 25°C and 35°C.

Three of the four met C^{ε} resonances are well resolved (peaks 3, 4 and 6). Peaks 3 and 4 move downfield towards the chemical shift value of the solvent-exposed met residues, whereas peak 6 displays a small upfield shift of 0.08 ppm.

The other distinct shift perturbations ($\Delta \geq$ 0.05 ppm) in the aliphatic methyl region occur in the resolved peaks 12, 15, 16, 17, 18 and 19 (Fig. 4.1).

Fig. 4.2 shows the region of thr C^{β} and ser C^{β}

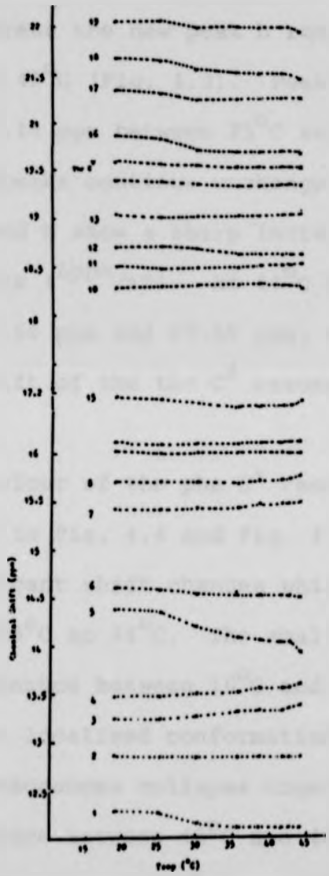

Fig. 4.1 Plot of chemical shifts of the methyl carbon resonances in the proton-decoupled ^{13}C NMR spectrum of RNase as a function of temperature, pD 3.2, 0.05 M NaCl. Peak numbers are those of Fig. 3.14.

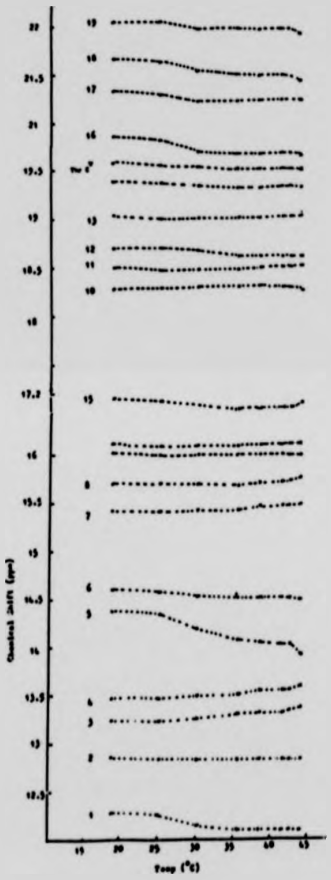

Fig. 4.1 Plot of chemical shifts of the methyl carbon resonances in the proton-decoupled ^{13}C NMR spectrum of RNase as a function of temperature, pD 3.2, 0.05 M NaCl. Peak numbers are those of Fig. 3.14.

resonances at 25°C, 35.5°C, 44°C, and 55°C. The intense peak (f-h) in Fig. 4.2 splits into three distinct peaks at 35.5°C. The new peak (f) which first becomes resolved at 35.5°C, can be seen to shift upfield progressively between 25°C and 44°C, whereas the new peak h remains unperturbed between 35.5°C and 42°C (Fig. 4.3). Peaks d and j both shift upfield by 0.18 ppm between 25°C and 35.5°C. Thereafter, these peaks continue unchanged. Between 42°C and 44°C peaks b and h show a sharp increase in their thermal coefficients ($^{\Delta ppm}/_{\Delta T}$). At 44°C a new band of peaks is seen between 67.66 ppm and 67.89 ppm, these corresponding to the chemical shift of the thr C^{β} resonance in the heat-denatured protein.

The behaviour of the phe C^{γ} resonances during thermal unfolding is shown in Fig. 4.4 and Fig. 4.6. The resonances do not show significant shift changes whilst the temperature is increased from 25°C to 44°C. The small thermal shift of the phe-8 C^{γ} resonance between 16°C and 25°C can be attributed to minor localised conformational changes. The three phe C^{γ} resonances collapse together at the main transition temperature between 46°C and 48°C to give three well-resolved resonances at 136.81 ppm, 137.08 ppm and 137.15 ppm in the spectrum of the heat-denatured RNase.

At 25°C one single arg C^{ζ} resonance is well resolved at 157.73 ppm (Fig. 4.6, peak 29). This resonance shows characteristics of fast exchange behaviour by its progressive upfield shift between 16°C and 38°C. Above 38°C, it coalesces with the main arg C^{ζ} peak (Fig. 4.6, peaks 26-28). Above 38°C the main arg C^{ζ} peak moves

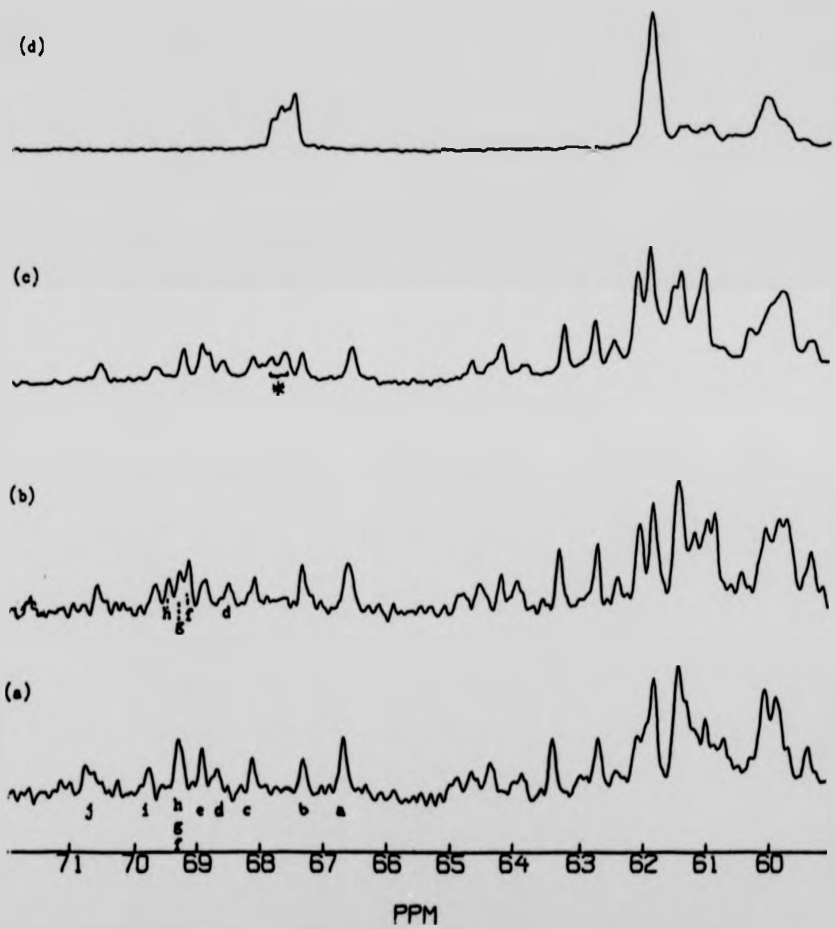

Fig. 4.2 The thr C^{β} (peaks a-j) and ser C^{β} (62.0 ppm-65.0 ppm) regions of the proton-decoupled ^{13}C NMR spectrum of RNase at various temperatures, pD 3.2, 0.05 M NaCl. The peak letters indicate the positions of individual thr C^{β} resonances. The peaks marked * in spectrum (c) correspond to the thr C^{β} resonances in the heat-denatured protein.
(a) 25°C
(b) 35.5°C
(c) 44°C
(d) 55°C

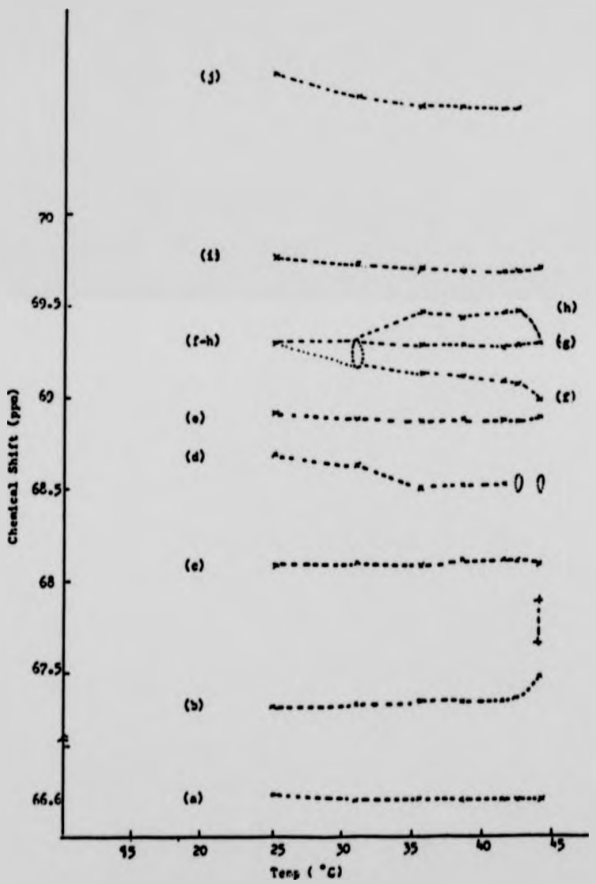

Fig. 4.3 Temperature dependence of the chemical shifts of the thr C^{β} resonances of RNase, pD 3.2, 0.05 M NaCl. Peak letters are those of Fig. 4.2.

⇨ , broad unresolved peak;

+---+ , thr C^{β} peaks of denatured protein.

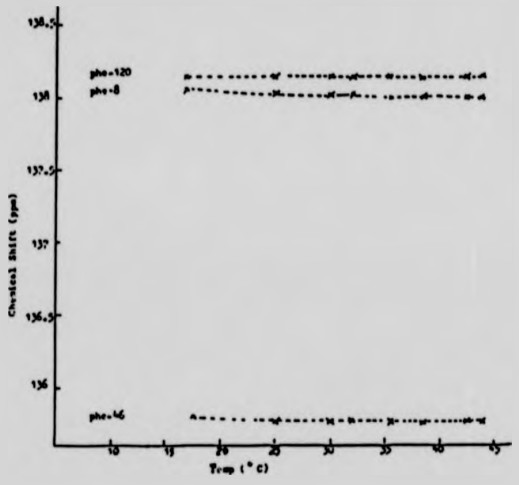

Fig. 4.4 Temperature dependence of the chemical shifts of the phe C^{γ} resonances of RNase, pD 3.2, 0.05 M NaCl.

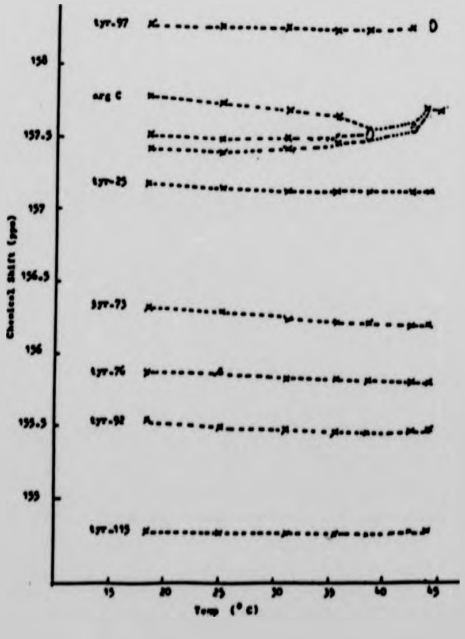

Fig. 4.5 Temperature dependence of the chemical shifts of the tyr C^{ζ} and arg C^{ζ} resonances of RNase, pD 3.2, 0.05 M NaCl.

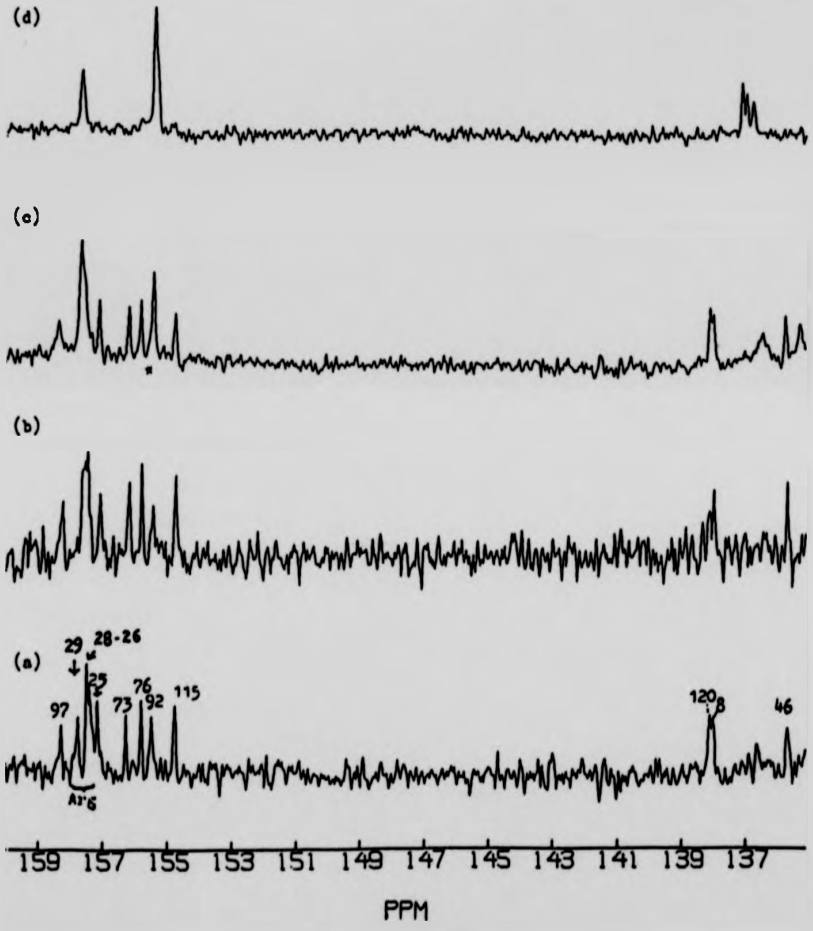

Fig. 4.6 The tyr C^{ζ}, arg C^{ζ} and phe C^{γ} region of the proton-decoupled ^{13}C NMR spectrum of RNase at various temperatures, pD 3.2, 0.05 M NaCl. The numbers above each tyr C^{ζ} resonance (115, 92, 76, 73, 25, 97) and each phe C^{γ} resonance (46, β, 120) are assignments to specific residues (this work; Santoro *et al.*, 1979). The resonance marked * in spectrum (c) corresponds to the tyr C^{ζ} resonance in the heat-denatured protein.
(a) 25°C
(b) 38.5°C
(c) 44°C
(d) 55°C

progressively downfield with increasing temperature and finally resonates at 157.79 ppm.

At pD 3.2, below 44°C the six tyr C^{ζ} resonances are always well resolved. These resonances have each been assigned to their specific amino acid residue in the present study (Chapter 3, Section 3.5.2.5). Between 25°C and 35.5°C the C^{ζ} resonances of tyr-73 and tyr-76 show shift perturbations of up to 0.07 ppm (Fig. 4.5). These small shifts are attributed to localised conformational changes around these tyr residues. As the temperature is increased above 35.5°C, the six tyr C^{ζ} resonances remain unchanged. At 44°C the tyr-97 C^{ζ} resonance broadens and the intensity of the peak at 155.49 ppm increases (Fig. 4.6(c)). The broadening of the tyr-97 C^{ζ} resonance suggests an intermediate exchange behaviour. The resonance at 155.49 ppm corresponds to the tyr C^{ζ} resonance of the denatured protein.

Within the transition temperature range (46°C-48°C) at least two species, the 'native' and the denatured states, are present in slow exchange. The collapse of the sharp resolved peaks of the spectrum occurs in most cases at an equal rate.

4.2.2 Discussion

At low temperatures the progressive thermal shift of many of the resonances indicates a fast exchange between the native and locally modified conformations.

The thermal shift characteristics of the met residues, of the other aliphatic residues and of the

polar residues such as thr, arg and tyr, are discussed separately.

4.2.2.1 Met Residues

Peak 3 is assigned specifically to the met-29 C^{ε} atom, peak 4 tentatively to the met-13 C^{ε} atom and peak 6 tentatively to the met-30 C^{ε} atom (Chapters 3 and 6). The remaining met C^{ε} resonance is hidden under the broad multiplet at 16.09 ppm. At all temperatures below the main transition temperature, none of the met C^{ε} resonances coincide with the met C^{ε} resonances in the spectrum of the denatured protein. This strongly suggests that the four met groups are markedly inequivalent, each lying in a non-solvent-like environment.

Of the three resolved peaks, 3 and 4 appear to move towards the chemical shift value of the solvent-exposed met C^{ε} resonances. In the native state, the met-29 residue is fairly well exposed to the solvent. Met-13, on the other hand, is protected externally by leu-51 (Carlisle *et al.*, 1974). However, it has been postulated that with careful control of experimental conditions it is possible to partially expose the met-13 side-chain by rotation about its C^{α}-C^{β} axis so that it extends out into the solvent with no major disruption of other residues (Richards and Wyckoff, 1971). In addition, Matheson and Scheraga (1979(a)) suggested that at pD 5.5, and above 30°C, one of the most important stabilising interactions on the N-terminal portion of RNase, the met-13-val-47 hydrophobic interaction, weakens. The perturbation of peak 4 demonstrates

that the met-13 residue is involved in some of these suggested conformational changes. However, at temperatures below 46°C, this peak does not resonate at around 15.2 ppm, the position of the met C^{ε} resonances of the denatured protein. That is, the unfolding of the met-13 residue proposed by Richards and Wyckoff (1971) and Matheson and Scheraga (1979(a)) may not be as drastic as it was believed to be.

In summary, the two met residues which are most exposed to the solvent (met-29 and met-13) (Lee and Richards, 1971) show thermal shift changes which tend towards the met C^{ε} resonance of the denatured protein. The anomalous thermal shift of peak 6 may be attributable to localised heat-induced structural changes similar to those observed in the hydrophobic residues (see following section).

4.2.2.2 Other Hydrophobic Residues

At pD 3.2, in the temperature range between 25°C and 35.5°C, significant shift changes are observed in the resonances which arise from hydrophobic residues such as ile, val and leu. Similar shift characteristics are observed in aqueous solutions both with and without NaCl (0.05 M) present. That is, the thermal shifts are independent of the ionic strength of the protein solution. Furthermore, at pD 5.5, with or without cytidine-2'-phosphate (40 mM) present, these thermal shifts are still observed between 25°C and 48°C but to a smaller extent.

There has been previous evidence for a predenaturational conformational change in RNase in the temperature range between 29°C and 45°C at pH 5.0-pH 6.5 (Matheson and Scheraga, 1979(b)). The exact nature of this conformational change is not yet known. The most plausible explanation proposed so far is that this structural change is related to the conformational change which RNase undergoes on forming an enzyme-inhibitor complex. There are several proposals regarding the exact position of these structural changes, two of which are that they appear to be localised in the area of the polypeptide chain near his-48 and lys-41, or that they occur in the portion of the molecule between asp-14 and tyr-25 (French and Hammes, 1965; Meadows *et al.*, 1969). All the proposals imply structural movements involving the active site cleft.

However, in the present studies, the shift perturbations of the ^{13}C methyl resonances observed on increasing the temperature differ from those induced either by the binding of inhibitors or by a change in pD (see Fig. 6.7 and Fig. 3.15). This implies that the heat-, inhibitor- and pD-induced conformational changes are not identical.

It is necessary to consider the distribution of hydrophobic residues in the RNase molecule. There is a cluster of hydrophobic residues comprising of phe-8, val-47, val-54, ile-81, ile-106, val-108 and phe-120, buried at the end of the cleft opposite the active site residues his-12, his-119 and lys-41 (Appendix II(a)).

In addition, hydrophobic pockets comprising of specific segments are present in the native RNase structure, the most significant being formed by the segments 106 to 118 (Matheson and Scheraga, 1978). This 13-residue pocket is predicted by Matheson and Scheraga (1978) to be the nucleation site for the folding of RNase. The many short-range hydrophobic interactions present stabilise the pocket in the native protein structure. The juxtaposition of the nucleation pocket and the active site cleft makes it difficult to consider the two regions independently. The factors which affect the conformation of the groups in the two hydrophobic areas may thus be related.

It is therefore reasonable to explain the heat-induced shift perturbations partly by the thermal effects on hydrophobic bonds and partly by a heat-induced conformational change in the active site cleft. The conformational change is dependent on the pD of the protein solution, being greater at low pD values. At high pD values or in the presence of a bound inhibitor, the thermal shifts observed in this study are small. This concurs with the observation that at temperatures below 45^{o}C, the conformation of the RNase molecule is thermally stable at around pD 5.5-pD 6.5 and even more so when it is also bound to an inhibitor.

From what is known about the thermodynamics of hydrophobic associations, an increase in temperature can strengthen hydrophobic bonds. Therefore, the shift perturbations observed could arise from changes in the interactions between the various hydrophobic groups. These changes can induce a limited rotation about the

C^{α}-C^{β} bond of the ile residue, causing an alteration in the magnetic environment of the ile $C^{\gamma 2}$ methyl group. This rotation is feasible because the ile residues in RNase are not in the helical portions of the protein. It is known that the helical backbone can restrict rotation about the C^{α}-C^{β} and C^{β}-$C^{\gamma 1}$ bonds in the side-chains (Wittebort *et al.*, 1979). Similar restricted rotation about the C^{α}-C^{β} or C^{β}-C^{γ} bonds caused by changes in hydrophobic associations is conceivable for the other aliphatic groups in hydrophobic contact.

The difference between the thermal behaviour of the various hydrophobic groups is interesting. Currently the core of the protein, consisting of the phe, ile, leu, val, cys, met-30, ser-90 and tyr-97 residues, is believed to 'melt' in a single cooperative step at a temperature above the overall transition temperature of the molecule (Matheson and Scheraga, 1979(a)). Comparing the shift perturbation of the phe C^{γ} resonances with the aliphatic methyl resonances, this one-step cooperative melting hypothesis may be correct as far as the actual unfolding of the protein is concerned, but the predenaturational changes in the hydrophobic residues take place very differently. At pD 3.2, the phe C^{γ} resonances remain stable from 25°C up to the main transition temperature of 46°C-48°C, whereas many of the aliphatic methyl resonances shift continuously throughout this temperature range. (At pD 5.5, the direction and magnitude of the shift of the phe-120 C^{γ} resonance in the range 25°C to 40°C can be accounted for by the temperature-

dependence of the pKa value of the nearby his-12 or his-119 residue.)

One explanation for the difference in behaviour of the phe C^{γ} resonances is as follows. The large phe side-chains are normally kept close to their own backbones by the orientation of the C^{α}-C^{β} bonds (Matheson and Scheraga, 1978). If the induced conformational changes in the protein are very small and localised, there will be very little alteration in the environment of the phe C^{γ} centres.

The three phe residues in RNase are near to the active site his side-chains. The absence of shift perturbations in the phe C^{γ} resonances shows that the predenaturational changes which affect the active site conformation must be small.

4.2.2.3 Polar Residues

4.2.2.3.1 Thr Residues

The results obtained in this study suggest that one component of the peak f-h must arise from a residue which is involved in early unfolding at below the main transition temperature. Previous studies have suggested the preliminary unfolding of segments 13-25 and a change in the solvent-exposure of residues 1-12 during the thermal denaturation of RNase (Matheson and Scheraga, 1979(a)). Thr-17 is found in the segment 13-25 and thr-3 in segment 1-12. From the characteristics of

their perturbations, peak f may arise from thr-17 C^{β} and peak h from thr-3 C^{β}. The chemical shift of peak j is pD-dependent. At pD 5.5, it shifts upfield. Hence its upfield shift in the temperature range 25°C to 35.5°C can be accounted for by the temperature-dependence of the pKa value of a nearby glu or asp group, rather than by an early unfolding of the thr residue. This explanation can likewise be used to account for the thermal shift of peak d between 25°C and 35.5°C. Apart from thr-3 and thr-17, the thr residues which are near a glu or asp group are thr-87, thr-99 and thr-100. Peaks j and d can thus be tentatively attributed to two of these residues.

The spectrum at 44°C shows a mixture of 'native' and denatured species present in slow exchange. The thr C^{β} resonances of the 'native' component of the spectrum are identical to those at around 42°C. The protein structure appears to undergo steady conformational changes such that the 'native' form, at 42°C, just before denaturation, is different from the 'native' form at 25°C.

4.2.2.3.2 Tyr Residues

Line broadening of the tyr-97 C^{ζ} resonance at 42°C occurs at pD 3.2. When the thermal denaturation of RNase is studied at pD 5.5, broadening of this resonance is not observed at temperatures below the main unfolding temperature (Fig. 4.7). This pD-dependent characteristic prompts the suggestion that the broadening of the tyr-97 C^{ζ} resonance at pD 3.2 arises from a slow

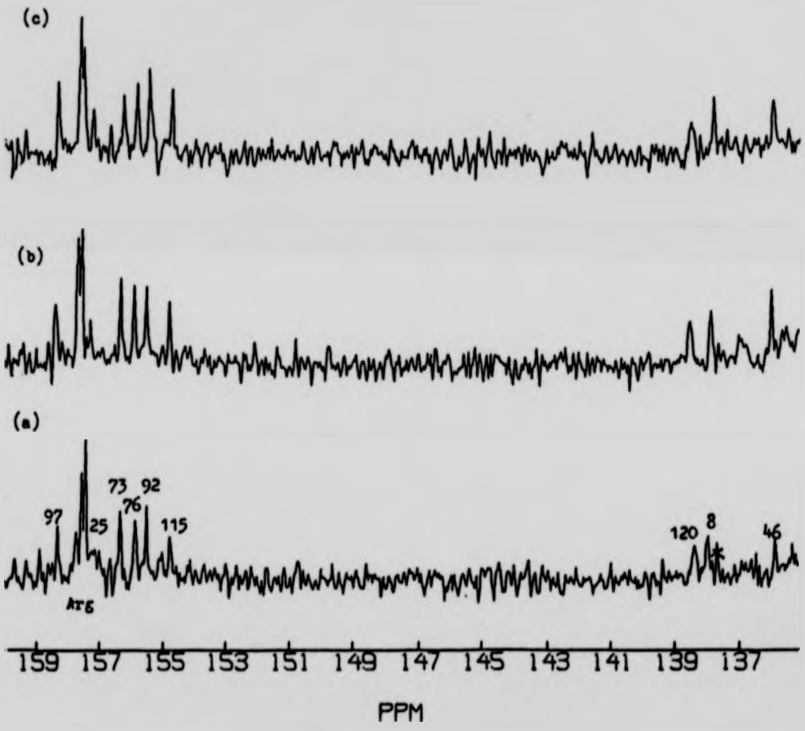

Fig. 4.7 The tyr C^{ζ}, arg C^{ζ} and phe C^{γ} region of the proton-decoupled ^{13}C NMR spectrum of RNase at various temperatures, pD 5.5, 0.05 M NaCl.
The numbers above each tyr C^{ζ} resonance (115, 92, 76, 73, 25, 97) and each phe C^{γ} resonance (120, 8, 46) are assignments to specific residues (this work, Santoro *et al.*, 1979).
(a) 25°C
(b) 41°C
(c) 48°C

heat-induced protonation-deprotonation exchange taking place in a nearby carboxylic acid group with increasing temperature. This suggestion is feasible because the glu-86 carboxylate group is about 5.3 Å from the tyr-97 C^{ζ} centre (Stanford, personal communication), a separation which may be sufficient to reveal direct through-space effects.

The coincidence of the tyr-92 C^{ζ} resonance with the solvent-exposed tyr C^{ζ} resonance at as low a temperature as 25°C is consistent with the fact that tyr-92 is the first residue in RNase to normalise under the conditions used in this study.

Notably, no significant thermal perturbations in the tyr-25 C^{ζ} resonance are seen at pD 3.2. At pD 5.5 and below 40°C, this resonance appears as a broad signal (Fig. 4.7). The broadening at low temperature in combination with high pD, implies a hindered rotation about the C^{β}-C^{γ} bond. This may be due to the presence of a hydrogen bond between the hydroxylic proton of tyr-25 and the carboxylate group of asp-14 at pD values above pD 5.0 (Lenstra *et al.*, 1979). With an increase in temperature to above 40°C, this hydrogen bond is broken, allowing tyr-25 to rotate freely, thus giving a decrease in the linewidth of the tyr-25 C^{ζ} resonance.

At both pD 3.2 and pD 5.5 the tyr-25 C^{ζ} resonance remains distinct throughout the predenaturation temperature range. The local unfolding of tyr-25 suggested in previous studies (Burgess and Scheraga, 1975; Matheson and Scheraga, 1979(a)) is not apparent in the present ^{13}C NMR studies.

In a parallel set of studies carried out in this research using ^{1}H NMR, no predenaturational thermal changes are observed in the assigned tyr-25 C^{δ} resonance at pD 3.2 (Fig. 4.8). Hence it appears that the local unfolding at below the main transition temperature is not as significant as previously suggested.

4.2.2.3.3 Arg Residues

Of the four arg residues, only arg-10 and arg-33 are capable of forming intramolecular hydrogen bonds. The guanidino group of arg-33 hydrogen- bonds to one or more of the backbone carbonyl oxygen atoms after his-12. Arg-10 is part of a hydrogen bonding system involving glu-2, arg-10 and asn-34 (Carlisle *et al.*, 1974; Borkakoti, personal communication).

Although arg-10 and arg-33 can form intramolecular hydrogen bonds, the arg-10 C^{ζ} atom is completely inaccessible to the solvent due to its position in the crystal structure. The arg-33 C^{ζ} centre, however, is equally as exposed to the solvent as the arg-39 and arg-85 C^{ζ} centres. Therefore, one can expect little difference between the chemical shifts of the C^{ζ} resonances of arg-33, arg-39 and arg-85.

The resonance at 157.73 ppm (peak 29, Fig. 4.6) is tentatively assigned to arg-10 C^{ζ}. This assignment is speculative since it is based solely on a correlation between the known environment of the arg residues in the crystal structure and the ^{13}C chemical shift data obtained in the present studies. However, it is not unreasonable

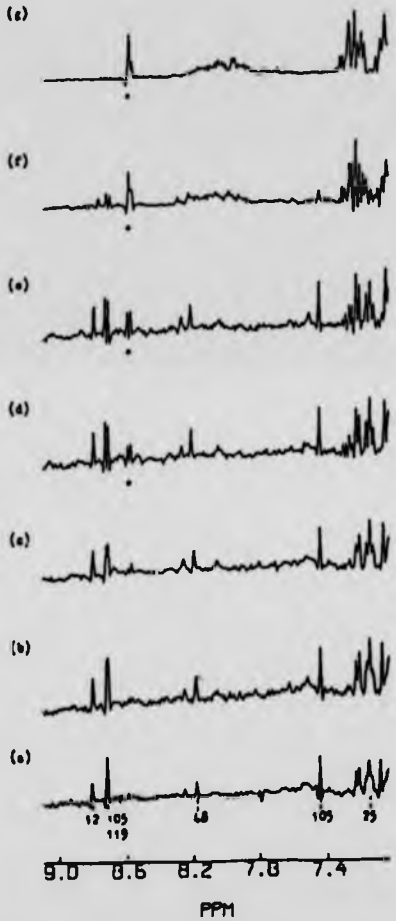

Fig. 4.8 ^{1}H NMR spectra (7.0 ppm-9.0 ppm) of RNase at various temperatures, pD 3.2, 0.05 M NaCl. Peak 25 is the C(2,6) H resonance of tyr-25, and peak 105 at 7.45 ppm is the C(4)H resonance of his-105. Other peaks labelled 48, 105, 119 and 12 are his C(2)H resonances. The peaks labelled * are the his C(2)H resonances of the denatured protein.

(a) 27°C
(b) 30°C
(c) 35°C
(d) 40°C
(e) 44°C
(f) 47°C
(g) 50°C

to expect a downfield shift as a result of hydrogen bonding. This resonance shifts towards the main arg C^{ζ} band with increasing temperature. If the assignment is correct, the thermal shift agrees with the results from previous studies, that is, the N-terminal segment 1-12 undergoes an initial change in its solvent-exposure before the actual denaturation takes place (Matheson and Scheraga, 1979(a)).

4.2.2.4 Predenaturation Conformation (44°C to 46°C)

The structure of RNase just before the main unfolding process is different from the native state which exists at lower temperatures, as is evident from the linewidths and chemical shifts observed. Notably, the resonances of the polar residues (thr, tyr and arg) arising from the denatured protein are distinctly visible in the spectrum at 44°C. In contrast, none of the hydrophobic phe C^{γ}, ile $C^{\gamma 2}$, ile C^{δ} and met C^{ε} resonances in the denatured protein are seen at this temperature. This suggests that the polar residues, which are in the main near to the surface of the protein, change their exposure to the solvent at lower temperature than do the more-buried hydrophobic residues. This change in exposure destabilises the rest of the protein molecule at a temperature near to the main transition temperature, and on a further temperature increase of approximately 5°C, the entire molecule unfolds cooperatively. That is, the main unfolding is two-state. This postulation is supported by the results obtained in the present study

using ^{1}H NMR. The areas of the four resolved his C(2)H resonances appear to decrease simultaneously (Fig. 4.8). The present observations concur with those of Benz and Roberts (1975(a)). It should also be added that the unfolded state, as detected by ^{13}C NMR, is not a completely random coil (Howarth and Lian, 1981) (Appendix XI); Section 4.4 of this Chapter).

4.2.3 Summary

The ^{13}C NMR results reveal predenaturational conformational changes involving specific hydrophobic residues, in particular ile, val and thr. A distinct conformational change occurs between 25°C and 35.5°C. This change is explained partly by the thermal effects on the groups involved in short-range hydrophobic interactions and partly by a predenaturational conformational change at the active site cleft.

The normalisation of one arg C^{ζ} resonance at a temperature below the main transition temperature possibly implies that the N-terminal region of the protein undergoes initial changes in its solvent-exposure before the gross denaturation step.

The main unfolding step is essentially a two-state process, with initial loosening of the protein molecule by an increase in the solvent-exposure of some of its hydrophilic groups. There is no evidence in this study to suggest the early unfolding of tyr-25, or of any of the phe residues, either at pD 3.2 or pD 5.5. All these residues are well resolved and readily identifiable in the ^{13}C NMR spectra

obtained. The early broadening of the tyr-97 C^{ζ} resonance at pD 3.2 and the shift of at least one thr C^{β} resonance at the same pD can be attributed to a protonation-deprotonation process in nearby carboxylate groups.

The deviations in the structure of thermally unfolded RNase from the completely random coil conformation are significant. The hydrophobic residues appear to show more heterogeneity in their chemical shifts than do the hydrophilic residues. This strongly suggests that the thermally-unfolded protein is stabilised by residual hydrophobic interactions which perhaps resemble those present in the nucleation pocket of RNase.

4.3 HEW LYSOZYME: PREDENATURATIONAL TRANSITIONS

4.3.1 Results

The resolved resonances are all significantly broadened at temperatures below 25°C. Between 25°C and 35°C shift changes are observed in many of these resonances. Above 45°C the temperature coefficient of chemical shift (Δppm/ΔT) increases significantly for some specific resonances. For example, between 45°C and 50°C, the temperature coefficients of the ile-98 $C^{\gamma 2}$ (peak 1), ile-88 C^{δ} (peak 5), ile-98 C^{δ} (peak 6), ile-88 $C^{\gamma 2}$ (peak 10) and leu-56 $C^{\delta 1}$ (peak 23) resonances are significantly larger than those of the ile-78 $C^{\gamma 2}$ (peak 2 or 3, tentative assignment), ile-58 $C^{\gamma 2}$ (peak 9), leu-17 $C^{\delta 2}$ (peak 25a), val-92 $C^{\gamma 2}$ (peak 28) and val-99 $C^{\gamma 1}$ (peak 29) resonances (Fig. 4.9).

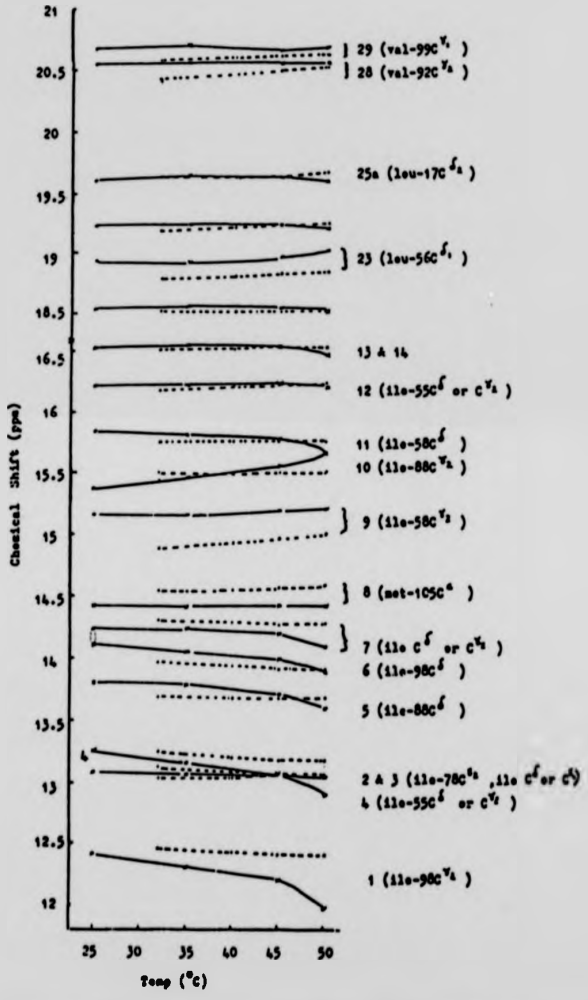

Fig. 4.9 Temperature dependence of the chemical shifts in the methyl region of the proton-decoupled ^{13}C NMR spectrum of lysozyme, pD 3.2, in D_2O. Peak numbers are those of Fig. 3.4, and Table 3.2. The assignments to specific residues are shown in parenthesis (this work).

——— , free lysozyme, pD 3.2

..... , + 100 mM NAG, pD 3.2

Between 45°C and 50°C in the region of the trp C^{γ} resonances (108 ppm-113 ppm) one half of the resonance assigned to the trp-28 and trp-111 C^{γ} atoms shifts downfield by 0.24 ppm whilst the other trp C^{γ} resonances in the rest of this region are not significantly perturbed (Fig. 4.10(a)).

The spectral region between 136 ppm and 158 ppm consists of peaks from the nonprotonated aromatic carbon atoms - trp $C^{\epsilon 2}$, phe C^{γ}, tyr C^{ζ} and arg C^{ζ}. With the exception of the main arg C^{ζ} peak at 158 ppm, all the resonances in this region show significant shift perturbation especially above 45°C (Fig. 4.10(b) and (c)). At lower temperatures, the thermal shifts of the trp-108 $C^{\epsilon 2}$, phe-34 C^{γ}, trp-62 $C^{\gamma 2}$, phe-3 or phe-38 C^{γ}, tyr-53 C and tyr-23 C^{ζ} resonances are too large to be ignored.

All the perturbed resonances are distinct and narrow throughout the temperature range explored. This behaviour corresponds to a fast exchange condition between the folded conformational structures.

Between 25°C and 55°C at both pD 3.2 and pD 5.0, three distict arg C^{ζ} peaks are resolved (Fig. 4.10(c)). The downfield resonance at 158 ppm coincides with the solvent-exposed arg C^{ζ} resonance. The three peaks remain distinct throughout the temperature range used in this study. At 60°C, the upfield peak (at 157.78 ppm) cannot be distinguished above the background noise. The broadening of this resonance occurs over a narrow temperature band.

When N-acetylglucosamine (NAG) is added, then

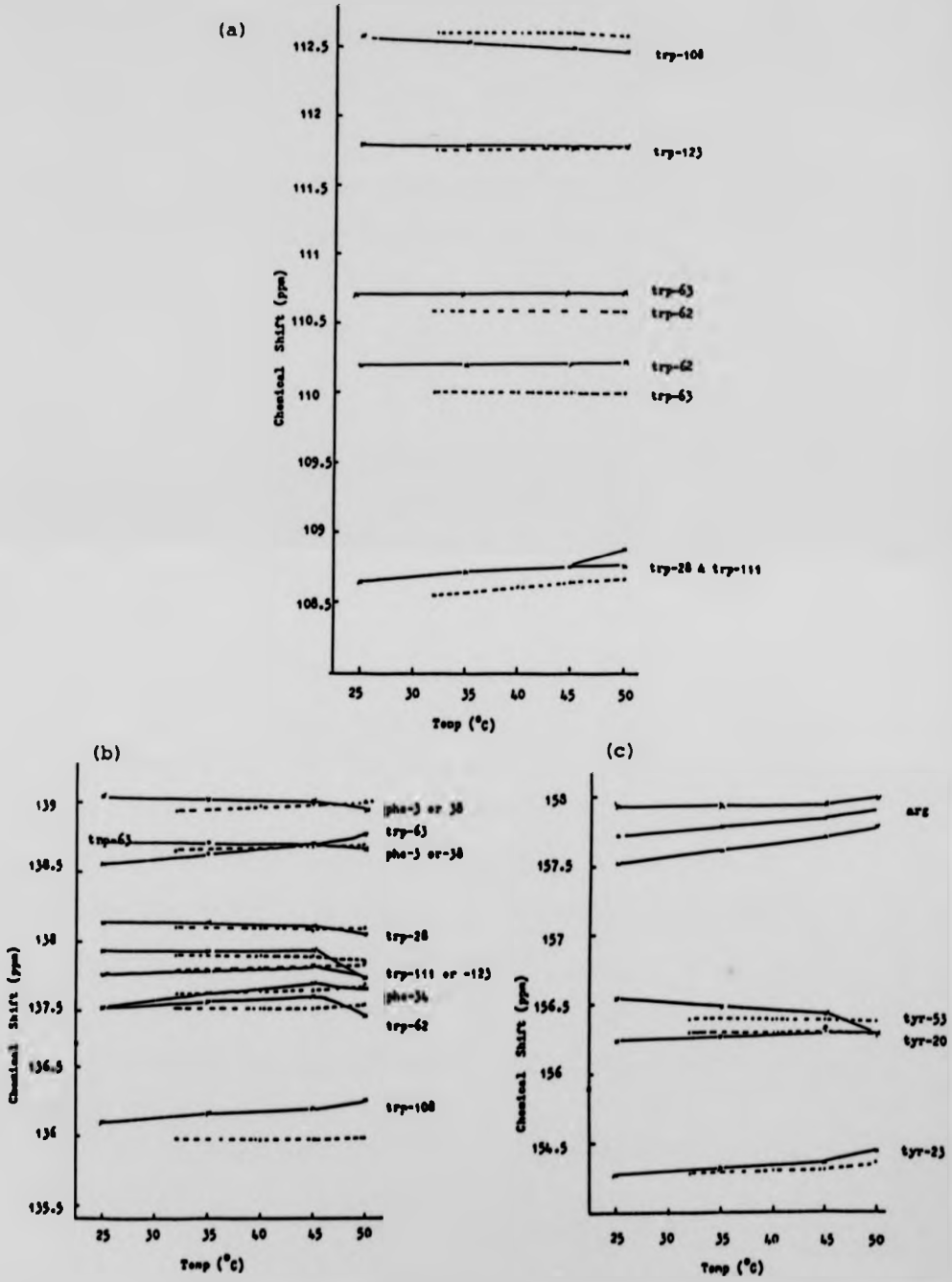

Fig. 4.10 Temperature dependence of the chemical shifts of
(a) the trp C^{γ} resonances
(b) the trp $C^{\varepsilon 2}$ and phe C^{γ} resonances
(c) the tyr C^{ζ} and arg C^{ζ} resonances
in the proton-decoupled natural abundance ^{13}C NMR spectrum of lysozyme.
——— , free lysozyme, pD 3.2
- - - - , + 100 mM NAG, pD 3.2

within the limits of experimental error (± 0.04 ppm), the thermal shifts described in the preceding paragraphs are not observed.

At around the transition temperature of approximately 70°C, at least two species, the 'native' and the 'denatured' forms are present in slow exchange. In the various regions of the spectrum, the rate of collapse of each of the sharp resolved peaks is the same.

4.3.2 Discussion

4.3.2.1 Linewidths

The observed non-specific line broadening of the resolved resonances cannot be attributed to the self-association of lysozyme molecules for the following reasons. Firstly, under the pD and concentration conditions used in this study, self-association is known to be minimal. Secondly, the C^{γ} resonances of trp-62 and trp-63 remain separate throughout the temperature range used. In the aggregated state of the protein, these two resonances coalesce to form a broad peak at 110.8 ppm (Shindo *et al.*, 1977).

Therefore the general line broadening of the resonances at low temperatures must be due to an increase in the viscosity of the protein solution.

4.3.2.2 Hydrophobic and Aromatic Residues

As the temperature is increased there may be specific regions of the protein where expansion and/or conformational changes are more likely to occur. The general conformational mobility of lysozyme is known. Residues 70-73, 82-84, 101-103, asp-18, thr-47, arg-61 and glu-121 are all known to be susceptible to additional motion - and conformational - changes due to their higher exposure to a solvent. On the other hand phe-3, ile-88, val-92 and val-99 are buried, being parts of regular secondary structures. They are less likely to be influenced by changes in temperature (Imoto *et al.*, 1972).

The results obtained in this study for the methyl groups do not agree completely with the fact that the more solvent-exposed side-chains have a greater thermal motion than those which are buried. Hydrophobic residues such as ile-88, leu-56 and the val groups are observed to be susceptible to changes in temperature, in addition to the more exposed hydrophilic groups.

In both the methyl and the aromatic regions of the spectrum, it is possible to differentiate shift characteristics in the resolved resonances. For example, in the temperature range from 25°C to 35°C, the magnitudes of the shift changes of the ile-98 and ile-88 methyl resonances are significantly greater than those of ile-58. Between 45°C and 50°C, ile-98, ile-88 and leu-56 appear to be more perturbed than the val, ala, thr and the other resolved ile resonances. The met-105 C^{ϵ} resonance remains

unchanged throughout the temperature range studied. The differential thermal shifts of the aromatic resonances between 136 ppm and 139 ppm (trp $C^{\varepsilon 2}$, phe C^{γ}) at lower temperatures ($25^{o}C$-$35^{o}C$) further suggest that the heat-induced changes are not uniform throughout the protein structure.

Cozzone *et al.* (1975), from observations of non-protonated ^{13}C aromatic resonances, concluded that the vicinity of subsites D and E is the primary locus for structural change at temperatures between $20^{o}C$ and $30^{o}C$. Their conclusions were, however, drawn from a set of very tentative assignments. Their preliminary assignment of the tyr-53 C^{ζ} resonance has since been reassigned definitely to tyr-23 C^{ζ} (Allerhand, 1979; this work).

There are two main reasons for the need to reexamine the temperature-dependent changes as observed in the ^{13}C NMR spectrum. Firstly, in the present study, resolved resonances other than those arising from residues near subsites D and E are perturbed at temperatures below $35^{o}C$. Examples of these perturbed resonances are: trp-108 $C^{\varepsilon 2}$, trp-111 $C^{\varepsilon 2}$ or trp-28 $C^{\varepsilon 2}$, trp-62 $C^{\varepsilon 2}$, phe-34 C^{γ}, phe-3 C^{γ} or phe-38 C^{γ}, tyr-23 C^{ζ}, ile-98 $C^{\gamma 2}$ and ile-98 C^{δ}. Whereas trp-108, trp-111 and trp-28 are positioned near to subsites D and E, the other residues are not (Appendix VII(b)). In addition, the resonance of the leu-56 $C^{\delta 1}$ atom, which is near to subsites D and E, remains constant below $35^{o}C$.

Secondly, Cozzone *et al.* related the temperature-dependent conformational transition in solution, between $20^{o}C$ and $30^{o}C$ at pD 4.75, to the crystalline phase transition

unchanged throughout the temperature range studied. The differential thermal shifts of the aromatic resonances between 136 ppm and 139 ppm (trp $C^{\varepsilon 2}$, phe C^{γ}) at lower temperatures ($25^{o}C$-$35^{o}C$) further suggest that the heat-induced changes are not uniform throughout the protein structure.

Cozzone *et al.* (1975), from observations of non-protonated ^{13}C aromatic resonances, concluded that the vicinity of subsites D and E is the primary locus for structural change at temperatures between $20^{o}C$ and $30^{o}C$. Their conclusions were, however, drawn from a set of very tentative assignments. Their preliminary assignment of the tyr-53 C^{ζ} resonance has since been reassigned definitely to tyr-23 C^{ζ} (Allerhand, 1979; this work).

There are two main reasons for the need to reexamine the temperature-dependent changes as observed in the ^{13}C NMR spectrum. Firstly, in the present study, resolved resonances other than those arising from residues near subsites D and E are perturbed at temperatures below $35^{o}C$. Examples of these perturbed resonances are: trp-108 $C^{\varepsilon 2}$, trp-111 $C^{\varepsilon 2}$ or trp-28 $C^{\varepsilon 2}$, trp-62 $C^{\varepsilon 2}$, phe-34 C^{γ}, phe-3 C^{γ} or phe-38 C^{γ}, tyr-23 C^{ζ}, ile-98 $C^{\gamma 2}$ and ile-98 C^{δ}. Whereas trp-108, trp-111 and trp-28 are positioned near to subsites D and E, the other residues are not (Appendix VII(b)). In addition, the resonance of the leu-56 $C^{\delta 1}$ atom, which is near to subsites D and E, remains constant below $35^{o}C$.

Secondly, Cozzone *et al.* related the temperature-dependent conformational transition in solution, between $20^{o}C$ and $30^{o}C$ at pD 4.75, to the crystalline phase transition

from the tetragonal form (A) to the triclinic form (B). However, from x-ray crystallography, it is seen that the differences in the two crystalline forms of lysozyme are strictly localised. Variation of the conformation of the crystal structure does not significantly affect the ring current shift of the ^{1}H NMR signals (Perkins and Dwek, 1980). Rather, the ring current shift interactions are influenced to a greater extent by thermal motions in the protein side-chains.

The extent of the shift perturbations of the resonances strongly suggests thermal expansion of the lysozyme structure. The increase in the volume of a protein must be associated with an increase in the degrees of vibrational freedom of the main chain. If the protein as a whole expands steadily over the temperature range used, changes in ring current effects will be observed in all the ring current shifted resonances. The absence of a thermal shift in the met-105 C^{ε} resonance implies that this 'whole-molecule expansion' model is inadequate, especially bearing in mind that the met-105 residue is surrounded by four aromatic residues - trp-28, trp-108, trp-111 and tyr-23 (Appendix I).

A model which assumes increases in the thermal vibrations of certain aromatic rings about the aromatic C^{β}-C^{γ} bond as sections of the protein become looser, is more feasible. Ile-98 is situated near trp-63, trp-62 and trp-108 (Appendix I and Appendix IV(c)), and ile-88 is close to phe-3 (Appendix IV(b)). The ile-98 methyl resonances are perturbed significantly over the whole temperature range between 25^{o}C and 50^{o}C, whereas the ile-88 methyl resonances

only show thermal shifts above 35°C. Therefore it appears that the area around ile-98, trp-63 and trp-108 is affected at a lower temperature (below 35°C) than that around phe-3 and ile-88.

The regions of the protein which become looser with increasing temperature can perhaps be identified to some extent from the ^{13}C NMR results. The vicinity of a wider area around the substrate groove rather than just the vicinity around subsites D and E, appears to be the primary locus for the structural changes, particularly at lower temperatures. There are three reasons for suggesting this:

(a) The thermal shifts observed in the resonances of residues in the groove, namely ile-98, trp-108 and tyr-53, are more significant than those of any other resolved resonances.

(b) The thermal shifts of the resolved resonances of lysozyme bound to NAG are either absent, or smaller than those of free lysozyme. This decrease is most clearly seen in the ile-98 methyl resonances. The NAG holds the active site in a fixed conformation which remains stable under varying thermal conditions.

(c) The substrate groove is not of fixed dimensions. Initial expansion of the protein is most likely to occur around this flexible region where the residues are most mobile.

4.3.2.3 Arg Residues

The more-upfield arg C^{ζ} resonance at 157.8 ppm coalesces with the main solvent-exposed arg C^{ζ} resonance at 158.0 ppm at temperatures well below the main transition temperature. This strongly suggests that long-chain polar residues and those near to the protein surface are likely to normalise somewhat before the main transition temperature is reached.

4.3.3 Summary

Clearly, it is difficult to produce a rigorous explanation for the temperature-dependence of the spectrum of lysozyme. The ^{13}C chemical shift data obtained in this study rule out a significant conformational change at any one temperature. The observed changes are consistent with increasing mobility of the protein residues, possibly accompanied by some swelling of the general protein structure. The substrate groove is probably the primary locus for this swelling. These changes are in addition fully reversible.

The unfolding process of lysozyme at pD 3.2 can be viewed as a one-step gross-unfolding mechanism with small conformational changes at the predenaturation temperature.

The observations made in this study enhance the need to re-examine the behaviour of proteins over a wide range of temperatures. The small conformational differences,

if present, may reveal why allosteric enzymes such as lysozyme have an operating temperature and pH at which their activity is optimised.

4.4 THE DENATURED STATE OF RIBONUCLEASE A AND HEW LYSOZYME

4.4.1 Results and Discussion

The nature of the thermally denatured state of RNase at pD 3.2 as observed by ^{13}C NMR has been described previously by Howarth and Lian, 1981 (Appendix XI). The spectrum of thermally denatured RNase at pD 5.5 resembles that at pD 3.2 except for the pD-dependent shifts of the glu side-chain resonances.

Only very small differences are observed between the spectra of urea-denatured and heat-denatured RNase at pD 3.2 (Fig. 4.11). It appears therefore that the structure of the unfolded state is largely independent of the denaturant used and of the pD at which denaturation takes place.

The nature of the unfolded state of lysozyme is also investigated in the present study. Fig. 4.12 shows the spectra of lysozyme when denatured by 3 methods - heat, urea and performic acid oxidation - all at pD 3.2. The resonances observed between 11.45 ppm and 11.73 ppm arise from the ile C^{δ} methyl groups. It is clear in all three cases that the five ile methyl groups are magnetically inequivalent.

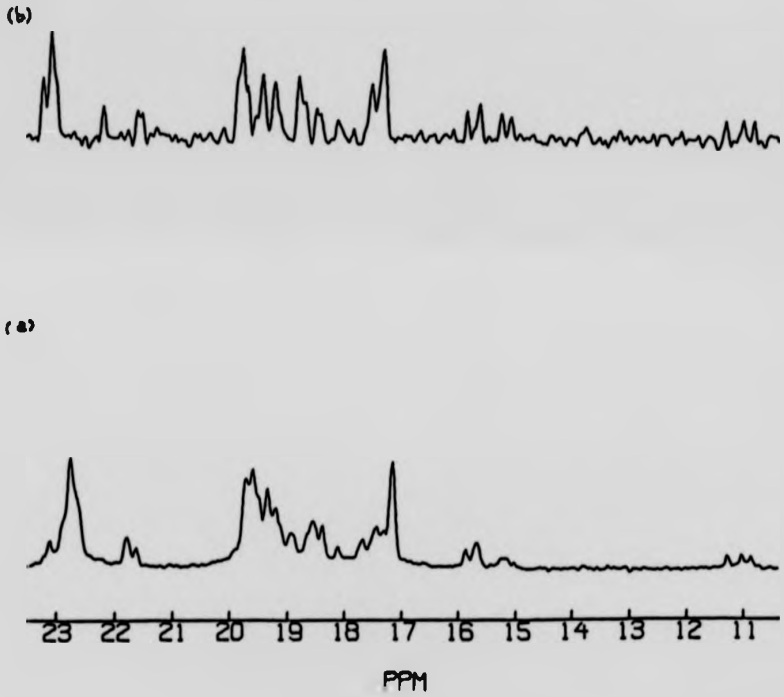

Fig. 4.11 Portions of proton-decoupled ^{13}C NMR spectrum of unfolded RNase.
(a) Thermally denatured at 55°C, pD 3.2, 6 mM in D_2O.
(b) Urea-denatured at 25°C, pD 3.2, 6 mM in D_2O.

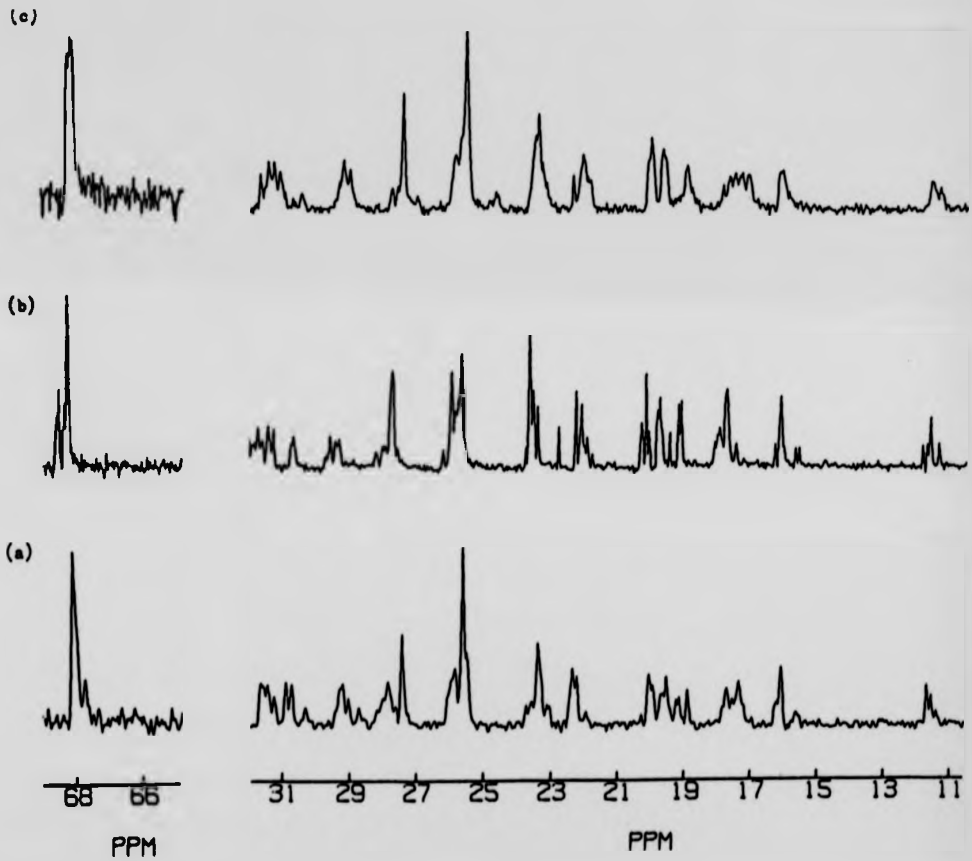

Fig. 4.12 Portions of proton-decoupled ^{13}C NMR spectrum of unfolded lysozyme.
(a) Thermally denatured at 75°C, pD 3.2, 6 mM in D_2O.
(b) Urea-denatured at 25.0°C, pD 3.2, 6 mM in D_2O.
(c) Oxidised by performic acid at 50°C, pD 3.2, 5 mM in D_2O.

The main features of the spectra of denatured lysozyme appear to be very similar to those of denatured RNase. The residues with hydrophobic groups attached, such as ile, phe and thr show resolved resonances, whereas the hydrophilic residues such as glu and tyr show slightly broadened single resonances. The heterogeneity in the chemical shifts of the ile and thr groups of the denatured protein is still present even when the disulphide bridges have been cleaved using performic acid oxidation.

The spectra of lysozyme denatured in the three different ways differ from each other in detail. Of the three spectra in Fig. 4.12, that of urea-denatured lysozyme shows the greatest chemical shift heterogeneity for resonances from like carbon atoms. It is possible that the final state attained on urea unfolding is more rigidly structured than that attained by heat denaturation or performic acid oxidation. This concurs with the fact that urea is a weak denaturant when applied to lysozyme (Lapanje, 1978).

It appears that a hydrophobically bound structure may be a common feature of soluble denatured proteins. The hypothesis of a hydrophobically bound residual structure can in principle be tested by observing the state of the denatured protein in a less-polar solvent than D_2O. The polarity of D_2O can be decreased by the addition of a nonaqueous cosolvent such as ethanol or dioxane. The spectra of lysozyme when thermally denatured in 50% Ethanol-D_2O and in 40% Dioxane-D_2O cosolvent systems are shown in

Fig. 4.13. It appears that the hydrophobic ile C^{δ} carbons are magnetically more equivalent in the mixed solvents than in D_2O alone. The resonances of these carbons are now seen as a broad singlet at 11.7 ppm in the spectrum of the denatured lysozyme.

These results can be explained by an increase in the state of solvation of the hydrophobic ile side-chains caused by the presence of the nonaqueous cosolvent. The hydrophobic residues now begin to resemble the hydrophilic residues in their solvent exposure. Therefore, the hypothesis of a hydrophobically bound structure within the denatured protein is not unreasonable.

4.4.2 Summary

The deviation of the structure of each of the two denatured proteins from a random coil is significant. In each case the residual structure (after unfolding) is a structure stabilised by short-range hydrophobic interactions. For RNase, it has been proposed that the remnant structure is a molecular network based on the nucleation sites, which are essential for initiating the folding of this protein (Burgess and Scheraga, 1975; Anfinsen and Scheraga, 1975). It is possible that the retention of structured areas is a common feature of proteins particularly if folding is to occur efficiently.

Fig. 4.13. It appears that the hydrophobic ile C^{δ} carbons are magnetically more equivalent in the mixed solvents than in D_2O alone. The resonances of these carbons are now seen as a broad singlet at 11.7 ppm in the spectrum of the denatured lysozyme.

These results can be explained by an increase in the state of solvation of the hydrophobic ile side-chains caused by the presence of the nonaqueous cosolvent. The hydrophobic residues now begin to resemble the hydrophilic residues in their solvent exposure. Therefore, the hypothesis of a hydrophobically bound structure within the denatured protein is not unreasonable.

4.4.2 Summary

The deviation of the structure of each of the two denatured proteins from a random coil is significant. In each case the residual structure (after unfolding) is a structure stabilised by short-range hydrophobic interactions. For RNase, it has been proposed that the remnant structure is a molecular network based on the nucleation sites, which are essential for initiating the folding of this protein (Burgess and Scheraga, 1975; Anfinsen and Scheraga, 1975). It is possible that the retention of structured areas is a common feature of proteins particularly if folding is to occur efficiently.

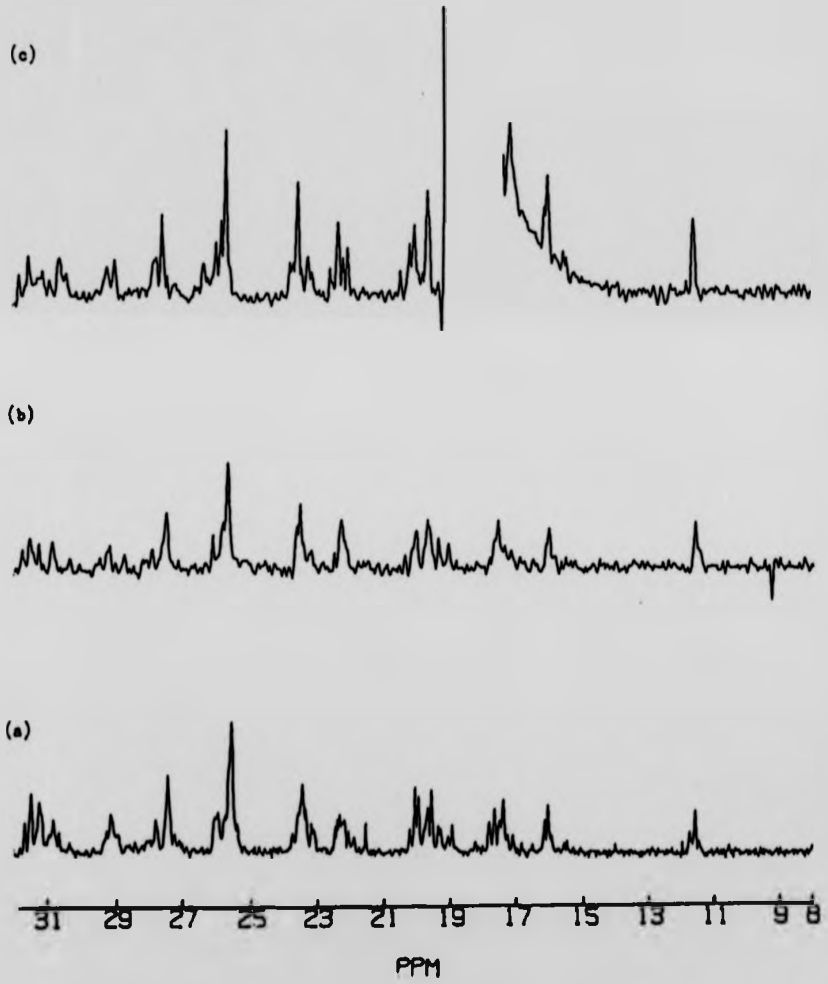

Fig. 4.13 Spectral region from 8.0 ppm to 32.0 ppm of proton-decoupled ^{13}C NMR spectrum of thermally unfolded lysozyme at 60°C, pD 2.3 in different solvent systems.
(a) D_2O
(b) 40% Dioxane, 60% D_2O
(c) 50% Ethanol, 50% D_2O

4.5 SUMMARY

Several insights into the process of thermal unfolding in proteins have resulted from this study. It has explicitly shown that predenaturational changes are very local, and, contrary to other studies, are not confined to the exposed residues. Rather, the thermal shift variations of the hydrophobic residues are significant, especially at low temperatures. This is the first time that hydrophobic residues have been monitored in the protein unfolding process because they remain 'silent' to other spectroscopic methods.

A hydrophobically-bound structure exists in the unfolded state of the proteins examined, this structure being independent both of the denaturant and of the pD used.

It is appropriate here to summarise the usefulness of high-resolution ^{13}C NMR spectroscopy for probing protein unfolding processes. Its advantage in this study is that many different types of residues throughout the protein structure can be examined concurrently. This is especially useful if the resolved resonances have been assigned to specific residues. Furthermore, the ^{13}C NMR technique can, in principle, distinguish between structures which fluctuate on the time-scale of the NMR method and those which fluctuate either faster or much slower. This method can also identify the stable regions of proteins.

CHAPTER 5

UREA UNFOLDING OF RIBONUCLEASE A AND HEW LYSOZYME

A. RIBONUCLEASE A

5.1 INTRODUCTION

Bovine ribonuclease (RNase) is the protein most often used in urea denaturation studies. So far, no convincing unfolding mechanism has been proposed although Benz and Roberts (1975(b)) in their ^{1}H NMR studies observed marked changes in the resonances of the his C(2) protons and other less definite changes in the aromatic and met S-methyl regions. From their results, they proposed:

(i) the presence of binding sites in RNase for urea at low denaturant concentrations;

(ii) the existence of at least two intermediate states in the unfolding process; and

(iii) similarity between the order of unfolding of the his residues in urea denaturation and in low pH thermal denaturation.

Since these proposed features were based only on the information from four (his) residues out of a total of the 124 present in RNase, their results are somewhat preliminary. Furthermore, Markley (1975(a)), Patel *et al.* (1975) and Lenstra (1979) have all reassigned the two active site his residue (12 and 119) resonances referred to by Benz and Roberts. His-12 now becomes his-119 and *vice versa*. In view of this, it is necessary to examine

the behaviour of other residues in the protein in the presence of increasing concentrations of urea.

In this research the mechanism of urea-unfolding and the structure of the denatured protein are investigated using high-resolution ^{13}C and ^{1}H NMR by means of which many more resolved resonances can now be identified. The nature of the urea-denatured protein is also examined.

5.2 MATERIALS AND METHODS

Urea from the Sigma Chemical Co. was used without further purification. Preweighed amounts of solid urea were added to RNase solution in D_2O (0.05 M NaCl) and the pD adjusted to either pD 3.2 or pD 5.5. The NMR spectra were acquired as described in Chapter 2. All experiments were carried out at $30^{o}C \pm 0.5^{o}C$.

5.3 RESULTS

5.3.1 ^{1}H NMR Studies (at pD 3.2 and pD 5.5)

At pD 3.2, changes in the chemical shifts of the his C(2)H resonances are seen at low concentrations of urea (< 2 M). The chemical shifts are plotted as a function of urea concentration in Fig. 5.1. The most significant shift perturbation is observed in the his-12 C(2)H resonance which shifts progressively downfield throughout the whole range of urea concentrations. At

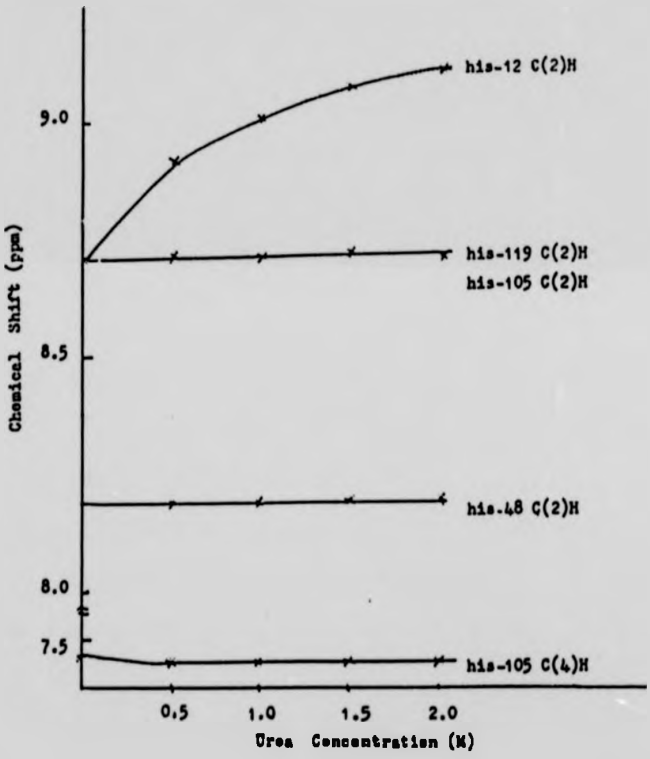

Fig. 5.1 The dependence of the chemical shift of the C(2)H resonance of his-12, his-119, his-105 and his-48 and the C(4)H resonance of his-105 of RNase on urea concentration, pD 3.2, 30°C.

2 M this resonance is 0.42 ppm downfield from its position in the spectrum of the native enzyme at pD 3.2. At 2.5 M urea, the peak corresponding to the C(2) proton of the his residues in the denatured protein is observed at 8.6 ppm. The areas of the four his C(2)H resonances do not appear to decrease simultaneously (Fig. 5.2).

In the present studies, at pD 5.5 the his-12 C(2)H resonance is broadened and it is not possible to follow the shift of this resonance in the presence of varying concentrations of urea. From the area of the his-C(2)H resonances, it can be seen that the two-proton resonance at 8.60 ppm (C(2)H of his-12 and his-119) in the spectrum of native RNase integrates for only one proton in the presence of 0.5 M urea. Since the his C(2)H peak of the denatured protein is not detected at this concentration of urea, it is reasonable to suggest that one component of the resonance at 8.60 ppm has shifted. At this pD value, the shift perturbations of his-119 C(2)H, his-105 C(2)H and his-105 C(4)H resonances are complete at 1 M urea. The magnitude of these shift perturbations is small, being between 0.02 ppm and 0.04 ppm.

5.3.2 ^{13}C NMR Studies (at pD 3.2)

5.3.2.1 Region between 11.0 ppm and 26.0 ppm (Methyl Resonances)

Small changes in the chemical shift of many resolved ^{13}C aliphatic resonances are seen at low concentrations of urea (< 2 M). As the urea concentration

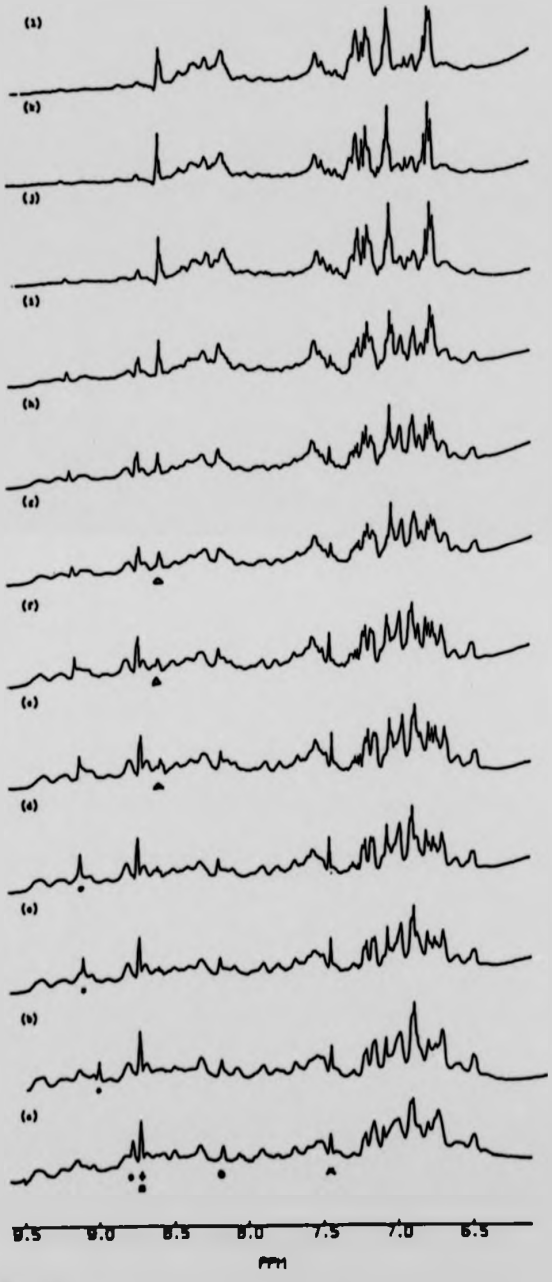

Fig. 5.2 ^{1}H NMR spectra (7.0 ppm-9.0 ppm) of RNase (6 mM, 0.05 M NaCl) with increasing amounts of urea, pD 3.2, 30°C. Peak designations are: •, his-12 C(2)H; +, his-105 C(2)H; □, his-119 C(2)H; O, his-48 C(2)H; X, his-105 C(4)H; Δ his C(2)H resonance of denatured protein.
(a) 0 M, (b) 1 M, (c) 2 M, (d) 2.2 M, (e) 2.5 M, (f) 2.8 M, (g) 3.2 M, (h) 3.4 M, (i) 3.9 M, (j) 4.2 M, (k) 4.7 M, (l) 5 M.

is increased, more-specific shift perturbations are observed in peaks 4, 5, 10, 12, 13 and in many ala (peak 9) and thr methyl resonances (between 19.5 ppm and 20.5 ppm) (Fig. 5.3(i)). The chemical shifts of some of the resolved resonances between 12.0 ppm and 28.0 ppm, when plotted as a function of urea concentration at pD 3.2, are shown in Fig. 5.4. Within this spectral region, many of the shift changes are complete at 2 M urea.

As the urea concentration is increased beyond 2.5 M, additional extensive changes in the spectrum are observed (Fig. 5.3(ii)). The linewidth of many of the resonances begins to increase. The signals representing the residues of denatured RNase become recognisable at 3.5 M urea. Since almost all the peaks of the denatured protein are present at this concentration of urea, a one-step unfolding rather than a stepwise unfolding process of the residues bearing the methyl groups is indicated.

5.3.2.2 Region between 66.0 ppm and 70.0 ppm (Thr C^{β} Resonances)

The thr C^{β} resonances appear between 66.0 ppm and 70.0 ppm at pD 3.2.. In the presence of low concentrations of urea, linewidth and shift changes are observed (Fig. 5.5); notably peak d appears to move upfield to coalesce with peak c when 1.5 M urea is added. The changes in the C^{β} resonances are complete at low concentrations of urea ($\leq$ 1.5 M). At 2.5 M urea, the resonance corresponding to the thr C^{β}

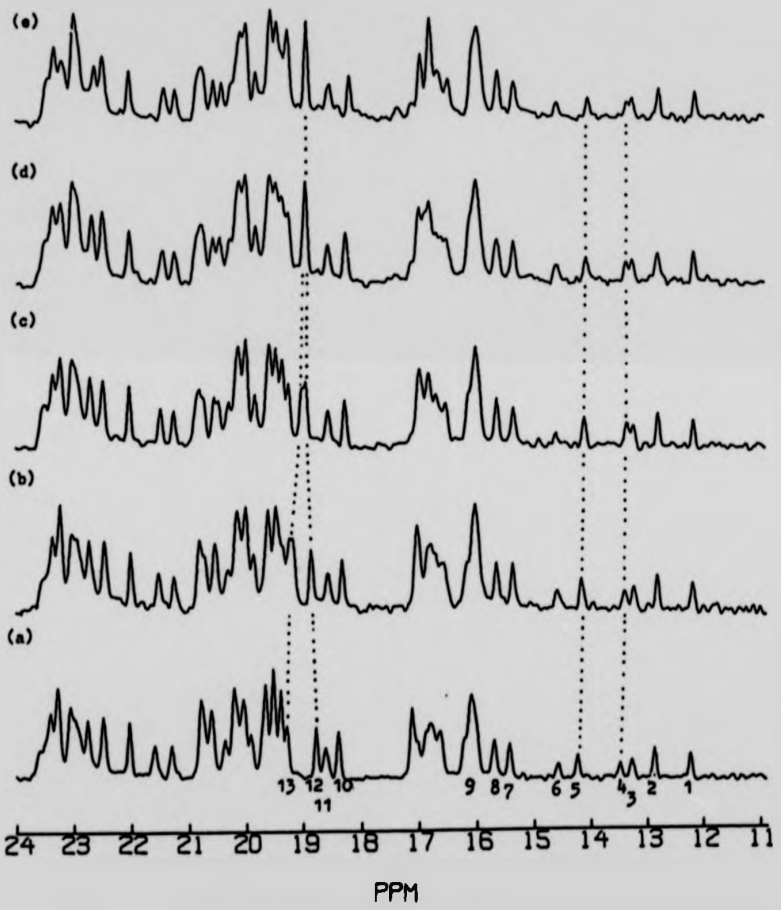

Fig. 5.3(i) Spectral region from 11.0 ppm to 24.0 ppm of the proton-decoupled ^{13}C NMR spectrum of RNase (6 mM, 0.05 M NaCl) to show the changes in the spectrum with increasing urea concentration, pD 3.2, 30°C. Peak numbers indicate the position of individual methyl carbon resonances.
(a) 0 M, (b) 0.5 M, (c) 1.5 M, (d) 2 M
(e) 2.5 M.

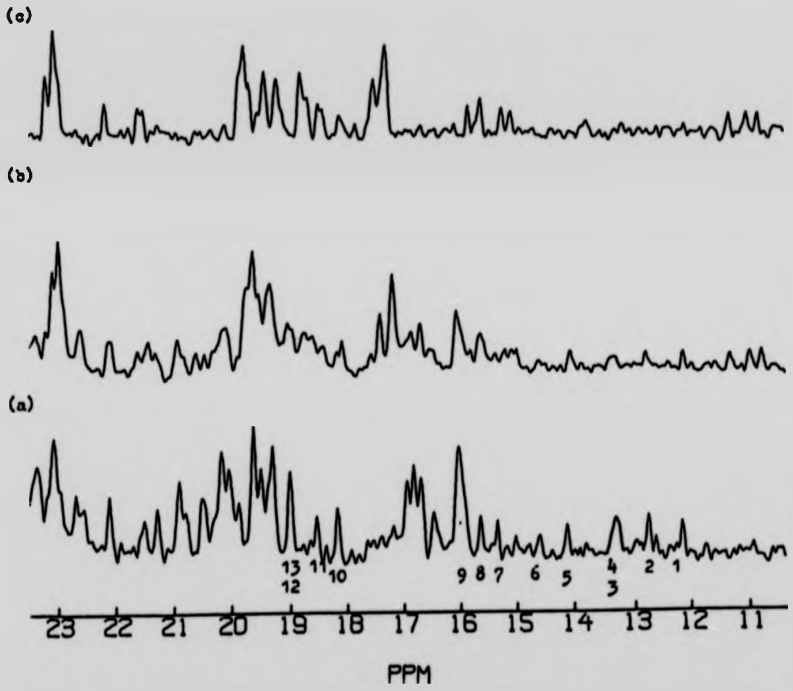

Fig. 5.3(ii) Spectral region from 11.0 ppm to 24.0 ppm of the proton-decoupled ^{13}C NMR spectrum of RNase (6 mM, 0.05 M NaCl) to show the changes in the spectrum with increasing urea concentration, pD 3.2, 30°C. Peak numbers indicate the position of individual methyl carbon resonances.
(a) 3 M, (b) 3.5 M, (c) 6 M.

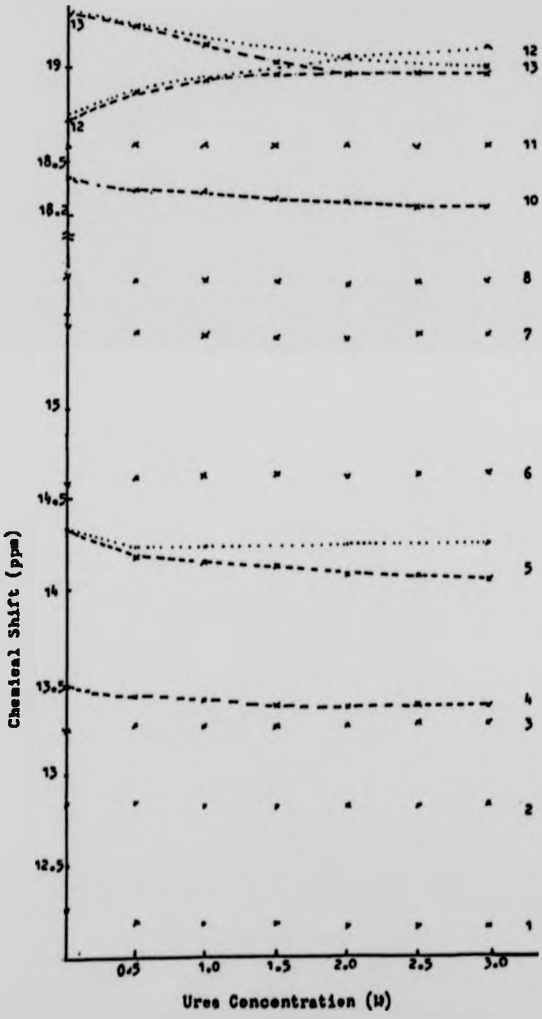

Fig. 5.4 The dependence of the chemical shift of methyl carbon resonances of RNase on urea concentration. Except for the values of the pD, sample conditions are given in the legend of Fig. 5.3(i). Peak numbers are those of Fig. 5.3.
------, pD 3.2; ....., pD 5.5.

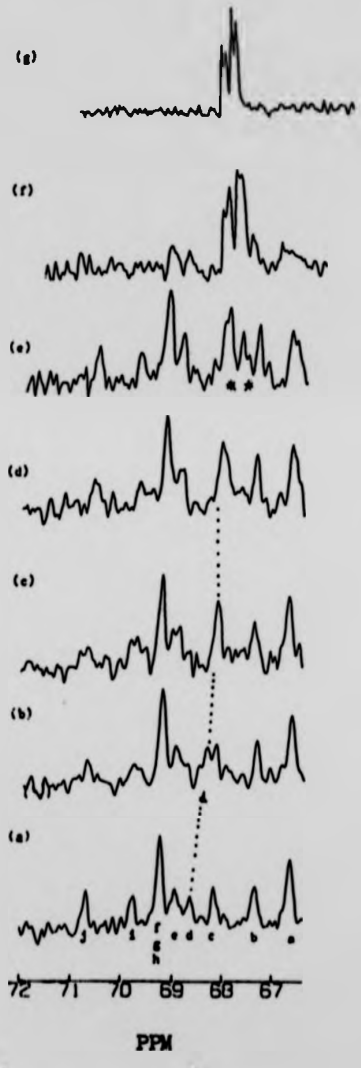

Fig. 5.5 The thr C^{β} region of the ^{13}C NMR spectrum of RNase (6 mM, 0.05 M NaCl) in the presence of 0 M to 6.0 M urea, pD 3.2, 30°C. The peak letters indicate the positions of individual thr C^{β} resonances. The peaks marked * in spectrum (e) correspond to the thr C^{β} resonances in the urea-denatured protein. (a) 0 M, (b) 0.5 M, (c) 1.5 M, (d) 2 M, (e) 2.5 M, (f) 3.5 M, (g) 6 M.

resonance of the denatured protein is detected (Fig. 5.5(e)).

5.3.2.3 Region between 154.0 ppm and 159.0 ppm (Tyr C^{ζ} Resonances)

The chemical shifts and linewidths of the tyr C^{ζ} resonances are not perturbed in the presence of less than 2 M urea. The tyr-97 C^{ζ} resonance begins to broaden at about 2 M urea. The tyr-25 C^{ζ}, and tyr-115 C^{ζ} resonances broaden when 2.5 M urea is present. The intensity and chemical shift of the tyr-76 C^{ζ} resonance is not perturbed even at 3.5 M urea (Fig. 5.6).

The chemical shift of the tyr C^{ζ} resonance of the denatured protein is very close to that of the tyr-92 C^{ζ} resonance in the native protein. Hence the broadening observed at 155.42 ppm when 2.5 M urea is added is due to the appearance of the tyr C^{ζ} resonance of the denatured protein.

5.4 DISCUSSION

The existence of several intermediate states in the unfolding process of RNase is indicated here. The intermediates are essentially the native structure with a few localised modifications. This seems to imply that for the protein to unfold, it is essential that the molecule undergoes some preparatory structural changes to afford a more efficient gross unfolding.

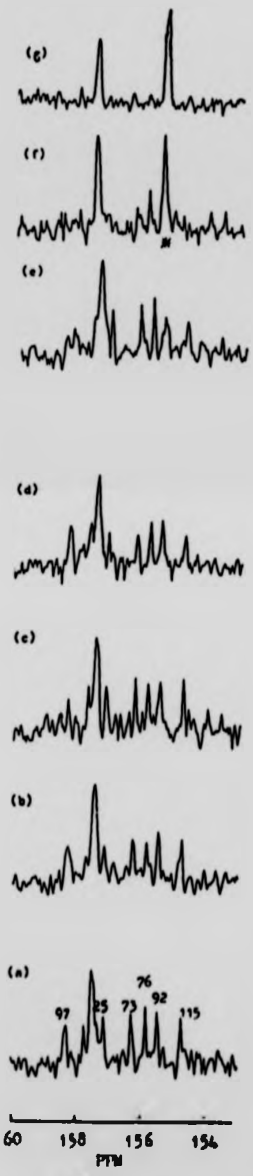

Fig. 5.6 The tyr C^{ζ} and arg C^{ζ} region of the ^{13}C NMR spectrum of RNase (6 mM, 0.05 M NaCl) in the presence of 0 M to 6 M urea, pD 3.2, 30°C. The numbers above each peak in spectrum (a) are assignments to specific tyr residues (this work; Santoro *et al.*, 1979). The peak marked * corresponds to the tyr C^{ζ} resonance in the urea-denatured protein. (a) 0 M, (b) 0.5 M, (c) 1.5 M, (d) 2 M, (e) 2.5 M, (f) 3.5 M, (g) 6 M.

5.4.1 The Effects of Low Concentrations of Urea (< 2 M)

5.4.1.1 ^{1}H NMR Studies (at pD 3.2 and pD 5.5)

There have been suggestions that urea binds to at least two sites at pD 5.5 (Benz and Roberts, 1975(b)). However, neither the nature of these binding sites nor the exact number of available urea binding sites in RNase is certain. In the present study, the shift of the his-12 C(2)H resonance with increasing concentration of urea at pD 3.2 is away from the position of the resonance of the solvent-accessible his residues. That is, the conformational changes produced by low urea concentrations do not result in a solvent-like environment for this his residue. It is likely that urea binds at a position close to the his-12 residue so as to perturb its magnetic environment directly.

The specificity of the shift perturbation of the his-12 C(2)H resonance is demonstrated by the fact that at low urea concentrations and pD 3.2, the C(2)H resonances of his-119 and his-105,the C(4)H resonance of his-105, and the aromatic proton resonances between 6.5 ppm and 7.3 ppm are not perturbed. The his-12 residue appears to be the strongest urea binding site in RNase, the C(2)H resonance of this residue being shifted at both pD 3.2 and pD 5.5 (this work; Benz and Roberts, 1975(b)).

Also, at pD 3.2 and pD 5.5, the complete absence of the resonances representing the his residues in the denatured protein shows that there is no appreciable unfolding at these low urea concentrations.

5.4.1.2 ^{13}C NMR Studies (at pD 3.2)

The small shift changes observed in most of the resolved resonances on the addition of 0.5 M urea are non-specific solvent shifts. More specific shift perturbations are noted for peaks 4, 5, 10, 12 and 13, these perturbations being complete at relatively low urea concentrations (≤ 2,0 M). The shifts observed in the presence of 2.0 M urea do not coincide with the shifts of the unfolded protein. That is, initial partial unfolding of RNase is not indicated by these shift changes.

Peak 4 has been assigned in this study to the met-13C$^{\epsilon}$ atom on the basis of its pD titration characteristics (Chapter 3, Section 3.5.2.3). The titration shift of this peak with increasing concentrations of urea may be attributable to the proximity of met-13 to his-12. When urea binds to his-12, the conformation of the protein surrounding this his residue would be expected to change, and this will in turn perturb the magnetic environment of the met-13 residue.

The existence of a his-12-urea interaction is further underlined by the titration shifts of peaks 12 and 13. At pD 5.5 peaks 12 and 13 show shift changes of similar magnitudes to those observed at pD 3.2, whereas peak 10 remains unperturbed throughout the urea concentration range used. Resonances in this part of the ^{13}C NMR spectrum (18.0 ppm to 20.0 ppm) normally arise from the val methyl carbons. From the specificity and magnitude of the shifts of peaks 12 and 13 at pD 3.2 and at pD 5.5,

it is probable that peaks 12 and 13 belong to val residues which are spatially close to the his-12 residue, for example, val-47 (The interatomic distance between his-12 C^{α} and val-47 $C^{\gamma 2}$ is 5.58 Å.). (It is feasible to attribute the shift perturbation of peak 10 at pD 3.2 to small conformational changes involving the active site cleft which accompany the interaction(s) between urea and RNase.)

The characteristics of peaks 12 and 13 at low urea concentrations are quite different from those observed during the thermal denaturation of RNase at pD 3.2 or pD 5.5. Under the latter conditions the two resonances remain unchanged right up to the temperature just before thermal unfolding. The proposal that differences in the mechanism of denaturation by the two processes exist is enhanced by the distinct differences in the behaviour of thr C^{β} resonances during urea and thermal unfolding at pD 3.2. Under the thermal unfolding conditions, one component of the multiplet f-g shifts steadily upfield when the temperature is increased from 25°C to 44°C (see Chapter 4, Section 4.2.1)and the thermal shift of peak d is complete at 35°C. When urea is used as the denaturant, only peak d moves upfield steadily in the presence of increasing concentrations of urea; the other thr C^{β} resonances are not perturbed.

Owing to an insufficient knowledge of the denaturation processes at molecular level, interpretation of the results is bound to be speculative. Any binding of urea to the active site his residues must perturb the ile (peak 5), thr (peak d) and some of the

val resonances *via* conformational changes rather than as a result of a direct interaction with the urea molecule. This must be so because these residues are farther than 7.0 Å from the active site his-12 residue.

Furthermore, there may be more than one binding site. Lapanje (1978), using guanidinium chloride as the denaturant, postulated that in addition to the charged groups on the proteins, the backbone peptide groups could also be major binding sites for the guanidinium ion. Therefore, this hypothesis must be considered when discussing the urea denaturation of RNase. Unfortunately, in the ^{13}C NMR spectrum, the main-chain C^{α} and carbonyl carbon resonances are not well-resolved even at high field and consequently these resonances cannot be analysed.

In summary, in the presence of urea at concentrations below that needed for gross denaturation, the RNase molecule appears to undergo localised changes. These changes can be attributed to the direct binding of urea to one or more sites, together with (i) a reduction in hydrophobic interactions, and/or (ii) a weakening of internal hydrogen bonds. Whatever the cause(s) of these localised changes, they do not appear to result in local unfolding.

5.4.2 The Effects of High Concentrations of Urea (> 2 M)

In the presence of 2.5 M urea, the resonances of the his residues in the denatured protein are clearly detectable in the ^{1}H NMR spectrum. At pD 3.2, the areas

of the different his resonances do not decrease in the same way as a function of urea concentration. It appears that the order of unfolding can be defined as his-119, his-12, then his-105. It is clear from Fig. 5.2 that the relative area of the his-48 C(2)H resonance is difficult to estimate. The results obtained in the present study concur with those of Benz and Roberts (1975(b)) who studied urea denaturation at pD 5.5.

The ^{13}C NMR resonances in the spectral regions from 11.0 ppm to 26.0 ppm and from 66.0 ppm to 72.0 ppm undergo little change in the urea concentration range between 2M and 2.5 M. A stable urea-protein complex appears to exist when the urea concentration lies within this range.

Between 2.5 M and 3 M urea, the ^{13}C spectra are less amenable to analysis because of line broadening, with a concomitant decrease in intensities. This can be explained in part by the increased internal and inter-state exchanges. The presence of these exchanges is particularly noticeable in the thr C^{γ} (19.5 ppm-20.5 ppm), thr C^{β} (66.0 ppm-72.0 ppm) and tyr C^{ζ} (154.0 ppm-159.0 ppm) resonances. For some of these resonances, broad and structureless peaks are seen. At these high concentrations of urea (> 2 M), the observed broadening indicates an exchange rate of approximately 25 Hz.

The loss of resolution could also be partly due to the low concentration of the native state. Intermediate exchange between different conformations implies that at 2.5 M to 3 M urea, the native structure is destabilised to some degree, even before it unfolds. The line broadening

is more significant in the thr, the tyr and one met resonances than in the methyl resonances of the hydrophobic residues ile, val and leu.

At 2.5 M urea resonances of the thr and tyr residues (and of the his residues in ^{1}H NMR) of the denatured protein are clearly detected. The ^{13}C NMR results appear to imply that the tyr-76 residue lags behind the other tyr residues during the unfolding process. As for the thr residues, there is no conclusive evidence to show preferential unfolding in one or more of these residues. From the present set of data one can only conclude broadly that the thr, tyr, and his residues (and perhaps one met residue) which are all generally nearer to the surface of the compact protein structure, unfold earlier than the buried hydrophobic residues. This conclusion concurs with that of Matheson and Scheraga (1979a) who investigated the thermal unfolding of RNase using non-specific surface labelling techniques.

5.4.3 The Mechanism of Urea Unfolding

From the above description a plausible mechanism for the urea denaturation process in RNase is:

$$N + U \rightleftharpoons (NU)_i \cdots \rightleftharpoons (NU)_s$$
$$(NU)_s \rightleftharpoons (NU)_j \cdots$$
$$(NU)_j \cdots \rightleftharpoons (NU)_D$$

where N represents the native state, $(NU)_i \cdots$ the urea-protein complexes formed between 0.5 M and 2 M urea,

$(NU)_S$ the 'stable' complex between 2 M and 2.5 M urea $(NU)_J$... the complexes at urea concentrations greater than 3 M and $(NU)_D$ the unfolded state.

The ^{13}C NMR and ^{1}H NMR results in this study show that the protein is essentially intact prior to gross unfolding, with early local conformational changes only involving a few residues. More often than not, the residues which show early normalisation of their resonances are those already near to the surface of the protein molecule. The main unfolding of the 'core' of the protein appears to occur in one step. This is best seen from the changes in the resolved ^{13}C resonances of the ile $C^{\gamma 2}$, ile C^{δ} and met C^{ε} atoms.

5.4.4 The Nature of the Unfolded State

The nature of the unfolded state of RNase brought about by urea denaturation has been discussed in greater detail in Chapter 4. Suffice to say here that the structure of the unfolded state deviates from a random coil structure.

5.5 CONCLUSIONS

The ^{13}C NMR results obtained in this study have demonstrated the existence of some early conformational changes in many of the protein residues. An intervening state exists in the presence of between 2 M and 2.5 M urea where an almost stable protein-urea complex is formed.

Finally, at urea concentrations higher than 2.5 M, gross unfolding occurs with the unfolding of some of the buried residues (ile, and val) lagging behind other more solvent-accessible groups (thr, his, tyr). These results concur with a hypothesised mechanism of denaturation by urea (and guanidinium chloride) which is as follows.

At low concentrations there are close contacts between the denaturant and sections of the protein molecule, for example, around the his-12 residue. These resulting interactions weaken the forces that stabilise the native conformation. This leads to an initial loosening of the protein structure followed by the penetration of more denaturant molecules into the structure. By increasing the urea concentration still further, more denaturant molecules are bound, which in turn leads to complete unfolding.

B. HEW LYSOZYME

5.6 INTRODUCTION

The mechanism of the urea denaturation of HEW lysozyme is still not clear. Although a vast amount of work using different methods has been carried out (Snape, 1974, and references therein) the precise interaction between lysozyme and urea, particularly at low urea concentrations, is not yet established. In the crystalline state, Snape (1974) postulated that

one urea molecule binds at the acetamido specificity pocket and that at least three other urea molecules bind to other parts of the active site. Barnes *et al.* (1972), using circular dichroism, concluded that upon interaction of 8 M urea with lysozyme, a conformational rearrangement occurs around the disulphide bond or bonds with little or no disruption of the α-helical structure.

It is now known that urea does not act by the direct large-scale replacement of bound water. Rather, the direct binding of urea to globular proteins is important (Lapanje, 1978). Bradbury and King (1969) examined the ^{1}H NMR spectra of lysozyme-urea solutions at pH 2.8 as a function of urea concentration and concluded that the unfolding of the protein proceeds in at least two steps.

It is hoped that with the ability to look at individual atoms in the protein molecule using high-resolution ^{13}C NMR some further insight into the nature of the urea-lysozyme interaction may be obtained.

5.7 MATERIALS AND METHODS

Preweighed amounts of solid urea (Sigma Chemical Co.) were added to HEW lysozyme solution in D_2O and the pD adjusted to pD 3.2. The NMR spectra were acquired as described in Chapter 2. All experiments were carried out at $25^{o}C \pm 0.5^{o}C$.

5.8 RESULTS

The spectra of lysozyme in the presence of different concentrations of urea at pD 3.2 are shown in Fig. 5.7. A general decrease in the line widths of the resonances is observed on the addition of 1 M urea. Above this concentration, the linewidths remain constant up to 4 M urea.

The most obvious and significant shift changes are observed in the resonances assigned to met-105 C^{ε} and to the two leu residues between 21.72 ppm and 21.93 ppm (Fig. 5.7). These two sets of shift perturbations are complete at low concentrations of urea (1 M) under the experimental conditions used in this study. Further addition of up to 4 M urea does not appear to cause further shift perturbations.

Line broadening of many of the methyl resonances begins to appear when the urea concentration is increased to 4 M. Many of the individual resonances are however, still discernible. There appears to be more broadening of the main ala and thr methyl resonances than of the ile and val methyl resonances at this concentration.

No spectrum in Fig. 5.7 resembles the spectrum of lysozyme at pD 3.2 obtained at temperatures higher than 25°C. This means that the spectra shown in Fig. 5.7 are specific for lysozyme in the presence of urea at a concentration below that required for gross unfolding. In addition, the spectrum of lysozyme in the presence of 100 mM N-acetylglucosamine (NAG) at pD 3.2 and 45°C (Fig. 3.10)

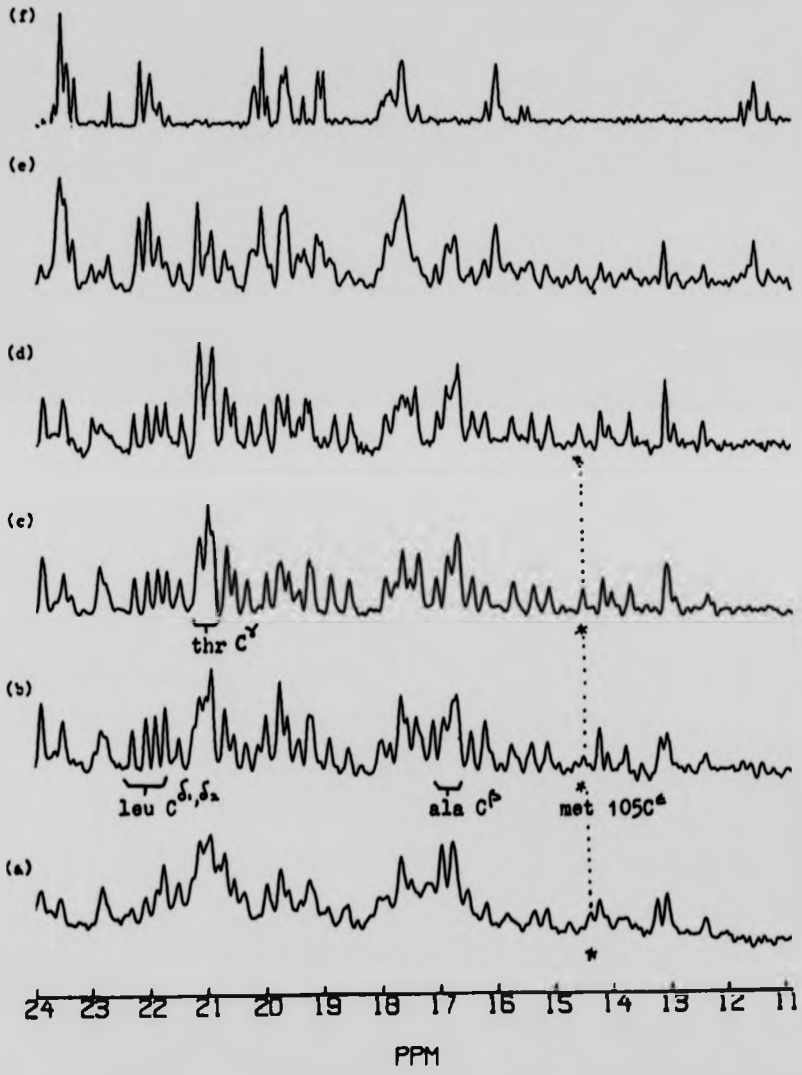

Fig. 5.7 Spectral region from 11.0 ppm to 24.0 ppm of the proton-decoupled ^{13}C NMR spectrum of lysozyme (7 mM in D_2O) to show changes in the spectrum with urea concentration, pD 3.2, 25°C. The met-105 C^{ε} resonance (*) is identified. The resonances tentatively assigned to the methyl carbon atoms of ala, thr and leu residues are also indicated.
(a) 0 M, (b) 1 M, (c) 2 M, (d) 4 M, (e) 6 M, (f) 8 M.

differs significantly from the spectra shown in Fig. 5.7.

At 6 M urea, the spectrum shows the urea-denatured lysozyme present in slow exchange with the 'native' lysozyme. The denaturation process appears to be essentially one-step because significant differential line broadening and/or early normalisation of the resonances are/is not detected. All the resonances of the denatured protein are distinguishable in the spectrum using 6 M urea (Fig. 5.7(e)).

Analysis of the aromatic regions of the spectra is severely hampered by the poor S/N ratio. The nonprotonated resonances of arg C^{ζ} and tyr C^{ζ} (153.0 ppm-159.0 ppm) are not perturbed by the addition of urea over the concentration range studied. In the trp $C^{\varepsilon 2}$ and phe C^{γ} region (137.0 ppm-139.0 ppm) shift changes are apparent. In the presence of 1 M urea the resonance assigned to trp-63 $C^{\varepsilon 2}$ (*) shifts upfield by 0.15 ppm. The resonance at 138.13 ppm (o) has been assigned to either trp-28 $C^{\varepsilon 2}$ or trp-111 $C^{\varepsilon 2}$ by Allerhand *et al.* (1977). This resonance remains unperturbed throughout the urea titration (Fig. 5.8). The phe C^{γ} resonances are also not significantly perturbed by the addition of low concentrations of urea. As the other trp C^{ε} resonances have not been assigned on a one-to-one basis (except for the trp-108 $C^{\varepsilon 2}$ resonance at 136.39 ppm (+) analysis of the resonances between 137.0 ppm and 139.0 ppm cannot be carried out in detail.

As the concentration of urea is increased, decreases in the linewidths of the protonated (C^{δ}) aromatic resonances of tyr-20, tyr-23 and tyr-53 (and also of other unassigned protonated aromatic resonances between 129.0 ppm

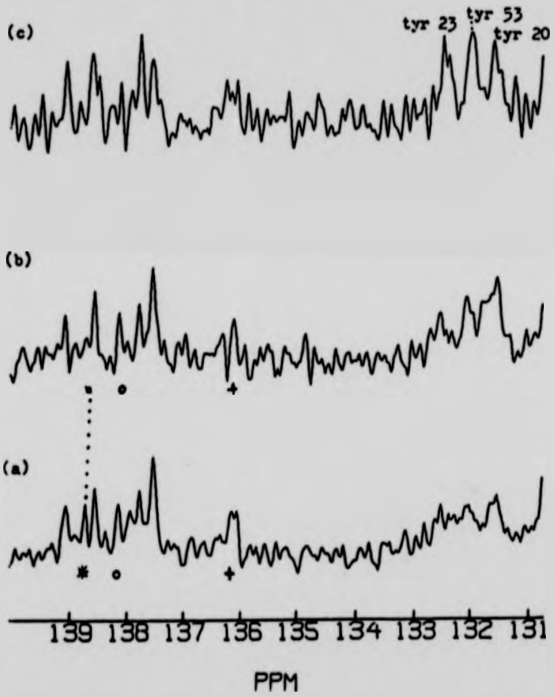

Fig. 5.8 Spectral region from 131.0 ppm to 140.0 ppm of the proton-decoupled ^{13}C NMR spectrum of lysozyme (7 mM in D_2O) to show changes in the spectrum with urea concentration, pD 3.2, 25°C.
The resonances of the δ-carbons of tyr-23, tyr-53 and tyr-20 are identified in spectrum (c). The other identified resonances are: *, trp-63 $C^{\varepsilon 2}$; 0, trp-28 $C^{\varepsilon 2}$ or trp-111 $C^{\varepsilon 2}$; +, trp-108 $C^{\varepsilon 2}$.
(a) 0 M, (b) 1 M, (c) 2 M.

and 133.0 ppm) are also observed (Fig. 5.8).

5.9 DISCUSSION

Until the lysozyme-urea interactions are known, the initial decrease in linewidths (and $^1/T_2$) of many resolved resonances must be tentatively attributed to either a decrease in the viscosity of the urea-lysozyme solution (that is, a solvent effect) and/or a general loosening of the lysozyme structure.

The progressive decrease in the linewidth of each of the tyr C^{δ} resonances prompts the conclusion that some loosening of the lysozyme molecule with increasing urea concentration is present. This loosening is not an unreasonable assumption because in crystallographic studies, many of the conformational changes observed on urea binding are associated with regions of the native structure which are in strained or irregular conformation (Snape, 1974).

Using ^1H NMR, Campbell (1977) observed that aromatic ring-flips in the tyr and phe side-chains of proteins are common. For this motion of these aromatic rings to occur, adjacent groups must be mobile. In the present ^{13}C NMR study, decreases in the linewidths of the tyr and phe methine resonances are also observed on increasing the temperature. These results suggest that apart from the general solvent effect on the linewidths of the resonances, more-specific changes such as greater internal motions of the tyr and phe residues are also present.

The perturbation of the resonances between 21.73 ppm and 21.93 ppm is specific for the interaction of lysozyme with urea. The five resolved methyl resonances in this region of the spectrum remain unchanged on further addition of urea above 0.5 M. This is interesting because this region of the ^{13}C spectrum of lysozyme is particularly susceptible to changes in conditions such as temperature, pD and the addition of sugar inhibitors. The presence of urea appears to have stabilised the area around the residues which give rise to these resonances. These residues are most likely to be leu (or thr) residues.

The magnitude and direction of the shift change of the met-105 C^{ε} resonance is similar to that induced by the binding of NAG. In the latter case, this shift perturbation is attributed predominantly to a movement of the trp-108 ring, as evidenced by a shift in the resolved trp-108 $C^{\varepsilon 2}$ resonance (Chapter 3, Section 3.4.3.1.5.1). In the present study, when 1 M urea is added the shift of the trp-108 $C^{\varepsilon 2}$ resonance is unperturbed.

Clearly, other possible interactions involving met-105 must be explored. Can the shift of the met-105 C^{ε} resonance be an indication of a movement of the disulphide bridge cys-30-cys-115 which is in close proximity to the methyl group of the met-105 residue? Barnes *et al.* (1972) have postulated that urea may bind to one of the disulphide bridges. Alternatively, the shift change in the met-105 C^{ε} resonance may possibly be explained by some more-complex movements within the protein molecule.

Snape (1974) postulated that when the centrally bound urea molecule occupies the acetamido specificity site

of lysozyme, it relaxes strained features arising from intermolecular contacts. The removal of these native strains is sufficient to trigger significant internal perturbations. The four aromatic rings - trp-28, trp-108, trp-111 and tyr-23 - which surround met-105 all undergo some movement, mainly in the form of rotations about $\alpha-\beta$ and $\beta-\gamma$ bonds. All these movements are associated with the rotation of peptides, notably 17, 22, 23 and 11. The movement of the sulphur atom of met-105, however, was not detected in this crystallographic study.

The results from the present ^{13}C NMR studies do not seem to concur with the proposed structural movements deduced from x-ray crystallography. No perturbations are observed in the assigned trp-108 $C^{\varepsilon 2}$, trp-28 $C^{\varepsilon 2}$ (or trp-111 $C^{\varepsilon 2}$), tyr-23 C^{ξ} and leu-17 $C^{\delta 1}$ resonances. Rather, the met-105 C^{ε} resonance shows significant perturbation. It is possible that the conformational changes in the aromatic residues are present but are not detected as ^{13}C chemical shift perturbations. It must also be borne in mind that the studies carried out by Snape (1974) were on the crystalline state and that the structural changes are essentially crystalline in origin. The same changes may not be present in the solution phase.

In an attempt to form an analogy between the binding of urea and the binding of the acetamide side-chain of NAG, the spectra in the presence of the two ligands (urea and NAG) are compared. The shift changes observed in the two are quite different. The

absence of the upfield shift of peak 9 (discussed in Chapter 3, Section 3.4.3.2.5.1) in the spectrum of lysozyme containing urea is most distinct.

At all concentrations up to 4 M urea, premature normalisation of specific resonances in both the aromatic and aliphatic regions is not observed. At 4 M urea, many of the trp resonances in the aromatic region of the spectrum begin to show exchange broadening. In addition, at this concentration there are indications that the main ala and thr methyl resonances begin to show greater line-broadening than the other methyl resonances. This suggests that there may be some preferential initial unfolding involving residues which are normally situated near to the surface of the protein molecule. Possible examples include at least four ala and four thr residues. The met, leu, val and ile residues which are generally considered to be less exposed to the solvent, are not likely to undergo initial structural perturbations.

5.10 CONCLUSIONS

The studies prompt some major conclusions. Firstly, the shift changes induced by urea are different from those induced by NAG. This calls for a reappraisal of the nature of the conformational changes involved when the acetamido specificity site of lysozyme is occupied.

Secondly, there appear to be two types of localised conformational change. One type perturbs the shifts of met-105 C^{ε}, trp-63 $C^{\varepsilon 2}$ and perhaps one leu

methyl resonance. These changes are complete at 1 M urea and they suggest that the urea molecule binds to lysozyme. The other type of conformational change is related to the internal motion of the tyr residues. The ring-flip of each tyr residue continues to increase over the whole range of urea concentration.

The gross unfolding of lysozyme by urea occurs in one step. No residues appear to unfold prematurely, although the loosening of a restricted section of the protein molecule, to allow for increased internal motion and for the alteration of the solvent exposure of the surface residues, appears to be present. It must be emphasised that the conclusions drawn here are only speculative as they are based on unusual shifts in one met, one trp, one leu and three tyr residues out of the total of 129 residues present in HEW lysozyme.

CHAPTER 6

RIBONUCLEASE A: INHIBITOR BINDING

6.1 INTRODUCTION

The nature of the sites responsible for the interactions between ribonuclease A (RNase) and its substrate ribonucleic acid has previously been investigated mainly through the use of x-ray diffraction and NMR spectroscopy (Arus *et al.*, 1981, and references therein). These studies have shown the existence of at least three phosphate binding sites, namely p_0, p_1 and p_2, and two sites for the binding of the nucleoside moieties, namely B_1R_1 and B_2R_2 (Fig. 6.1). Pyrimidine nucleotides were found to bind preferentially to site $B_1R_1p_1$ and purine nucleotide to $B_2R_2p_2$ (Richards and Wyckoff, 1971).

According to the data obtained by various techniques there is only one strong pyrimidine-binding site in RNase both in solution and in the crystalline state. Changes in the NMR spectra of RNase and of mononucleotides observed on the formation of a RNase-mononucleotide complex can be attributed to the attachment of a mononucleotide at this site. So far, in both ^1H and ^{13}C NMR studies, only the resonances of the active site residues - his-12, his-119, his-48 and lys-41 - have been studied in detail and found to be perturbed by the binding of various inhibitors (Jentoft *et al.*, 1981; Walters and Allerhand, 1980; Arus *et al.*, 1981).

However, two groups of residues in the protein are involved in the formation of RNase-mononucleotide

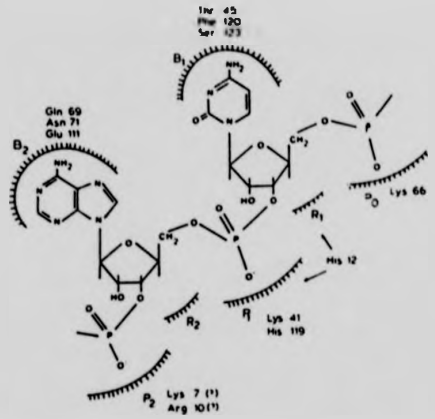

Fig. 6.1 Schematic illustration of the binding of an RNA fragment to RNase. In each subsite are listed the amino acids the participation of which is known or postulated. Taken from Arus *et al.* (1981).

complexes, namely those around the pyrimidine ring (site B_1) or purine ring (site B_2), and those which are in (or which border) the active site cleft (Fig. 6.1). These two groups of residues are a considerable distance from each other (≥ 12 Å). It is, therefore, reasonable to expect conformational changes to involve residues other than the his-12, his-119 and lys-41 residues.

The aim of the present work is to further characterise the RNase-inhibitor interactions by using high-resolution ^{13}C and ^{1}H NMR techniques. It is hoped that questions regarding the inhibitor-induced conformational changes to residues other than those in the active site cleft will be answered in some detail and that the

observed shift perturbations will allow assignments to be made.

6.2 MATERIALS AND METHODS

Cytidine-2'-phosphate (2'CMP) was supplied by the Sigma Chemical Co., cytidine-3'-phosphate (3'CMP) by PL Biochemicals Inc., Milwaukee, Wisconsin, U.S.A., and cytidine and cytidine-5'-phosphate (5'CMP) by BDH Chemicals Ltd. Reagent grade $CuSO_4$, $MnCl_2$ and Na_2HPO_4 were used.

All the cytosine inhibitors were used without further purification. When tested, the ^1H NMR spectrum of 2'CMP showed no trace of 3'CMP.

For each RNase-inhibitor solution, 1.5 ml of RNase solution in D_2O (0.05 M NaCl) was mixed with 0.8 ml of the inhibitor solution in D_2O (0.05 M NaCl). The final concentration of RNase was 6.0 mM. The final concentrations of the inhibitors in their respective solutions were: 2'CMP:40 mM, pD 5.5; 2'CMP:40 mM, pD 7.0; 3'CMP:65 mM, pD 5.5; 5'CMP:80 mM, pD 5.5; cytidine:80 mM, pD 5.5 and phosphate ion:80 mM, pD 5.5. For each experiment the pD of the solution was adjusted to the appropriate value and it was then left overnight to equilibrate. Readings of pD were taken before and after acquisition of the spectrum, the readings always agreeing to within 0.05 pD unit.

In order to study the effects of Cu^{2+} and Mn^{2+} ions, small amounts of highly concentrated salt solutions in D_2O (0.5 M to 1.0 M of $CuSO_4$ or $MnCl_2$) were added to

RNase to give the desired concentration of metal ions.

The ^{13}C and ^{1}H NMR spectra were obtained as described in Chapter 2.

6.3 STRUCTURE OF COMPLEXES OF RNase WITH CYTOSINE NUCLEOTIDES - A REVIEW

At present there is only one set of x-ray crystallographic data which gives measurements of coordinates of the atoms of the bound nucleotides, 2'CMP and 3'CMP, and the interatomic distances between these nucleotides and the protein RNase S in the complexes (Pavlovsky *et al.*, 1977). This data, although only tentative, shows that in the bound state the two nucleotides are present in the anti conformation* and that the ribose ring has a 3-endo conformation*. These results disagree with earlier models which proposed that, when bound to RNase, 3'CMP has the anti conformation and 2'CMP has the syn conformation*. The earlier proposal, however, was based on model building and hence was only qualitative in nature.

The crystallographic data of Pavlovsky *et al.* (1977) also revealed that two hydrogen bonds exist between the cytosine ring and the protein. These are $>C^{2}=O\cdots H-N$ (the main chain of thr-45) and $>N^{3}\cdots H-O$ (the side chain of thr-45) (Fig. 6.2). In contrast with the earlier hypothesis of Richards and Wyckoff (1971) Pavlovsky found no crystallographic evidence of a third hydrogen bond between the NH_2 group of the cytosine ring and the CH_2OH group of ser-123 in the complexes considered. The distance between the nitrogen and oxygen atoms of these

*Appendix IX gives the structure and conformation of the cytosine inhibitors discussed in this Chapter.

groups was found to be greater than 4 Å. No water molecule capable of participating in the hydrogen bond as an intermediate link was detected. More data is, however, needed to settle this controversy.

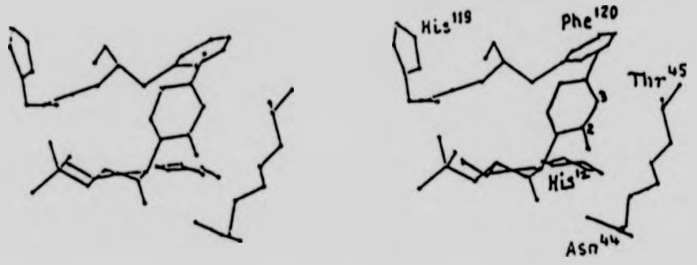

Fig. 6.2 Stereoprojection of a fragment of the structure of the complex of RNase S with cytidine-3'-phosphate. Taken from Pavlovsky *et al.* (1977).

No crystallographic data is at present available concerning the structure of the RNase-5'CMP complex. On the basis of the chemical shift changes of the three inhibitor protons, C(6)H, C(5)H and C(1')H, Meadows *et al.* (1969) postulated that the cytosine ring in each of the cytosine mononucleotides binds in essentially the same manner. However, Gorenstein and Wyrwicz (1974) concluded, in disagreement with Meadows that the changes in the C(5)H and C(1')H chemical shifts on binding 3'CMP and 5'CMP were different. Gorenstein and Wyrwicz proposed a model in which 5'CMP had an anti conformation at all pH values and 3'CMP had an anti conformation at low pH (< 6.0) and a syn conformation at higher pH (> 6.0) values.

However, in a subsequent study, Karpeisky and Yakovlev (1977) measured the nOe between C(6)H and C(1')H and showed that at both high and low pH values, bound 3'CMP is in an anti conformation.

Combining the crystallographic data of Pavlovsky *et al.* (1977) and the ^{1}H NMR results (Meadows *et al.*, 1969; Karpeisky and Yakovlev, 1977) it appears as if all three mononucleotides, 2'CMP, 3'CMP and 5'CMP, adopt the anti conformation in the bound state. In addition, it seems that at least two hydrogen bonds exist between the cytosine ring and the protein molecule in each complex. More data is clearly required to finally establish the precise conformation of each of the bound inhibitors.

All the pyrimidine mononucleotides are at present assumed to bind in broadly the same manner, as shown in Fig. 6.2, but with some differences in orientation. In the case of 2'CMP, 3'CMP and 5'CMP binding, the differences in orientation are obviously necessary to allow for the different positions of the phosphate group. Since the major contributions to the binding energy come from the interaction of the phosphate group with his-12 and lys-41 (and the binding of the cytosine ring) the conformation of both the enzyme and the inhibitor must be altered, within limits, to maximise these interactions. This partly arises from the fact that the his-12 residue, unlike the lys-41 and his-119 side-chains, is rigidly held. Although the his-119 imidazolium ring is not known to form ionic bonds with the phosphate group in the mononucleotide, the

mere presence of the inhibitor would be expected to perturb the orientation of this imidazolium ring (and the residues in close proximity to his-119). This is due to the fact that his-119 has considerable freedom of movement within the active site (Appendix III) (Borkakoti *et al.*, 1982).

6.4 RESULTS AND DISCUSSION

6.4.1 ^{1}H NMR Studies

Fig. 6.3(i) shows the aliphatic region of the ^{1}H NMR spectra of RNase at pD 3.2 and pD 5.5 and in the presence of 2'CMP, 3'CMP, 5'CMP, cytidine and phosphate ion. The peak (H7) at 0.62 ppm at pD 3.2 broadens slightly on increasing the pD value to pD 5.5. This peak shifts upfield to coalesce with H11 at 0.53 ppm in the presence of all three mononucleotide inhibitors (Fig. 6.3(i): e, f, g). To confirm this upfield shift the ^{1}H NMR spectrum is examined in conjunction with the ^{13}C NMR spectrum. Table 6.1 shows the shifts of corresponding methyl ^{1}H and ^{13}C resonances under the conditions indicated. The identification of corresponding ^{1}H and ^{13}C methyl resonances is based on the observation of a prominent ^{13}C peak when the single proton-frequency irradiation method is used. The proton irradiation frequency (in ppm) in each case is as shown in Table 6.1.

At pD 3.2, selective irradiation at the frequency of peaks H11 and H7 in the ^{1}H NMR spectrum gives the decoupled peaks 11 and 7 respectively, in the

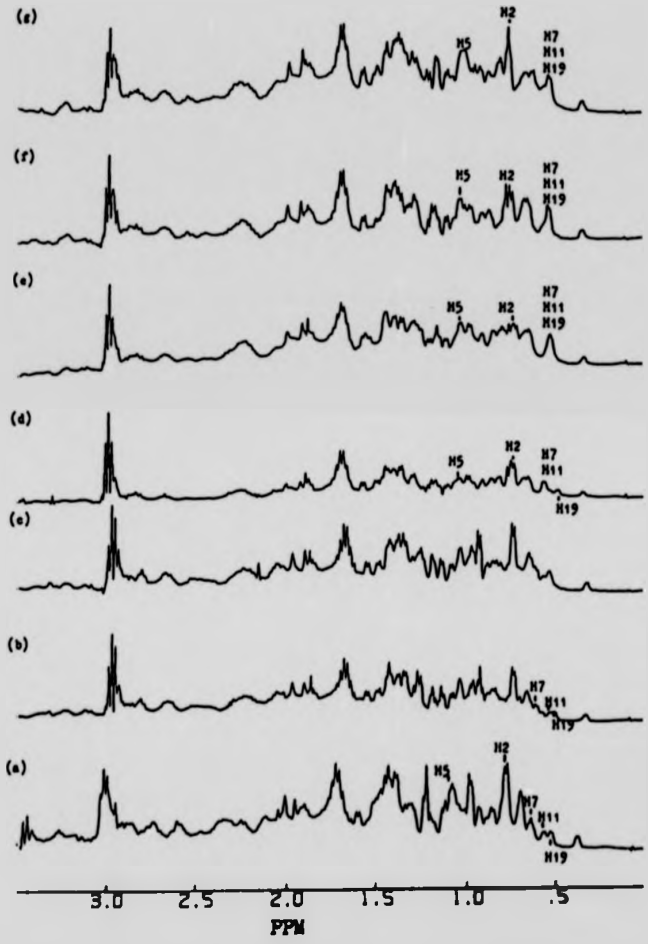

Fig. 6.3(i) Aliphatic region from 0 ppm to 3.5 ppm of ^{1}H NMR spectrum of RNase (6 mM in 0.05 M NaCl) in the presence of various inhibitors at 25°C.

(a) free protein, pD 3.2
(b) free protein, pD 5.5
(c) + 80 mM phosphate, pD 5.5
(d) + 80 mM cytidine, pD 5.5
(e) + 80 mM 5'CMP, pD 5.5
(f) + 65 mM 3'CMP, pD 5.5
(g) + 40 mM 2'CMP, pD 5.5

The peak designations indicate the positions of individual methyl groups.

TABLE 6.1 ^{13}C NMR and ^{1}H NMR Chemical Shifts of Methyl Resonances in RNase and RNase Complexes[a]

RNase, pD = 3.2		RNase, pD = 5.5		RNase + Cytidine		RNase + 5'CMP		RNase + 3'CMP		RNase + 2'CMP	
^{13}C Res.[b]	^{1}H Res. δppm[c]	^{13}C Res.	^{1}H Res. δppm	^{13}C Res.	^{1}H Res. δppm	^{13}C Res.	^{1}H Res. δppm	^{13}C Res.	^{1}H Res. δppm	^{13}C Res.	^{1}H Res. δ ppm
19	0.527			19	0.48						
11	0.56(6)	7[d]	0.55(6)	7	0.55	7	0.53(3)	7	0.53(3)	7	0.53
		11		11		11		11		11	
		19				19		19		19	
7	0.62					13	0.65(6)			13	0.65(6)
13						(and others)[e]				(and others)[e]	
1	0.75	1	0.72-	1	0.73-	1	0.75			1	0.76(8)
2		2	0.75	2	0.75	2				2	
8		8		8		8	0.74			8	
10		10		10		10				10	
5	1.02	5	1.02	5	1.00	5	1.04	5	1.04	5	1.02
12		12	0.96	12		12		12		12	
4	2.00										

[a] The conditions of the samples are described in Fig. 6.3
[b] Peak numbers are as shown in Fig. 6.5
[c] The ^{1}H NMR chemical shifts, δ ppm, are relative to external Me_4Si. The frequency shown is that used in each single proton-frequency experiment
[d] Peak 7 retains some residual coupling in the single proton-frequency decoupling experiment using this sample
[e] More than one decoupled peak is observed

^{13}C spectrum (see Fig. 3.14). At pD 5.5, when the sample is irradiated at 0.53 ppm two sharp ^{13}C resonances, peaks 11 and 19 are observed. Peak 7, however, shows residual coupling. In each of the RNase-mononucleotide complexes, irradiation at 0.53 ppm gives three distinctly decoupled peaks: 7, 11 and 19. Finally, in the RNase-cytidine complex spectrum, irradiation of H19 gives a sharp peak at 22.05 ppm (peak 19) in the ^{13}C spectrum. (All the peak numbers referred to in the ^{13}C NMR spectrum discussed here are as shown in Fig. 6.5.)

Detailed analysis of the ^{1}H spectra shown in Fig. 6.3(i) is hampered by poor resolution. There are very few differences between the spectrum of RNase at pD 5.5 and of RNase in the presence of 80 mM phosphate at the same pD. In contrast, the addition of cytosine inhibitors causes upfield shifts of some methyl groups to give an intense peak at around 0.53 ppm.

Peak I in each of the RNase-cytosine inhibitor complex spectra has not been definitely assigned (Fig. 6.3(ii)). This resonance was first assigned to phe-120 (Meadows *et al.*, 1969), then to tyr-25 (Markley, 1975(a))and more recently reassigned again to phe-120 (Lenstra *et al.*, 1979). In the present work, the assignment of peak I is confirmed using two techniques: spin-decoupling and nOe difference experiments.

At pD 5.5, the C^{δ} peak of tyr-25 is well resolved at 7.12 ppm. In the presence of the mononucleotides, this peak shifts downfield slightly. Spin-decoupling experiments showed that the peak at 7.12 ppm is coupled to the assigned tyr-25 C^{ε} peak at 6.48 ppm (Fig. 6.4(b)).

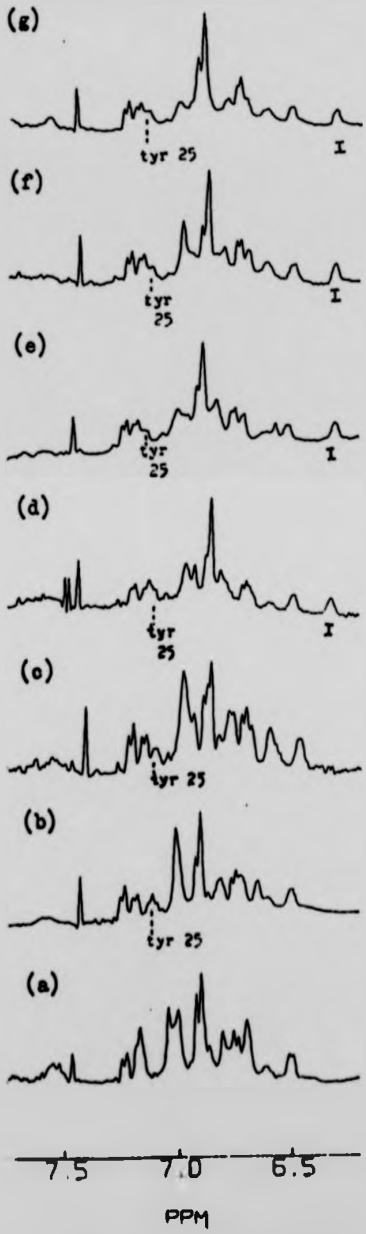

Fig. 6.3(ii) Aromatic region from 6.0 ppm to 8.0 ppm of ^{1}H NMR spectrum of RNase in the presence of various inhibitors at 25°C. The conditions for each spectrum (a-g) are the same as for Fig. 6.3(i). The tyr-25 C(2,6)H resonances are identified. Peak I is a new peak originating from the RNase-cytosine inhibitor complex.

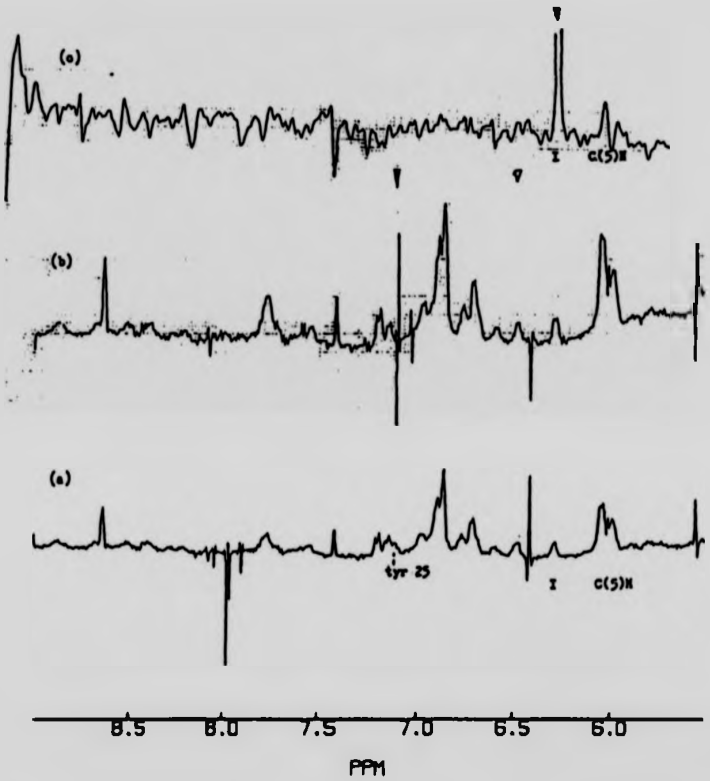

Fig. 6.4 (a) Aromatic region of ^{1}H NMR spectrum of RNase (6 mM, 0.05 M NaCl) in the presence of 2'CMP (40 mM), pD 5.5, 25°C. The tyr-25 C(2,6)H resonances and the 2'CMP C(5)H resonance are identified. Peak I is a new peak originating from the complex.

(b) Double resonance (spin decoupling) spectrum of the same sample as (a). The filled arrow indicates the position of the irradiation and open arrow the position of the decoupled tyr resonance.

(c) nOe difference spectrum of the same sample as (a). A selective r.f. saturating field was applied at the position of peak I. The difference spectrum was obtained in the manner described in Chapter 2, Section 2.3.5.

Peak I cannot, therefore, arise from the protons of the tyr-25 residue.

Saturation of peak I results in a large nOe on the C(5)H peak of 2'CMP (Fig. 6.4(c)). Peak I must, therefore, belong to an aromatic residue in the protein which is close to the C(5)H atom of the cytosine ring of 2'CMP. Fig. 6.2 is a drawing of a section of the structure of the 3'CMP-RNase S complex, as extracted from Pavlovsky *et al.*, 1977. The distance between the two closest atoms (N^4 of the base and one of the carbon atoms of the phe-120 ring) is approximately 3.3 Å for a complex with 3'CMP, and 3.8 Å for a complex with 2'CMP. Hence, peak I must be attributed to the aromatic protons of phe-120.

The phe-120 ring protons show an upfield shift whilst the pyrimidine ring protons, C(5)H and C(6)H, move downfield when each of the cytosine inhibitors binds to RNase (this work; Meadows *et al.*, 1969). This suggests that the two aromatic rings are neither coplanar nor stacked, in each of the complexes. This is confirmed by the x-ray crystallographic results of Pavlovsky *et al.* (1977), who found that the angle between the phe-120 ring and the pyrimidine ring is approximately 130°, that is, the rings do not overlap.

6.4.2 ^{13}C NMR Studies

6.4.2.1 General Considerations

Fig. 6.5 shows the region of the ^{13}C spectrum

of RNase between 11.0 ppm and 24.0 ppm in the presence of each of the five inhibitors. At pD 5.5 and 25°C, all the spectra show no significant line broadening when compared with the spectrum of the free protein at the same pD and temperature. At the concentrations of inhibitors used, virtually the whole enzyme exists in the complexed form. The rate of exchange between the complexed and free species is no longer an important factor in determining linewidths. At pD 7.0, there is evidence of slight line broadening in each resolved peak in the spectrum of the RNase-2'CMP complex. This is attributed to a decrease in the binding constant at pD values greater than pD 7.0 and to the rate of exchange now becoming an important factor. Thus, at pD 5.5, the position of each peak represents the chemical shift of the fully complexed form.

The addition of each inhibitor can cause either an upfield or a downfield shift in many of the peaks, resulting in coalesced peaks in some cases. The four RNase-cytosine inhibitor complexes each give a different spectrum. This suggests that there are considerable differences in the binding of each of these related inhibitors. To establish the components of unresolved peaks, the heteronuclear double resonance experiments described in Chapter 2, Section 2.3.3 were used. It is possible to distinguish the ile and met methyl resonances in the region between 12.5 ppm and 14.0 ppm because the proton resonances of the ile and met methyl groups are well separated in the ^{1}H NMR spectrum of RNase. In addition,

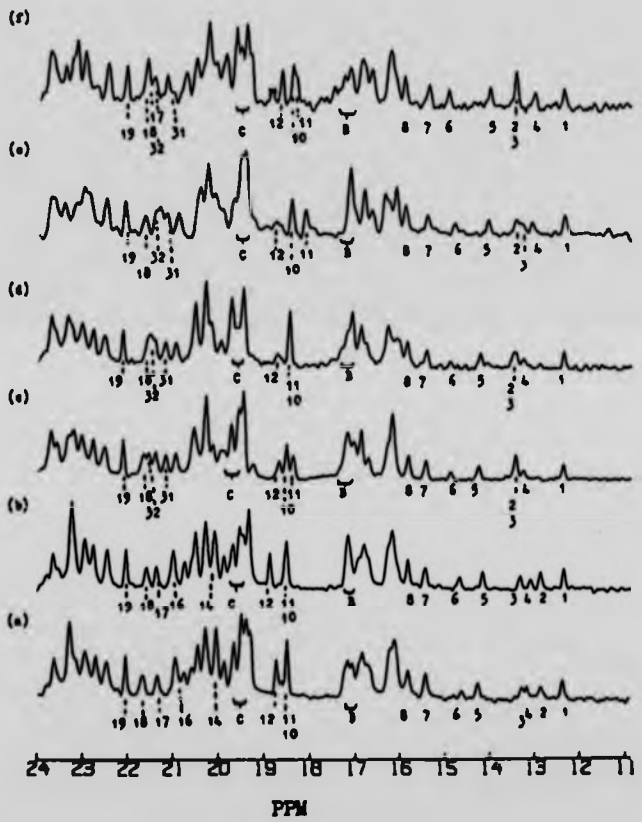

Fig. 6.5 Spectral region from 11.0 ppm to 24.0 ppm of the proton-decoupled ^{13}C NMR spectrum of RNase (6 mM in 0.05 M NaCl) in the presence of various inhibitors at 25°C, pD 5.5.

(a) free protein
(b) + 80 mM phosphate
(c) + 80 mM cytidine
(d) + 80 mM 5'CMP
(e) + 65 mM 3'CMP
(f) + 40 mM 2'CMP

The numbers indicate the positions of individual methyl carbon resonances. The letters indicate the positions of groups of unresolved methyl carbon resonances.

the spectrum of Methyl Met-29 C^{ε} RNase in the presence of cytidine is also examined (Fig. 6.6). Peak 3 in the ^{13}C spectrum of native RNase is assigned to the met-29 C^{ε} centre (Chapter 3, Section 3.5.2.1). This peak is, however, not observed in the spectrum of the free Methyl Met-29 C^{ε} RNase. Therefore, combining the data from Fig. 6.6 and Figs. 6.5(c), 6.5(d), and 6.5(f), peak 4 must arise from a met C^{ε} centre and peak 2 from an ile methyl carbon in each figure. The sharp peak at 13.5 ppm in Figs. 6.5(c), 6.5(d) and 6.5(f) hence comprises of peaks 2 and 3.

Fig. 6.7 shows a plot of the chemical shifts of peaks 1 to 8 and peaks 10 to 12 in the spectrum of both free- and bound-RNase. Within the limits of experimental error ($\pm$ 0.04 ppm) the addition of the phosphate anion causes only very small shift changes with the exception of peaks 2, 4 and 12.

For all changes in chemical shifts observed on ligand binding, an attempt is made to distinguish between direct and conformationally transmitted effects. One of the methods used was to examine the ^{13}C resonances of RNase in the presence of Cu^{2+} ions at pD 5.5. When the Cu^{2+}/ protein molar ratio is 0.3, peaks 10 or 11, 14, 19 and some of the peaks in region C are significantly broadened (Fig. 6.8(b)). In addition, two resolved and tentatively assigned carboxylate carbon peaks are significantly broadened, these broadenings indicating the participation of carboxylate groups when Cu^{2+} binds to RNase. Allewell and Wyckoff (1971) have suggested the probable participation

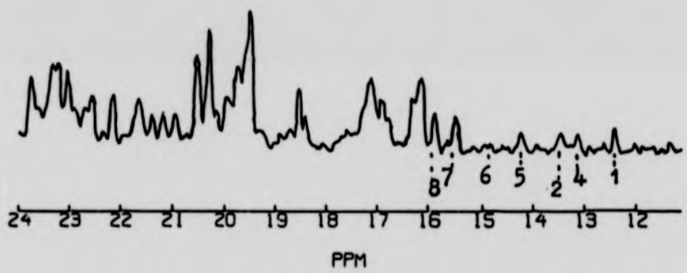

Fig. 6.6 Spectral region from 11.0 ppm to 24.0 of the proton-decoupled ^{13}C NMR spectrum of [Methyl Met-29 C^{ε}] RNase (5 mM in 0.05 M NaCl) in the presence of cytidine (80 mM) at 25°C, pD 5.5. Peak numbers are those of Fig. 6.5.

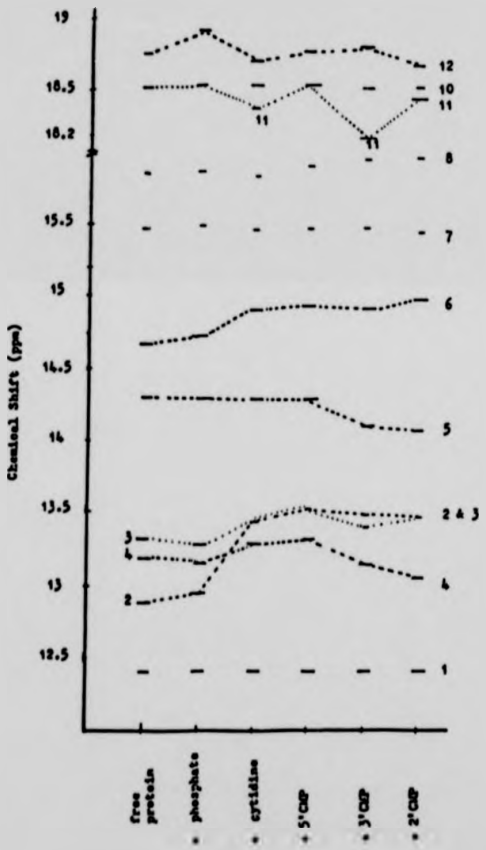

Fig. 6.7 Chemical shifts of the methyl carbon resonances of RNase (6 mM in 0.05 M NaCl), pD 5.5, 25°C, in the absence and presence of inhibitors. The concentration of each inhibitor present is the same as in Fig. 6.5. Peak numbers are those of Fig. 6.5.

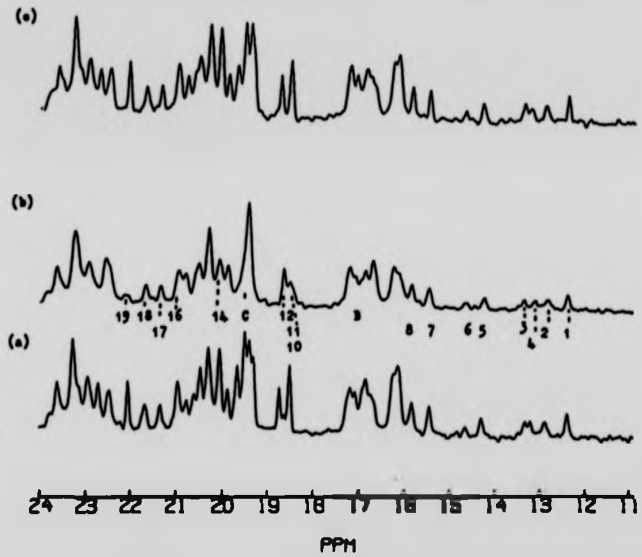

Fig. 6.8 Effect of Cu^{2+} and Mn^{2+} on the resonances in the spectral region from 11.0 ppm to 24.0 ppm of the proton-decoupled ^{13}C NMR spectrum of RNase in 0.05 M NaCl, pD 5.5, 25°C.
(a) free protein (6 mM)
(b) + Cu^{2+} (1.8 mM)
(c) + Mn^{2+} (0.8 mM)
Peak numbers and letters are those of Fig. 6.5.

of at least four carboxylate groups when Cu^{2+} binds to RNase S. The ^{1}H NMR spectrum of the RNase-Cu^{2+} complex obtained in the present studies shows the resolved his-12, his-105 and his-119 peaks to be significantly broadened. Reported ^{13}C NMR studies (Walters and Allerhand, 1980) and ^{1}H NMR studies (Ihnat, 1972) have shown that there are at least two binding sites for Cu^{2+} in RNase - one at the his-105 residue and the other at the active site (his-12 and his-119). When Cu^{2+} complexes with RNase, conformationally transmitted changes in the protein molecule are not apparent. That is, the broadening results from dipolar interactions which depend solely on the distance r between the Cu^{2+} ion and the binding centre in the protein, rather than as a result of conformational changes.

Are the observed broadenings in Fig. 6.8(b) due to the binding of Cu^{2+} to his-105 or to the active site? Fan and Bersohn (1975) showed by means of ^{1}H NMR that Mn^{2+} binds preferentially to or near his-105 at pD 5.7. The effect of Mn^{2+} on the ^{13}C resonances of 8.0 mM RNase in D_2O is examined in the present study. Fig. 6.8(c) shows the ^{13}C NMR spectrum of a sample of RNase in the presence of 1.0 mM Mn^{2+} (that is, the Mn^{2+}/protein molar ratio is 0.13). There is no broadening in any of the resolved methyl resonances. The ^{1}H NMR spectrum of the same sample of RNase-Mn^{2+} solution showed the resolved his-105 C(4)H resonance to be severely broadened, whilst the his-119 C(2)H and his-12 C(2)H appear to be only slightly affected. Therefore, the broadening of peaks 10 (or 11), 14 and 19 and those in region C of Fig. 6.8(b) is perhaps

due to the relaxation effect caused by the Cu^{2+} ion bound at the active site (his-12 and his-119).

In each RNase-cytosine inhibitor complex spectrum, peaks 11 and 14 and those in region C (Fig. 6.5) are significantly perturbed. (The absence of a significant shift of peak 11 in the RNase-5'CMP complex spectrum implies a slight difference in the structure between this complex and those of the other RNase-cytosine inhibitor complexes.) Combining the results obtained from Cu^{2+} and cytosine-inhibitor binding, it appears that points of contact involving more than one methyl group in RNase are present and that these contacts are common to all the complexes examined. It is also appropriate to attribute the perturbations of peaks 11 and 20 and those in region C in the RNase-cytosine inhibitor complexes to directly transmitted shift effects. Unfortunately, interatomic distances between the Cu^{2+} ion and the amino acid side-chains in the protein are not available to provide a more quantitative analysis. All the other observed shift changes induced by the binding of cytosine inhibitors appear to result from either (i) conformational changes in the protein, or from (ii) protein-inhibitor interactions at points other than those involving the his-12 and his-119 residues.

In contrast, peak 19 is not perturbed in the presence of the cytosine inhibitors. This may indicate that the broadening of the peak by Cu^{2+} results from the binding of this ion at sites other than those involved in the cytosine inhibitor binding (Allewell and Wyckoff, 1971, and references therein).

Based on what is known about the structure of the RNase-cytosine inhibitor complexes an attempt is made to rationalise some of the observed shift perturbations. Table 6.2 shows the interatomic distances between the centres of hydrophobic groups around the active site cleft calculated from x-ray data supplied by Stanford (personal communication).

6.4.2.2 Ile Methyl Resonances (Peaks 2 and 5)

It has been postulated (Richards and Wyckoff, 1971) that the side-chain hydroxyl group of ser-123 forms a hydrogen bond with the NH_2 group of the cytosine ring. The conformation of the protein around ser-123 may thus be expected to change. If this postulation is correct, then peak 2 can possibly be attributed to an ile methyl group which is in close proximity to the ser-123 residue, that is, the ile-81 C^{δ} group (Table 6.2). In addition, the proximity of the ile-81 C^{δ} atom to the thr-45 C^{γ} atom enhances this assignment (Appendix VIII). Peak 2 is perturbed in the same manner when each of the cytosine inhibitors is bound to RNase. It appears that this methyl group undergoes the same conformational changes on formation of each of the RNase-cytosine inhibitor complexes.

Peak 5, on the other hand, shifts upfield by 0.2 ppm only when 2'CMP or 3'CMP is added. This resonance is shifted upfield in a similar manner and to the same extent by variation of either pD or temperature (Chapter 3,

TABLE 6.2 Intercarbon Distances[a] in Ribonuclease A[b]

Residue	Carbon Atom	Ser-123 C^{β}	Ile-106 $C^{\gamma 2}$	Phe-120 C^{ζ}	Phe-120 C^{γ}	Lys-41 C^{ε}	Thr-45 C^{γ}	Phe-8 C^{ζ}	His-12 C^{α}
Ile-81	γ_2	5.2	3.89	5.43	7.86		4.62		
Ile-81	δ	3.23	5.10	5.37	7.97		4.24		
Ile-106	γ_2	4.76		3.86	6.20		6.08		
Ile-106	δ	7.56		5.22	6.34		7.99		
Ile-107	γ_2	8.74							
Ile-107	δ	7.53							
Thr-45	γ			3.95					
Val-47	γ_2	7.36					5.00		5.58
Val-108	γ_1			5.75	5.10			4.10	
Met-30	ε					3.80			

[a]Distances are expressed in Angstroms

[b]The distances are calculated from coordinates supplied by Stanford (personal communication).

Section 3.5.2.3 ; Chapter 4, Section 4.2.2.2). The pD- and temperature-dependent shifts are attributed to a structural change involving the sliding of the cleft residues relative to one another. It is likely that when 2'CMP or 3'CMP binds to RNase, a similar type of conformational change occurs. The position of the ile-106 residue relative to the active site cleft (Chapter 1 and Appendix II(a)) and the proximity of the ile-106 C^{γ_2} atom to the phe-120 C^{ζ} atom (Table 6.2 and Appendix VIII) suggest that peak 5 arises from the ile-106 $C^{\gamma 2}$ atom. The absence of a similar shift change in peak 5 when either 5'CMP or cytidine is added implies that the conformational changes described above may not be significant when either of these two inhibitors is bound.

The methyl groups represented by peaks 2 and 5, in the ^1H NMR spectrum of free RNase, resonate at around 0.72 ppm (peak H2) and 1.02 ppm (peak H5) respectively (Fig. 6.3(i)). In the presence of 2'CMP or 3'CMP, peak H2 shifts downfield to around 0.77 ppm, but in the presence of 5'CMP or cytidine, it appears at 0.75 ppm. Peak H5 resonates at between 1.00 ppm and 1.04 ppm under conditions shown in Table 6.1. On saturation of either peak H2 or peak H5 in each RNase-cytosine inhibitor complex using low r.f. power, no nOe is observed in the C(6) or C(5) proton resonances of the cytosine ring. This suggests that the methyl protons are somewhat more than 5.0 Å away from the cytosine ring protons (Olejniczak *et al.*, 1981; Bothner-By and Gassend, 1973). It is more likely that the shift perturbations observed in peaks 2 and

5 in the ^{13}C NMR spectrum arise from localised changes in the protein conformation rather than from a direct ring current shift in the cytosine ring (Perkins and Dwek, 1980).

6.4.2.3 Met Methyl Resonances (Peaks 3, 4 and 6)

Peak 4, which has been tentatively assigned to met-13 C^{ε} (Chapter 3, Section 3.5.2.3) is shifted upfield when 2'CMP (Δ = 0.14 ppm) or 3'CMP (Δ = 0.08 ppm) is added. In the presence of cytidine or 5'CMP, this peak shifts downfield by 0.06 ppm – 0.08 ppm. The perturbation of peak 4 must therefore be related to the conformational change arising from the interaction between the neighbouring his-12 residue and each of the inhibitors. When 2'CMP or 3'CMP binds to RNase, the his-12 imidazolium ring forms an ionic bond with the phosphate group, but when 5'CMP binds, such a bond is known not to be present (Meadows *et al.*, 1969). However, his-12 also interacts with the 2'OH group of the ribose located in site R_1 (Pavlovsky *et al.*, 1977). The change in the pKa value of his-12 C(2)H, as observed by ^1H NMR, when 5'CMP or cytidine binds to RNase, is attributed to the interaction of this his residue with the 2'OH group of the ribose. That is, the his-12 residue is involved in interactions with each of the cytosine inhibitors although the nature of these interactions is different in each case. Thus, peak 4 is perturbed when either 2'CMP, 3'CMP, 5'CMP or cytidine is present.

Peak 3 (Met-29 C^{ε}) and peak 6 both undergo a

distinct downfield shift in the presence of each of the inhibitors (Fig. 6.7). Fig. 6.9 shows the position of the lys-41 side-chain, and the residues around it in the crystal structure of RNase at pH 5.7 (Borkakoti, personal communication). It is likely that a change in the conformation of the lys-41 side-chain will perturb the magnetic environment around the met-30 C^{ε}, and, to a lesser extent, the met-29 C^{ε} atoms. The met-30 C^{ε} atom is 3.8 Å from the lys-41 C^{ε} atom and peak 6 is thus tentatively assigned to met-30 C^{ε}.

The lys-41 side-chain is free to rotate about the C-C single bond. Small conformational changes in the rest of the protein molecule can cause this mobile side-chain to alter its position. In the formation of RNase-mononucleotide complexes, interaction between the lys-41 N^{ζ} atom and the oxygen atom of the phosphate group is believed to be maximised (Metzler, 1977). However, this interaction need not be the only cause for a movement of the lys-41 side-chain. When cytidine, which has no phosphate group, binds to RNase, the perturbations of the met C^{ε} peaks are identical to those caused by the binding of 5'CMP. Furthermore, on the addition of phosphate anions, the perturbations of the met C^{ε} peaks are much smaller than those caused by the presence of the cytidine inhibitors.

Although a binding site for the phosphate anion involving his-12, his-119 and lys-41 is believed to exist, two features of phosphate ion binding must be borne in mind. Firstly, the free phosphate ion-imidazole interaction is different from those in mononucleotide complexes.

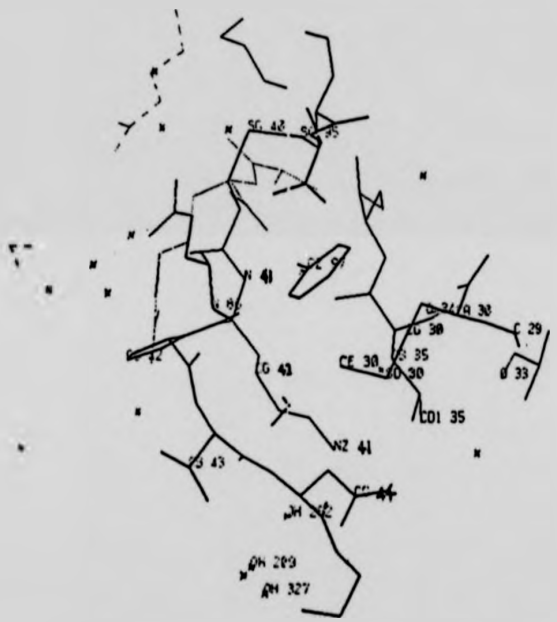

Fig. 6.9 Stereoplot of part of the active site of RNase showing the proposed orientation of the lys-41 side chain and the area around this side-chain (Borkakoti, personal communication).

Secondly, the phosphate-RNase binding constant is lower than the mononucleotide-RNase binding constant (Benz and Roberts, 1975). Both these factors can account for the smaller shift changes in the phosphate-RNase complex compared with those observed in the mononucleotide-RNase complexes.

In summary, the movement of the lys-41 side-chain may be caused by a combination of several factors. These include: the necessity to maximise the interaction between the phosphate group on the mononucleotide inhibitor and the lys-41 N^{ζ} atom, and a conformational change around the his-119 and his-48 side-chains. In order to attain the phosphate-lys-41 interaction, the part of the peptide chain containing lys-41 must be pulled nearer to the phosphate group which lies on the opposite side of the active site cleft. The residues in the peptide chain around the hinge region of the protein (Appendix II(b)) will thus have to slide relative to one another resulting in a closure of the cleft. On the other hand, when cytidine (which has no phosphate group) binds, conformational changes induced by interactions between the his residues, 12 and 119, and the nucleoside must be important (Jentoft *et al.*, 1981).

6.4.2.4 Other Methyl Resonances (Region between 16.5 ppm and 22.0 ppm)

With the exception of the tentative assignment of peaks 12 and 13 to the methyl groups of val-47 (Chapter 5, Section 5.4.1.2) the resonances in this region have not yet been assigned to specific amino acid residues.

In the region marked B, the most significant changes are seen in the spectra obtained using 5'CMP, 3'CMP and 2'CMP as the inhibitors (Fig. 6.5(d), 6.5(e) and 6.5(f)). The changes observed in each of the RNase-inhibitor complex spectra differ from one another. The perturbations must arise from the structural changes caused by the presence of the nucleotide inhibitor because the presence of either a phosphate anion or a cytidine molecule alone does not appear to cause these perturbations (Fig. 6.5(b), 6.5(c)).

In the region between 18.0 ppm and 19.0 ppm the peaks are designated as 10, 11 and 12 (Fig. 6.5). The binding of a phosphate ion causes a significant downfield shift (Δ = 0.15 ppm) in peak 12. This same peak shifts downfield by 0.26 ppm in the presence of low concentrations of urea at pD 3.2 and pD 5.5 (Chapter 5, Section 5.4.1.2). In the ^{1}H NMR studies, the his residue most significantly perturbed in the presence of either urea or phosphate ion belongs to his-12 C(2)H (this work, and Meadows *et al.*, 1969). This implies that the his-12 imidazolium ring is a probable binding site for both the urea molecule and the phosphate ion. It is therefore not unreasonable to attribute peak 12 in Fig. 6.5(b) to the methyl group of a val residue near his-12, that is, val-47.

Peak 12 is also significantly perturbed in the presence of all the cytosine inhibitors, this perturbation probably resulting from the interaction of his-12 with the bound inhibitor in each case (see Section 6.4.2.3).

In the presence of a mononucleotide, the peak is broadened. This reflects a hindered rotational freedom of the side-chain as a result of the tighter binding of each mono-nucleotide, when compared with that of urea, phosphate or cytidine.

When each of the four cytosine inhibitors is added to RNase, distinct shift changes are observed in the spectral region between 20.0 ppm and 22.0 ppm (Fig. 6.5). The sharp intense peak 14 disappears in the presence of all four cytosine inhibitors. In each case two new peaks appear further downfield at around 21.20 ppm (peak 31) and at around 21.58 ppm (peak 32).

It has been established earlier in Section 6.4.2.1 that peaks 11 and 14 are perturbed as a result of the close proximity between the methyl groups represented by these peaks, and the bound ligands. These two peaks are, however, not perturbed when either urea or phosphate ion binds to RNase at his-12. It appears that even though a common his group (his-12) is involved in the binding of each ligand, the precise structure of the binding site of urea and phosphate must differ from those of the cytosine inhibitors (or Cu^{2+} ion).

Based on the known primary shifts of the methyl groups of amino acids (Howarth and Lilley, 1978), the resonances in the region between 16.5 ppm and 22.0 ppm are known normally to arise from the methyl groups of val, thr and leu. The val residues are distributed throughout the RNase chain. Val-43 and val-47 are situated in the active site cleft, the val-47 $C^{\gamma 2}$ atom being 5.0 Å

from the thr-45 C^{γ} atom. Val-108 $C^{\gamma 1}$ is 4.06 Å from the ile-106 C^{δ} atom. In addition, many val residues, for example, val-47, val-108 and val-118, are found in the same region as the his and phe residues that are in or around the active site. As for the thr residues, the crystallographic data discussed in Section 6.3 show that two hydrogen bonds exist between thr-45 and the cytosine ring when the inhibitors bind to RNase. The formation of these bonds is likely to cause conformational changes around this residue and one would expect the shifts of the methyl groups of thr-45 and of the val residues around this thr residue to be perturbed. Combining the crystallographic data and NMR results it is possible to tentatively attribute peak 11 to a val methyl group and peak 14 to a thr methyl group. Both these methyl groups must be in close proximity to the his-119 or his-12 residue and the bound ligands. Amongst the likely candidates are thr-45, val-108 and val-118.

There are only two leu residues in RNase, leu-35 and leu-51. The leu-35 C^{ζ} atom is 4.84 Å away from the lys-41 N^{ξ} atom (Fig. 6.9 and Table 6.2). A change in the conformation of the active site cleft, together with a movement of the lys-41 side-chain is likely to perturb the magnetic environment of leu-35.

Therefore, except for peaks 11 and 14 and those in region C, the changes in the chemical shifts and line-widths of the resonances between 16.0 and 22.0 ppm can be attributed to conformationally transmitted changes involving

the val, thr and leu residues. However, one cannot rule out the possibility that the shift changes arise from contacts between these protein side-chains and points on the inhibitor other than those points in the inhibitor already in contact with the his-119, his-12 and lys-41 side-chains. Attempts to resolve the latter possibility using nOe experiments proved unsuccessful. Although an nOe between a nucleus on the ligand and one on the protein can be used to establish a point of contact, the likelihood of interference from spin diffusion makes this method highly unreliable.

6.4.2.5 Other ^{13}C Resonances

The resonance assigned to lys C^{δ} at 27.0 ppm exhibits similar perturbations when either cytidine, 5'CMP, 3'CMP or 2'CMP bind to RNase. This suggests the participation of lys residues when each of the inhibitors bind. The glu C^{γ} peak at 35.0 ppm consistently shifts upfield in the presence of each of the four cytosine inhibitors. This resonance must belong to a glu residue, such as glu-49, which is in close proximity to the residues in the active site.

As far as the phe residues are concerned, the ^{1}H NMR results obtained in this research and by Lenstra *et al.* (1979) show that the tentatively assigned phe resonances broaden on addition of the cytosine inhibitors (Fig. 6.3(ii)). This broadening is attributed to the restricted rotational freedom of the phe side-chains

about the C^{β}-C^{γ} bond when the protein is in a bound state. For the same reason, the ^{13}C resonances of the phe C^{γ} atoms are broadened to such an extent that they disappear into the background noise. Hence, analysis of the phe C^{γ} resonances in the ^{13}C spectra is not possible at this time.

6.5 SUMMARY

Much information has been gained from this study concerning the binding of inhibitors to RNase. It has explicitly confirmed the presence of conformational changes involving residues other than the active his residues (his-12, his-119 and his-48).

In the ^{1}H NMR studies, using double resonance techniques, the upfield resonance at 6.3 ppm is confirmed to arise from the phe-120 residue rather than from the tyr-25 residue. This definite assignment and the direction of the shift changes enhances the crystallographic evidence that the phe-120 ring is at an angle to the cytosine ring of the inhibitor, rather than their being in a stacked or coplanar conformation.

The ^{13}C NMR results show that the inhibitor-induced shift perturbations are not random; the same residues are being perturbed by each cytosine inhibitor although the magnitude of the resulting shift changes varies in each case, depending on the inhibitor used. The shift perturbations imply that conformational changes occur simultaneously in different regions of the RNase molecule on inhibitor binding. The occupation of

site B_1 by the cytosine ring is used to explain perturbations of the ile methyl resonances. The shift of the assigned met-29 C^{ε} carbon is attributed to a movement of the lys-41 side-chain. This same conformational change is used to tentatively assign the met-30 C^{ε} resonance. In addition to the ile and met side-chains, the methyl resonances of the val, thr and/or leu residues also show significant shift changes.

It is hence apparent that as further assignments of particular resonances become available, a more detailed picture of the interactions between RNase and each inhibitor will emerge.

CHAPTER 7

RESOLVED LIBRATIONAL MOTIONS OF GRAMICIDIN-S AND GLUTATHIONE DIMER AS STUDIED BY NUCLEAR MAGNETIC RESONANCE SPECTROSCOPY

7.1 INTRODUCTION

The study of the internal motions in proteins is of considerable importance to an understanding of their function. High-resolution ^{13}C NMR is in principle a very powerful method for the study of this problem, firstly because it permits simultaneous observation of spectral lines from many different residues, and secondly, because all the parameters measurable from each line are to some extent sensitive to motion. Numerous efforts have been made to derive information on internal motions in proteins from relaxation measurements. However, the principal problem encountered in this type of study is that of interpretation.

There has been considerable progress recently in the analysis of the motions of complex molecules by ^{13}C NMR relaxation and nOe measurements. London and Avitabile (1976) have presented a general theory of the relaxation parameters of atoms in a side-chain with freely rotating links attached to a rigid core. Although this model does not give very satisfactory fits with experimental data (London and Avitabile, 1977), its general approach may readily be developed to allow for restricted rotation of the links (London and Avitabile,

1978), and other comparable motions (Wittebort and Szabo, 1978) in a way which has been shown to fit a few experiments quite satisfactorily. Howarth (1978, 1979(b)) has developed a generalised version of this theory which reinterprets the restricted rotations as internal librations specified only by their average angular extent and rate. Jardetzky *et al.* (1980) have recently proposed a more abstract analysis of the ^{13}C relaxation data of BPTI. Richarz *et al.* (1980) analysed their ^{13}C relaxation data in terms of a "wobbling in a cone" model, where, in addition to the overall rotational motions of the molecule, the relaxation results showed librational motions of the polypeptide backbone and the amino acid side-chains.

In order to explain observations on natural rubber, Howarth (1980) found it necessary to assume librations of both slow, wide angle and fast, small angle, superimposed on a very slow pseudo-isotropic motion of the isoprene chain. The theoretical model which was developed for this analysis involves five motional parameters. The aim of the present work is to give this model as rigorous an experimental testing as reasonably practicable, and thus to go on to a more detailed experimental analysis of molecular flexibility.

Accordingly, the theory has been tested using two medium-sized molecules, gramicidin-S and glutathione dimer, for which T_1 data are available or measurable for at least three observation frequencies, together with nOe's at some of these frequencies. In the case of glutathione dimer the experiments were conducted in a 50% glycerol-D_2O solution with the aim of slowing the larger angled motions

preferentially and thus improving the resolution of the theoretical analysis of the underlying components of motion. Linewidths are not included in the analysis because they can often be misleadingly increased by conformational changes on the millisecond timescale.

Most of the data on these compounds cannot be convincingly reproduced by a single libration model, but the present model fits all the data so far obtained, within experimental error. It even passes such severe tests as giving the same underlying overall molecular rotation rate from data for different atoms in the same molecule and even when this is not assumed in advance. The one failure found so far is that the double-libration model still overestimates some nOe's in proteins, albeit not as badly as did the single-libration model.

7.2 MATERIALS AND METHODS

Gramicidin-S was obtained from the Sigma Chemical Co. and was used without further purification at a concentration of 8.8 mM in [D_4]-methanol.

Glutathione dimer was prepared by the method of Rall and Lehninger (1952) and was used at 160 mM concentration in 50% glycerol-D_2O for the reasons described in the introduction.

Ribonuclease A (Type II) and HEW lysozyme were obtained from the Sigma Chemical Co. Both were dialysed and lyophilised before use. The ^{13}C NMR relaxation studies were carried out using a 6 mM protein solution in D_2O at pD 3.2.

T_1 measurements were carried out at 22.6 MHz, and T_1 and nOe measurements at 45.2 MHz and 100.63 MHz on Bruker WH90, WH180WB and WH400 spectrometers, respectively, all at room temperature. The longitudinal relaxation times T_1 of the peptides at all three frequencies, and of the proteins at 22.5 MHz and 45.2 MHz were measured by the inversion-recovery method (Vold *et al.*, 1968; Freeman and Hill, 1969). The pulse sequence $(180^{o}\text{-}\tau\text{-}90^{o}\text{-}T)_n$ was used, where τ is a variable delay time and T was at least 4 times the longest T_1 to be measured (see Appendix IX(c). Between seven and ten spectra were recorded from each experiment. For the proteins, T_1 values were measured at 100.63 MHz using the saturation recovery method (Markley *et al.*, 1971; McDonald and Leigh, 1973) (see Appendix IX(d) for the microprogram used). Seven spectra were recorded using delay times of between 50 ms and 3 000 ms. The natural abundance ^{13}C NMR relaxation time measurements which were made in this study using 6 mM protein solution typically required 5 K to 10 K accumulations per spectrum.

NOe experiments on the WH400 spectrometer were carried out by obtaining eight scans with the decoupler turned on at all times and then by obtaining eight scans with the decoupler switched off during a delay time of 5.0 s and on during acquisition. Recycling through this loop 1 000 times yielded two sets of spectra that were fully decoupled, one with and one without nOe (see Appendix IX(e) for the microprogram used).

Measurements were repeated, with T_1 values

having an accuracy of ± 10% and nOe values on accuracy of ± 20%.

7.3 THEORETICAL

The main features of the relaxation theory of macromolecules were laid down some years ago (Doddrell *et al.*, 1972). For a carbon atom, under conditions of complete proton decoupling, the expressions for T_1, T_2 and nOe are given by the following equations.

$$1/T_1 = (1/10)A\Omega \quad (1)$$

$$1/T_2 = (1/20)A[\Omega + 4J_0(0) + 6J_1(\omega_H)] \quad (2)$$

$$nOe = 1 + [6J_2(\omega_H + \omega_C) - J_0(\omega_H - \omega_C)]\Omega^{-1}\gamma_H\gamma_C^{-1} \quad (3)$$

where

$$\Omega = J_0(\omega_H - \omega_C) + 3J_1(\omega_C) + 6J_2(\omega_H + \omega_C)$$

and

$$A = \hbar^2\gamma_H^2\gamma_C^2\Sigma\langle r_N^{-6}\rangle$$

Here γ_H and γ_C are the appropriate gyromagnetic ratios, N is the number of protons, $\langle r_N^{-6}\rangle$ is the motional average of the inverse sixth power of the carbon-hydrogen distance, ω_H and ω_C are the appropriate Larmor frequencies and $J_j(\omega)$ are the Fourier transform of the autocorrelation functions at frequency ω as given by

$$J(\omega) = \int_{-\infty}^{\infty} e^{i\omega\tau}\overline{|F(t)F(t+\tau)|}d\tau$$

The exact functional form taken by the spectral densities

$J_j(\omega)$ is dependent upon the model chosen to represent the motion of the system.

The 3-τ model developed by Howarth (1980) assumes that the common motion which underlies the rapid librations of individual atoms is anisotropic and may be described as a slow libration. Its jump correlation time is τ_S and its mean semi-angle is θ. The corresponding parameters for the second, faster libration are τ_G and X and all these are assumed to be superimposed on an overall isotropic rotation of diffusional correlation time τ_R. The autocorrelation function $\langle\overline{F(t+\tau)F(t)}\rangle$ is simply the product of the autocorrelation functions for the isotropic motion, the slow libration and the rapid libration discussed earlier, with correlation times respectively, τ_R, τ_S and τ_G. The resulting equations were used for the analysis described below.

Experimental T_1 values were fitted by a least-squares programme developed from a method published by Alcock *et al.* (1970). As this minimises the function $X^2 = [T_1(\text{expt})-T_1(\text{calc})]^2/T_1(\text{expt})$, it in effect favours the higher-field measurements, with their longer values of T_1. NOe's were not fitted for the peptides, as they are frequently less sensitive to the details of the underlying motion, but they were valuable as a check against false minima, and are recorded in the Tables. The methyl group T_1 values were not considered to be experimentally reliable, because there is some suspicion of non-exponential relaxation decay: also, they would test a different theory.

Some of the calculated parameters are less sensitive to the experimental data than others. With the data and theory used, it is estimated that the accuracy for τ_R is $\pm$ 10%, for τ_S $\pm$ 10%, for τ_G $\pm$ 14%, for θ $\pm$ 8% and for X $\pm$ 8%.

The overall correlation time for isotropic tumbling, τ_R, was at first allowed to vary freely for several resonances, as a test of the method of analysis. The calculated values of τ_R were found to lie within $\pm$ 10% of a mean value, which was then fixed as the τ_R for all resonances. Any effects of anisotropic motion are likely to appear as an apparent contribution to the slow libration. It was found that if the guessed starting value of τ_R was more than approximately 25% too small, new minima were found in some cases. These false minima could be reliably excluded because with the incorrect figures, ΣX^2 for all resonances was significantly larger both for values of T_1 and, independently, for values of the nOe.

The present method contrasts with that of Jardetzky *et al.* (1980) who treated measurements at different fields independently. Their resulting calculated motional parameters do not invariably harmonise, possibly because of T_2 errors, although they are generally consistent with the results obtained in this work.

7.4 RESULTS AND DISCUSSION

The T_1 values for gramicidin-S in methanol at 15.2 MHz and 67.5 MHz were taken from the work of Allerhand

and Komoroski (1973) and Komoroski *et al.* (1975). The other results were obtained in the present study. The gramicidin-S results are shown in Table 7.1 and the glutathione dimer results in Table 7.2. Nearly all the calculated T_1 values lie within the 10% band of the experimental error. The calculated values of nOe also lie within the experimental error of 20%. Thus, the two-libration model gives a very satisfactory fit with one of the largest available sets of experimental data.

7.4.1 Gramicidin-S

The measured T_1 values of the five different α-carbons are nearly identical. Based on the present analysis, no apparent or real slow, large-angle librational motion is detected and the overall tumbling of gramicidin-S is assumed to be effectively isotropic with an overall reorientation time, τ_R, of 0.362s. The presence of a rapid, small-angle librational component (τ_G = 97-107 ps, X = 0.47-0.51 rad) suggests a less tightly structured main chain. This rapid libration is a localised α-carbon libration common to many different molecules and probably not involving the entire side-chain. The above observations are consistent with the known structure of gramicidin-S in methanol (Allerhand and Komoroski, 1973) which takes the form of a cyclic decapeptide with four transannular hydrogen bonds.

In contrast, the side-chain motions all have a slow, wide-angle component of libration as well as a rapid one comparable with that found for the α-carbon.

TABLE 7.1

Gramicidin-S: nT_1 values for different resonances, motional frequencies, and amplitudes from ^{13}C relaxation data

	Resonance frequency										Motion amplitude/frequencies[f]				
	15.3 MHz[b]		22.6 MHz[c]		67.5 MHz[d]		100.6 MHz[c]								
α-CH	nT_1[a] (obs.)	nT_1 (calc.)	nT_1 (obs.)	nT_1 (calc.)	nT_1 (obs.)	nT_1 (calc.)	nT_1 (obs.)	nT_1 (calc.)	n.O.e. (obs.)	n.O.e. (calc.)	τ_G/ps	X/rad	τ_S/ps	θ/rad	τ_R/ns
Pro-α	150	155	150	158	204	200	243	243	2.19	2.28	88	0.310	Very large	Very small	0.362
Val-α	144	154	162	157	210	199	242	242	2.11	2.28	92	0.305	Very large	Very small	0.362
Phe-α	141	160	150	163	203	206	250	250	2.16	2.29	80	0.347	Very large	Very small	0.362
Orn-α	135	159	158	162	177	204	248	248	2.11	2.29	90	0.342	Very large	Very small	0.362
Leu-α	147	147	*e*	150	201	191	232	232	2.09	2.27	95	0.234	Very large	Very small	0.362
Side-chain CH_3															
Orn-β	*g*	306	210	210	244	255	270	301	2.46	2.40	20	0.400	714	0.65	0.362
Orn-γ	*g*	369	375	375	448	450	540	520	2.23	2.48	20	0.550	96	0.70	0.362
Orn-δ	393	388	400	400	496	479	550	552	2.28	2.49	20	0.550	85	0.73	0.362
Leu-β	340	336	343	343	424	423	480	500	2.67	2.39	20	0.400	41	0.70	0.362
Phe-β	198	198	200	200	240	244	280	291	2.00	2.37	20	0.400	2 000	0.98	0.362
Side-chain CH															
Val-β	180	206	210	210	241	254	300	300	2.39	2.41	20	0.390	700	0.67	0.362
Leu-γ	421	402	412	412	511	510	635	605	2.67	2.37	20	0.500	28	0.71	0.362
Phenylalanine CH															
Phe δ	213	177	180	180	235	219	265	261	2.02	2.39	20	0.230	600	0.60	0.362
Phe ε	211	197	200	200	250	243	290	288	2.09	2.40	20	0.350	570	0.60	0.362
Phe ζ	174	174	*g*	177	196	216	275	256	2.46	2.39	20	0.210	692	0.63	0.362
Proline CH_2															
Pro-β	*g*	236	240	246	308	292	330	331	2.23	2.51	20	0.400	360	0.70	0.362
Pro-γ	*g*	291	*g*	295	344	344	380	391	2.09	2.59	20	0.410	211	0.79	0.362
Pro-δ	150	198	*e*	201	244	244	270	288	*e*	2.43	20	0.340	540	0.62	0.362

[a] nT_1 Values in ms. [b] Results from Allerhand and Komoroski (1973). [c] Results obtained from this work at room temperature; concentration of 100 mg ml^{-1} in CD_3OD. [d] Results from Komoroski *et al.* (1975). [e] Accurate results could not be obtained because of interference of CD_3OD resonance. [f] τ_G = librational correlation time, X = mean librational angle (small-angle libration), τ_S = internal rotation or second librational correlation time, θ = second librational angle (large-angle libration), τ_R = overall reorientation correlation time. [g] Not available.

These slower librations have a τ_S value much smaller than the molecular rotational rate (τ_R) of this molecule. It is convenient to consider each side-chain in turn.

Qualitatively, the NT_1 values along the orn side-chain indicate fairly typical motional characteristics for a linear chain. The γ- and δ-carbons show substantially more motion than the β-carbon. On the basis of rotamer analysis, Jones *et al.* (1979) concluded that although internal rotation occurs in the side-chains, there is a distinct preference for one side-chain rotamer. Hence, the observation made in this study that the β-carbon is rather restricted in its motion concurs with the prediction of Jones *et al.* (1979). It is noted that the nOe does not vary significantly along the chain. Based on the above analysis, this implies that the orn side-chain may be flexible but "boxed".

The val side-chain appears to be almost as motionally restricted as the orn side-chain at C^{β}. But in contrast, the leu side-chain seems to be more flexible. This observation is again consistent with the rotamer population study (Jones *et al.*, 1979).

The phe side-chain appears to be inflexible and "boxed-in". The terminal C^{ζ} group has the smallest value of X in the entire molecule, presumably because the angle of the C^{ζ}-H bond is not affected by rotation about the C^{β}-C^{γ} bond. The T_1 differences between phe C^{δ} and phe C^{ε} are probably experimentally insignificant and therefore so too are the calculated differences in librational parameters. The side-chain moves as a whole, with a rate typical for

limited flexure at a C^{α}-C^{β} linkage (Howarth, 1978) plus some C^{β}-C^{γ} rocking.

Finally, the T_1 values of pro are in the order $C^{\gamma} > C^{\beta} > C^{\delta}$. The analysis shows motions consistent with London's (1978) detailed analysis. The author, however, assumed a single process of conformational change for the entire pro ring. From Table 7.1, the calculated variation in τ_s raises doubts about this assumption. It would seem that the pro C^{γ} motion is to some extent a combination of semi-independent angular motions of C^{β} and C^{δ}.

7.4.2 Glutathione Dimer

The data in Table 7.2 show that all the carbon atoms have a fast component of motion whose semi-amplitude is about 0.5 rad. However, the motion of cys C^{β} and cys C^{α} is somewhat restricted because of the S-S bridge. In addition, that of gly C^{α} has X = 0.56 which is consistent with earlier observations (Howarth, 1978). Evidently a side-chain partially restricts the rapid local motions of the α-carbon of an amino acid.

The slow librations in glutathione dimer have a novel feature. Their maximum semi-amplitude θ is almost constant for every protonated carbon in the molecule (0.90-1.13 rad.) rather than increasing with distance from the molecular centre. This indicates that the peptide chains extending from the cys C^{α} atoms are not moving like flexible, unrestricted, side-chains. One

TABLE 7.2

Glutathione dimer [d]: nT_1 values for different resonances, motional frequencies, and amplitudes from ^{13}C relaxation data

	Resonance frequency										Motion amplitude/frequencies [e]				
	22.6 MHz		45.2 MHz				100.6 MHz								
	nT_1 [a] (obs.)	nT_1 (calc.)	nT_1 (obs.)	nT_1 (calc.)	n O e [b] (obs.)	n O e (calc.)	nT_1 (obs.)	nT_1 (calc.)	n O e (obs.)	n O e (calc.)	τ_O/ps	X/rad	τ_S/ps	θ/rad	τ_R/ns
Cys-α	70	67	105	111	1.63	2.01	214	224	1.84	1.59	70	0.300	891	0.90	6.0
Cys-β	83	80	146	124	1.83	2.17	220	235	1.50	1.50	70	0.350	711	0.95	6.0
Glu-α	119	132	175	175	2.22	2.48	283	287	2.07	2.02	20	0.470	500	1.13	6.0
Glu-β	149	155	230	229	2.10	2.37	377	366	1.97	2.32	20	0.500	300	1.00	6.0
Glu-γ	145	170	240	249	2.22	2.05	385	398	2.03	2.02	20	0.560	304	1.00	6.0
Gly-α	171	185	266	279	2.13	2.05	419	470	1.93	1.97	20	0.560	247	1.00	6.0

[a] nT_1 values in ms. [b] n.O e values at 45.2 and 100.63 MHz were obtained from the intensity ratio between a gated decoupled spectrum and a normal decoupled spectrum. [c] See footnote *f* of Table 7.1. [d] Relaxation data at room temperature; sample concentration of 0.16 M in 50% glycerol–^2H_2O; pD 6.4.

explanation of this is that the dimer molecule is cross-linked not only by the S-S bond but also by hydrogen bonds. Electrostatic interactions between the charged terminal groups may also play a limited role although the conformation is apparently not affected by adding salt. The S-S and hydrogen bonds have a substantial but finite angular flexibility which determines θ. Within these constraints, some atoms move more rapidly than others, particularly if they are not dynamically constrained by side-chains and/or by associated solvent. Hence τ_S varies from 891 to 247 ps between cys C^{α} and gly C^{α} . The evidence shows that the motional characteristics of a peptide molecular loop with loose links differ from those of a relatively stiff cyclic peptide ring, such as that of gramicidin-S where no corresponding slow libration is detected.

An attempt is made to identify the angular constraints of the dimer using ^{1}H NMR. The standard method of identifying internal hydrogen bonds by solvent effects on NH resonances cannot be applied here. This is due to the anionic dimer being not readily soluble in dimethyl sulphoxide and the solution that can be made giving broad resonances which are characteristic of an aggregated product.

The ^{1}H NMR spectra of glutathione monomer (SH) and of the dimer (S-S) are compared. The monomer shows no shift inequivalence in the gly α-H atoms, and only 0.05 ppm in the cys β-H atoms. The dimer, on the other hand, shows a difference of 0.054 ppm for the gly α-H

atoms and of 0.342 ppm for the cys β-H atoms. The vicinal coupling constants between cys α-H and cys β-H are 5.31 Hz and 6.31 Hz in the monomer, 4.41 Hz and 9.58 Hz in the dimer. These observations are both consistent with the dimer being more conformationally restricted. For example, the approximate dihedral angles deduced from the cys coupling constants of the dimer *via* the Karplus equations, of about 50° and 170°, are consistent with the proposed cross-linked structure but inconsistent with an open-chain, conformationally-averaged molecule.

The glu α-H-β-H coupling constants are both close to 6.2 Hz in the monomer, but 5.6 Hz in the dimer. This lower value suggests that neither β-proton is *trans* to the α-proton. This in turn is sterically consistent with the presence of some interaction between the glu-NH_3^+ and the gly COO^- groups, either as proposed above or due to steric considerations.

When the monomer is dissolved in H_2O and the solvent resonance is radiofrequency saturated, the two amide proton resonances are substantially reduced in intensity due to saturation transfer by proton exchange. However, when the dimer is observed under similar conditions only the cys-NH resonance behaves in this way. The gly-NH resonance, which may be readily identified by its coupling patterns (a triplet), is appreciably less affected, as would be expected if the protons are involved in hydrogen bonds. Furthermore, the temperature dependence of the cys-NH resonances in the dimer gives further evidence that the cys-NH groups are not involved in intramolecular hydrogen bonds.

The above results concur with previous studies of cyclohexapeptide in water and in dimethyl sulphoxide (Kopple *et al.*, 1968; Kopple *et al.*, 1969). These systems have been shown to possess a favoured conformation in which two antiparallel extended peptide segments are bridged by two transannular hydrogen bonds.

All the above observations imply that structure 'A' is present (note the correction to structure 'A' found in Howarth and Lian (1982) (Appendix XII).

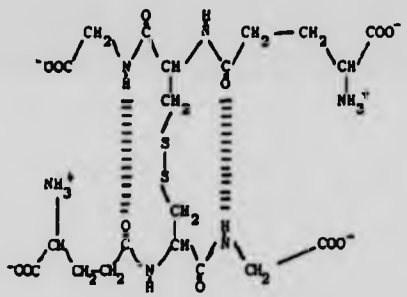

(A)

7.4.3 Proteins

Earlier studies (Howarth, 1978; Howarth, 1979) have shown that a single-libration model can explain many observed protein T_1 values at frequencies between 14 MHz and 68 MHz, and the nOe values obtained at up to 45 MHz. However, two queries have since arisen. One is a suggestion by Dill and Allerhand (1979) that the

same results may be explained in terms of a rigid rotor with unexpectedly long α-C-H bonds. The second is that the single-libration theory predicts a sharp increase in nOe for resonances in small proteins at very high observation frequencies, and also for larger proteins at somewhat lower frequencies. Measurements of such nOe's are now possible and in the present study such measurements were made in order to test the single-libration theory more rigorously and to compare it with the present theory.

In all three theories, there are no difficulties in explaining how T_1 and T_2 vary with observation frequency. The crucial test lies in the values of nOe. Allerhand's rigid-rotor theory predicts that when the observation frequency is much greater than $\tau_R/2\pi$, the nOe value should be 1.15, independent of the CH bond length.

The results in Table 7.3 shows that the α-carbons have a slow component of libration (τ_S = 7 ns, θ = 0.55-0.70 rad.) as well as a rapid one (τ_G = 40-60 ps, X = 0.35 rad.). The slower libration is a little faster than the overall rotational rate of the protein molecule. It is evident that although the single-libration theory predicts τ_G and X values of 10 ps and 0.3 rad. respectively, it predicts nOe values considerably larger than those actually observed. The double-libration theory gives a somewhat better fit with the experimental data. This is so because the double-libration theory does not exclude the possibility of some internal- or anisotropic-rotational motion at an intermediate rate, with an appropriate correlation time to give a lower nOe value. The observation of fast,

small-angle, and slow, wide-angle components of motion for the relaxation of C-α resonances indicates that, in addition to the overall rotational motion of the molecule, librational motions of the polypeptide backbone are present.

The lys side-chain shows the typical motional characteristics of a linear chain. The side-chain motions have a slow, wide-angle component of libration as well as a rapid one, comparable to that found for the α-carbons. The slower librations have τ_S typically 345 ps (Table 7.4). The presence of a slow librational contribution to this motion indicates constraint relative to what would be predicted for a truly unrestricted side-chain.

For each of the proteins tested, the rotational correlation time, τ_R, obtained using the 3-τ theory, is rather long. Perhaps a more realistic protein molecule including a greater variety of internal segmental motions than is allowed for in the present model is necessary.

7.5 CONCLUSIONS

The double-libration theory was devised in sufficiently general terms to be applicable to most molecules, and the above evidence shows that it withstands rigorous experimental testing better than do the other theories published to date. It yields sufficient detail to begin to allow some time-resolved conformational analysis of highly flexible molecules, although it requires further development and improved experimental data before

it can be used with confidence in proteins.

TABLE 7.3 Protein α-Carbon: nT_1 and nOe Values, Motional Frequencies, and Amplitudes from ^{13}C Relaxation Data

	Resonance Frequency																Motion Amplitude/ Frequencies[f]				
	15.2 MHz				22.6 MHz				45.2 MHz				100.6 MHz								
	nT_1	nT_1	nOe	nOe[e]	nT_1	nT_1	nOe	nOe	nT_1	nT_1	nOe	nOe[e]	nT_1	nT_1	nOe	nOe	τ_G	X	τ_e	θ	τ_R
	(obs)	(calc)	(obs)	(calc)	(obs)	(calc)	(obs)	(calc)	(obs)	(calc)	(obs)	(calc)	(obs)	(calc)	(obs)	(calc)	(ps)	(rad)	(ps)	(rad)	(ns)
Ribonuclease A	35.0[a]	35.0	-	1.4	-	-	-	-	150[b]	150	1.4	1.26 (1.3)	414	470	1.27	1.27	60	.35	7000	.55	20
Lysozyme	27.0[d] 29.0	31.0	-	1.55	-	-	-	-	92	140	1.33	1.25	409	411	1.21	1.27	40	.35	7000	.7	10
Myoglobin[c]	36.0	39.0	1.2	1.4 (1.3)	73	73	1.3	1.3 (1.3)	57	57	1.3	1.35	-	-	-	-	60	.35	7000	.65	30

[a] Results from Glushko *et al.* (1972)

[b] Results from Howarth (1978)

[c] Results from Vischer and Gurd (1975)

[d] Results from Dill and Allerhand (1979)

[e] Figures is parenthesis refer to nOe values calculated using the single libration theory (Howarth, 1978)

[f] See footnote of Table 7.1

TABLE 7.4 RNase Methylene Carbons: nT_1 and nOe Values, Motional Frequencies and Amplitudes from ^{13}C Relaxation Data

	15.2 MHz[a]				45.2 MHz[a]				100.6 MHz				Motion Amplitude/Frequencies[b]				
	nT_1	nT_1	nOe	nOe	nT_1	nT_1	nOe	nOe	nT_1	nT_1	nOe	nOe	τ_G	X	τ_s	θ	τ_R
	(obs)	(calc)	(obs)	(calc)	(obs)	(calc)	(obs)	(calc)	(obs)	(calc)	(obs)	(calc)	(ps)	(rad)	(ps)	(rad)	(ns)
Main C^{β}	130	98	-	1.82	220	276	1.6	2.14	527	513	1.86	1.87	36	.7	734	.7	20
Lys-C^{γ}	200	164	-	2.02	270	360	1.7	2.39	645	610	2.0	2.0	14	.78	530	.87	20
Lys-C^{δ}	380	367	-	2.08	360	-	-	2.71	792	841	2.34	2.7	32	.92	233	.98	20
Lys-C^{ε}	560	505	-	2.32	770	779	-	2.76	1000	973	2.45	2.63	23	.98	273	1.069	20

[a] Results from Howarth (1978)

[b] See footnote of Table 7.1

REFERENCES

Alcock, N. W., Benton, D. J. and Moore, P. (1970) *Trans. Faraday Soc.*, 66, 2210

Allerhand, A. (1979) *Methods in Enzymology*, 61, 458

Allerhand, A., Cochran, D. W. and Doddrell, D. (1970) *Proc. Natl. Acad. Sci. U.S.A.*, 67, 1093

Allerhand, A. and Komoroski, R. (1973) *J. Amer. Chem. Soc.*, 95, 8228

Allerhand, A., Norton, R. S. and Childers, R. F. (1977) *J. Biol. Chem.*, 252, 1786

Allewell, N. M. and Wyckoff, H. W. (1971) *J. Biol. Chem.*, 246, 4657

Anet, F. A. L. (1974) in "Topics in Carbon-13 NMR Spectroscopy", (G. C. Levy, ed.), Vol. 1, p. 209, Wiley-Interscience, New York

Anfinsen, C. B. and Scheraga, H. A. (1975) *Adv. Prot. Chem.*, 29, 205

Artymiuck, P. J. (1981) Personal Communication, Laboratory of Molecular Biophysics, Zoology Department, University of Oxford, U.K.

Arus, C., Paolillo, L., Llorens, R., Napolitano, R., Pares, X. and Cuchillo, M. (1981) *Biochim. Biophys. Acta*, 660, 117

Barnes, K. P., Warren, J. R. and Gorden, J. A. (1972) *J. Biol. Chem.*, 247, 1708

Benz, F. W. and Roberts, G. C. K. (1973) in "Physicochemical Properties of Nucleic Acid", (J. Duchesne,ed.), Vol. 3, p. 77, Academic Press, New York

Benz, F. W. and Roberts, G. C. K. (1975(a)) *J. Mol. Biol.*, 91, 345

Benz, F. W. and Roberts, G. C. K. (1975(b)) *J. Mol. Biol.*, 91, 367

Blake, C. C. F., Mair, G. A., North, A. C. T., Phillips, D. C. and Sarma, V. R. (1967) *Proc. R. Soc. London, Ser. B*, 167, 365

Block, K., Bernd, M. and Vignon, M. (1980) *J. Magn. Res.*, 38, 545

Borkakoti, N., Moss, D. S. and Palmer, R. A. (1982) *Acta Cryst.*, B38, 2210

Borkakoti, N. (1982) Personal Communication, Birkbeck College, University of London, U.K.

Bothner-By, A. A. and Gissend, R. (1973) *N. Y. Acad. Sci. Ann.*, 222, 668

Bradbury, J. H. and King, N. L. R. (1969) *Nature (London)*, 223, 1154

Bradbury, J. H. and Norton, R. S. (1974) *Int. Jnl. Pept. and Prot. Res.*, 6, 295

Briggs, J., Hart, F. A., Moss, G. P. and Randall, E.W. (1971) *J.C.S. Chem. Comm.*, 364

Burgess, A. W., and Scheraga, H. A. (1975) *J. Theor. Biol.*, 53, 403

Campbell, I. D., Dobson, C. M. and Williams, R. J. P. (1975) *Proc. R. Soc. London, Ser. A*, 345, 41

Campbell, I. D. (1977) in "NMR in Biology", (R. D. Dwek, ed.), Academic Press, London

Campbell, I. D. and Dobson, C. M. (1979) *Methods Biochem. Anal.*, 25, 1

Carlisle, C. H., Palmer, R. A., Mazumdar, S. K., Gorinsky, B. A. and Yeates, D. G. R. (1974) *J. Mol. Biol.*, 85, 1

Cassels, R., Dobson, C. M., Poulsen, F. M., and Williams, R. J. P. (1978) *Eur. J. Biochem.*, 92, 81

Cozzone, P. J., Opella, S. J., Jardetzky, O., Berthou, J. and Jolles, P. (1975) *Proc. Natl. Acad. Sci. U.S.A.*, 72, 2095

Dahlquist, F. W. and Raftery, M. A. (1968) *Biochemistry*, 7, 3269

Delepierre, M. (1982) Personal Communication, Department of Inorganic Chemistry, University of Oxford, U.K.

Deslauriers, R. and Smith, I. C. P. (1976) in "Topics in Carbon-13 NMR Spectroscopy", (G. C. Levy, ed.) Vol. 2, p.10, Wiley-Interscience, New York

Dickerson, R. F. and Geis, I. (1969) in "The Structure and Action of Proteins", p.72, W. A. Benjamin, Inc., California

Dill, K. and Allerhand, A. (1977) *J. Amer. Chem. Soc.*, 99, 4508

Dill, K. and Allerhand, A. (1979) *J. Amer. Chem. Soc.*, 101, 4376

Dobson, C. M. and Williams, R. J. P. (1975) *F.E.B.S. Lett.*, 56, 362

Dobson, C. M. (1975) D.Phil. Thesis, University of Oxford, U.K.

Doddrell, D., Glushko, V. and Allerhand, A. (1972) *J. Chem. Phys.*, 56, 3683

Egan, W., Shindo, H. and Cohen, J. S. (1978) *J. Biol. Chem.*, 253, 16

Fan, S. and Bersohn, R. (1975) *Biochim. Biophys. Acta*, 397, 405

Farrar, T. C. and Becker, E. D. (1971)in"Pulse and Fourier Transform NMR", p.75, Academic Press, New York

Ferridge, A. G. and Lindon, J. C. (1978) *J. Magn. Res.*, 31, 337

Freeman, R. and Hill, H. D. W. (1969) *J. Chem. Phys.*, 51, 3140

French, T. C. and Hammes, G. G. (1965) *J. Amer. Chem. Soc.*, 87, 4669

Glushko, V., Lawson, P. J. and Gurd, F. R. N. (1972) *J. Biol. Chem.*, 247, 3176

Gorenstein, D. G. and Wyrwicz, A. M. (1974) *Biochemistry*, 13, 3828

Howarth, O. W. (1978) *J.C.S. Faraday Trans.*, 2, 74, 1031

Howarth, O. W. and Lilley, D. M. J. (1978) *Prog. in NMR Spectroscopy*, 12, 1

Howarth, O. W. (1979(a)) *Biochim. Biophys. Acta*, 576, 163

Howarth, O. W. (1979(b)) *J.C.S. Faraday Trans.*, 2, 75, 863

Howarth, O. W. (1980) *J.C.S. Faraday Trans.*, 2, 76, 1219

Howarth, O. W. and Lian, L. Y. (1981) *J.C.S. Chem. Comm.*, 258

Howarth, O. W. and Lian, L. Y. (1982) *J.C.S. Perkin Trans.*, 2, 3, 249

Ihnat, M. (1972) *Biochemistry*, 11, 3483

Imoto, T., Johnson, L. N., North, A. C. T., Phillips, D. C. and Rupley, J. A. (1972) in "The Enzymes", (P. D. Boyer, ed.) Vol. 7, p. 665, Academic Press, New York

Jaenck, G. and Benz, F. W. (1979) *Biochem. Biophys. Res. Commun.*, 86, 885

Jardetzky, O., Ribeiro, A. A. and King, R. (1980) *Biochem. Biophys. Res. Commun.*, 92, 883

Jardetzky, O. and Roberts, G. C. K. (1981) in "NMR in Molecular Biology", Academic Press, New York

Jentoft, J. E., Gerken, T. A., Jentoft, N. and Dearborn, D. G. (1981) *J. Biol. Chem.*, 256, 231

Jones, W. C., Rothgeb, T. M. and Gurd, F. R. N. (1976) *J. Biol. Chem.*, 251, 7452

Jones, C. R., Kuo, M. C. and Gibbons, W. A. (1979) *J. Biol. Chem.*, 254, 10307

Karpeisky, M. Y. and Yakovlev, G. I. (1977) *F.E.B.S. Lett.*, 75, 70

Komoroski, R., Peat, I. R. and Levy, G. C. (1975) *Biochem. Biophys. Res. Commun.*, 65, 272

Kopple, K. D., Ohnishi, M. and Go, A. (1968) *Biochemistry*, 8, 4087

Kopple, K. D., Ohnishi, M. and Go, A. (1969) *J. Amer. Chem. Soc.*, 91, 4264

Lapanje, S. (1978) in "Physicochemical Aspects of Protein Denaturation", Wiley - Interscience, New York

Led, J. J. and Petersen, S. B. (1978) *J. Magn. Res.*, 32, 1

Lee, B. and Richards, F. M. (1971) *J. Mol. Biol.*, 55, 379

Lenstra, J. A., Bolscher, B. G. J., Stob, S., Beintema, J. J. and Kaptein, R. (1979) *Eur. J. Biochem.*, 98, 385

London, R. E. (1978) *J. Amer. Chem. Soc.*, 100, 2678

London, R. E. and Avitabile, J. (1976) *J. Chem. Phys.*, 65, 2443

London, R. E. and Avitabile, J. (1977) *J. Amer. Chem. Soc.*, 99, 7765

London, R. E. and Avitabile, J. (1978) *J. Amer. Chem. Soc.*, 100, 7159

Markley, J. L., Holsey, W. J. and Klein, M. P. (1971) *J. Chem. Phys.*, 55, 3604

Markley, J. L. (1975(a)) *Biochemistry*, 14, 3546

Jardetzky, O., Ribeiro, A. A. and King, R. (1980) *Biochem. Biophys. Res. Commun.*, 92, 883

Jardetzky, O. and Roberts, G. C. K. (1981) in "NMR in Molecular Biology", Academic Press, New York

Jentoft, J. E., Gerken, T. A., Jentoft, N. and Dearborn, D. G. (1981) *J. Biol. Chem.*, 256, 231

Jones, W. C., Rothgeb, T. M. and Gurd, F. R. N. (1976) *J. Biol. Chem.*, 251, 7452

Jones, C. R., Kuo, M. C. and Gibbons, W. A. (1979) *J. Biol. Chem.*, 254, 10307

Karpeisky, M. Y. and Yakovlev, G. I. (1977) *F.E.B.S. Lett.*, 75, 70

Komoroski, R., Peat, I. R. and Levy, G. C. (1975) *Biochem. Biophys. Res. Commun.*, 65, 272

Kopple, K. D., Ohnishi, M. and Go, A. (1968) *Biochemistry*, 8, 4087

Kopple, K. D., Ohnishi, M. and Go, A. (1969) *J. Amer. Chem. Soc.*, 91, 4264

Lapanje, S. (1978) in "Physicochemical Aspects of Proton Denaturation", Wiley - Interscience, New York

Led, J. J. and Petersen, S. B. (1978) *J. Magn. Res.*, 32, 1

Lee, B. and Richards, F. M. (1971) *J. Mol. Biol.*, 55, 379

Lenstra, J. A., Bolscher, B. G. J., Stob, S., Beintema, J. J. and Kaptein, R. (1979) *Eur. J. Biochem.*, 98, 385

London, R. E. (1978) *J. Amer. Chem. Soc.*, 100, 2678

London, R. E. and Avitabile, J. (1976) *J. Chem. Phys.*, 65, 2443

London, R. E. and Avitabile, J. (1977) *J. Amer. Chem. Soc.*, 99, 7765

London, R. E. and Avitabile, J. (1978) *J. Amer. Chem. Soc.*, 100, 7159

Markley, J. L., Holsey, W. J. and Klein, M. P. (1971) *J. Chem. Phys.*, 55, 3604

Markley, J. L. (1975(a)) *Biochemistry*, 14, 3546

Markley, J. L. (1975(b)) *Biochemistry*, 14, 3554

Markley, J. L. and Finkenstadt, W. R. (1975) *Biochemistry*, 14, 3562

Matheson, R. R. Jr. and Scheraga, H. A. (1978) *Macromolecules*, 11, 819

Matheson, R. R. Jr. and Scheraga, H. A. (1979(a)) *Biochemistry*, 18, 2437

Matheson, R. R. Jr. and Scheraga, H. A. (1979(b)) *Biochemistry*, 18, 2446

McDonald, G. G. and Leigh, J. S. (1973) *J. Magn. Res.*, 9, 358

McDonald, C. C. and Phillips, W. D. (1967), *J. Amer. Chem. Soc.*, 89, 6332

Meadows, D. H., Roberts, G. C. K. and Jardetzky, O. (1969) *J. Mol. Biol.*, 45, 491

Metzler, D. E. (1977) in "Biochemistry: The Chemical Reactions of Living Cells", Academic Press, New York

Nagayama, K. (1981) *Adv. Biophys.*, 14, 139

Niu, C. H., Matsuura, S., Shindo, H. and Cohen, J. S. (1979) *J. Biol. Chem.*, 254, 3788

Norton, R. S. and Allerhand, A. (1976(a)) *Biochemistry*, 15, 3438

Norton, R. S. and Allerhand, A. (1976(b)) *J. Biol. Chem.*, 251, 6522

Norton, R. S., Clouse, A. O., Addleman, R. and Allerhand, A. (1977), *J. Amer. Chem. Soc.*, 99, 79

Oldfield, E., Norton, R. S. and Allerhand, A. (1975) *J. Biol. Chem.*, 250, 6381

Olejniczak, E. T., Poulsen, F. M. and Dobson, C. M. (1981) *J. Amer. Chem. Soc.*, 103, 6574

Pavlovsky, A. G. Borisova, S. N., Vagin, A. A. and Karpeisky, M. Y. (1977) *Soviet Jnl. of Bio-Oceanic Chem.*, 3, 1378

Patel, D. J., Canuel, L. L. and Bovey, F. A. (1975) *Biopolymers*, 14, 987

Perkins, S. J., Johnson, L. N., Dwek, R. A. and Phillips, D. C. (1977) *F.E.B.S. Lett.*, 82, 17

Perkins, S. J., Johnson, L. N., Machin, P. A. and Phillips, D. C. (1978) *Biochem. J.*, 173, 607

Perkins, S. J. and Dwek, R. A. (1980) *Biochemistry*, 19, 245

Perkins, S. J., Johnson, L. N., Phillips, D. C. and Dwek, R. A. (1981(a)) *Biochem. J.*, 193, 553

Perkins, S. J., Johnson, L. N., Phillips, D. C. and Dwek, R. A. (1981(b)) *Biochem. J.*, 193, 573

Poulsen, F. M., Hoch, J. C. and Dobson, C. M. (1980) *Biochemistry*, 19, 2597

Rall, T. W. and Lehninger, A. L. (1952) *J. Biol. Chem.*, 194, 119

Richards, F. M. and Wyckoff, H. W. (1971) in "The Enzymes", (P. D. Boyer, ed.) Third Ed., Vol. 4, p. 647 Academic Press, New York

Richarz, R. and Wüthrich, K. (1978) *Biochemistry*, 17, 2263

Richarz, R., Nagayama, K. and Wüthrich, K. (1980) *Biochemistry*, 19, 5189

Sadler, P. J., Benz, F. W. and Roberts, G. C. K. (1974) *Biochim. Biophys. Acta*, 359, 13

Santoro, J., Juretschke, H. P. and Rüterjans, H. (1979) *Biochim. Biophys. Acta*, 578, 346

Saunders, M., Wishnia, A. and Kirkwood, J. G. (1957) *J. Amer. Chem. Soc.*, 79, 3289

Shindo, H. and Cohen, J. S. (1976) *Proc. Natl. Acad. Sci. U.S.A.*, 73, 1979

Shindo, H., Cohen, J. S. and Rupley, J. A. (1977) *Biochemistry*, 16, 3879

Shindo, H., Egan, W. and Cohen, J. S. (1978) *J. Biol. Chem.*, 253, 6751

Snape, K. W. (1974) Ph.D. Thesis, University of Oxford, U.K.

Stanford, M. (1981) Personal Communication, Birkbeck College, University of London, U.K.

Ugurbil, K., Norton, R. S., Allerhand, A. and Bersohn, R. (1977) *Biochemistry*, 16, 886

Visscher, R. B. and Gurd, F. R. N. (1975) *J. Biol. Chem.*, 250, 2238

Vold, R. L., Waugh, J. S., Klein, M. P. and Phelps, D. E. (1968) *J. Chem. Phys.*, 48, 3831

Walters, D. E. and Allerhand, A. (1980) *J. Biol. Chem.*, 255, 6200

Wilbur, D. J., Norton, R. S., Clouse, A. O., Addleman, R. and Allerhand, A. (1976) *J. Amer. Chem. Soc.*, 98, 8250

Wittebort, R. J. and Szabo, A. (1978) *J. Chem. Phys.*, 69, 1722

Wittebort, R. J., Rothgeb, T. M., Szabo, A. and Gurd, F.R.N. (1979) *Proc. Natl. Acad. Sci. U.S.A.*, 76, 1059

Wüthrich, K. (1976) in "NMR in Biological Research: Peptides and Proteins", North-Holland, Amsterdam

APPENDIX I

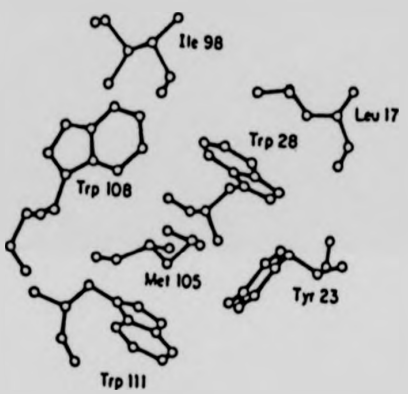

View of part of the hydrophobic box region of lysozyme. Taken from Poulsen *et al.* 1980.

APPENDIX II

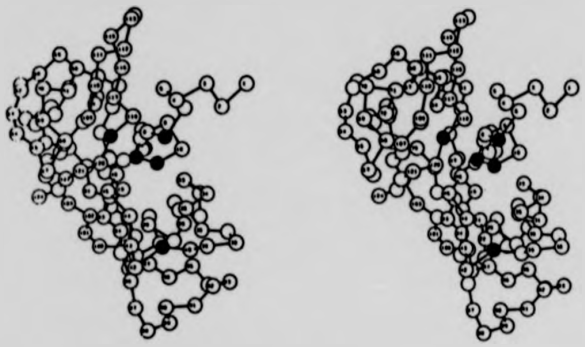

(a) Stereoscopic representation of the backbone chain of ribonuclease A showing only α-carbon atoms. The numbering corresponds to that of the amino acid sequence. α-carbon atoms for lys-7, gln-11, his-12, lys-41, and his-119 have been blacked in. Taken from Carlisle *et al.*, 1974.

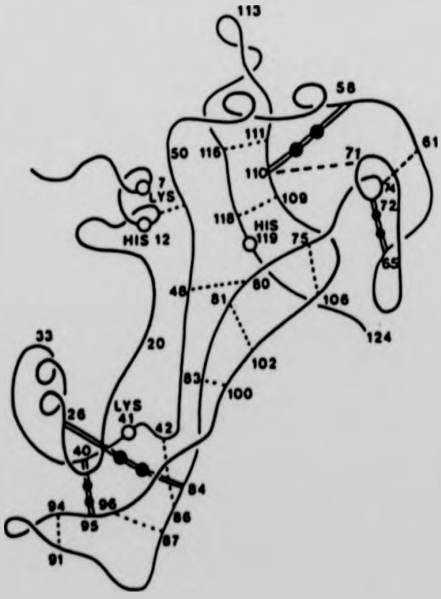

(b) Schematic drawing of the backbone chain of ribonuclease A (Borkakoti, personal communication).

○ ACTIVE SITE RESIDUES
HELIX
···· H-BONDS (SELECTED)
S-S BRIDGES

APPENDIX III

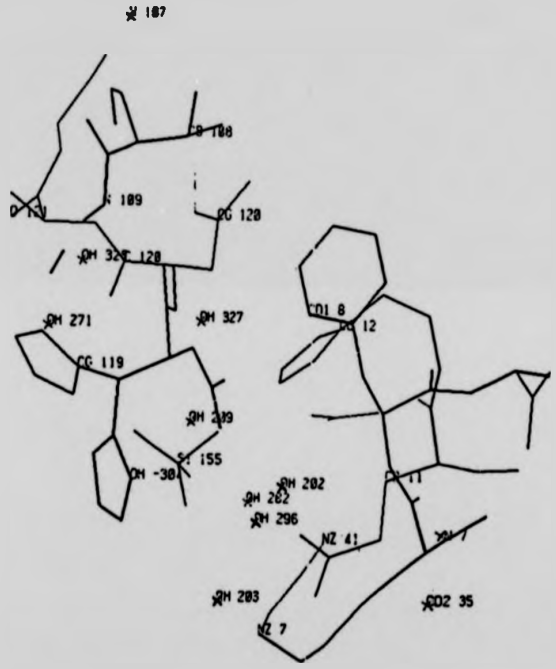

Stereoplot of part of the active site of ribonuclease A showing the possible orientations of the imidazole ring of his-119 (Borkakoti, personal communication).

APPENDIX IV

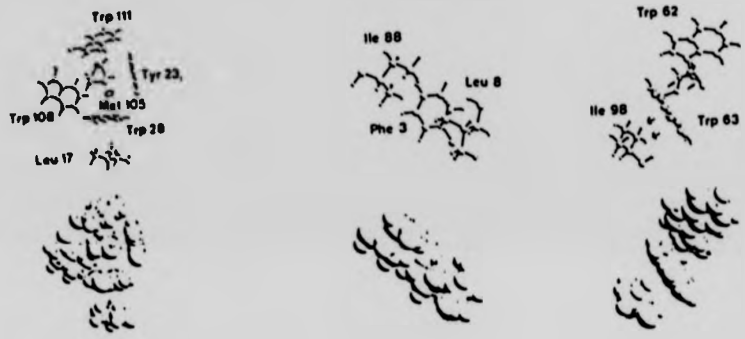

(a) (b) (c)

Computer drawings of local structures in the refined tetragonal crystal coordinates of lysozyme. Taken from Perkins and Dwek, 1980.

(a) The interactions in the aromatic box, where met-105 is surrounded by the rings of tyr-23, trp-28, trp-108 and trp-111.

(b) The interaction between phe-3, leu-8, and ile-88, where the ring of phe-3 is depicted beneath the side-chains of leu-8 and ile-88.

(c) The interaction between trp-63, trp-62 and ile-98.

APPENDIX V

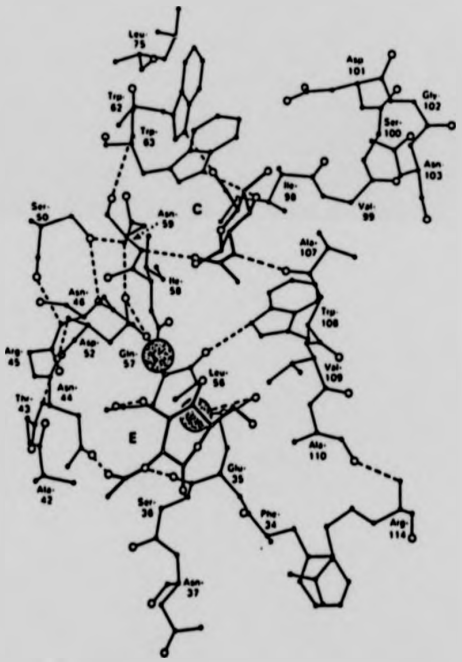

Active site cleft in native lysozyme drawn to show the position of the two Gd(III)-binding subsites and the sugar-binding subsites C and E. The sugar is shown with heavy lines, the Gd(III) is shadowed and the surrounding protein is shown with light lines. Taken from Perkins *et al.* (1981(b)).

APPENDIX VI

(i)

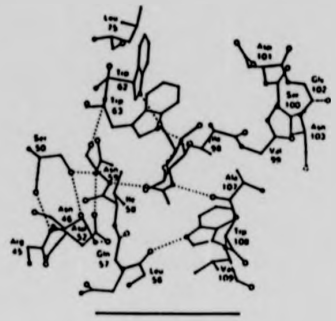

(ii)

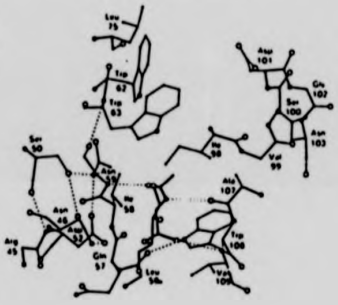

(a) Binding of β-NAG to subsite C-β(i) and of α-NAG to subsite C-α(ii) at the active site of lysozyme. The sugar is shown with heavy lines and the surrounding protein with light lines. Taken from Perkins *et al.* (1978).

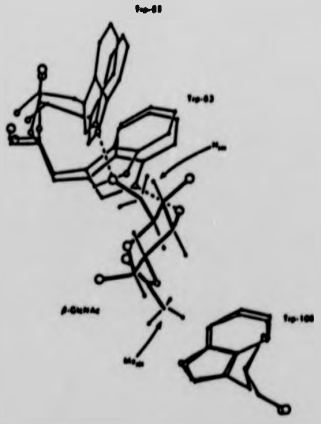

(b) Movements of the lysozyme tryptophan rings adjacent to subsite C that are observed in the tetragonal crystal structure of lysozyme-βNAG complex compared to native lysozyme. The tryptophan residues in bold outline indicate the lysozyme-inhibitor structure. The sugar is shown with heavy lines. Taken from Perkins. *et al.* (1981(a)).

APPENDIX VII(a)

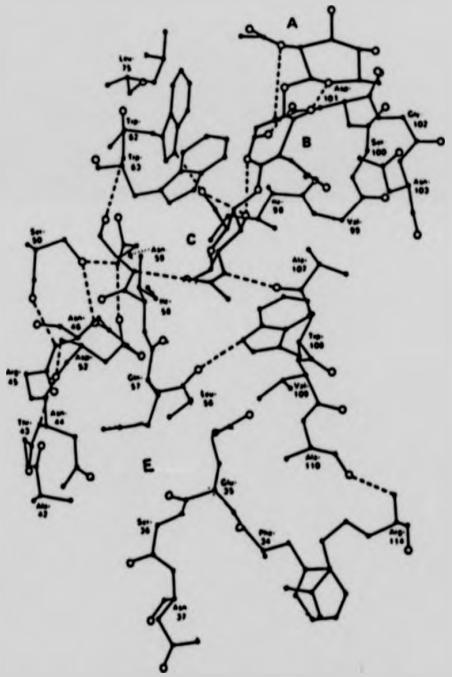

Active site of lysozyme showing the proposed binding of a trisaccharide substrate in the three subsites A-C in the cleft of lysozyme. Extracted from Perkins *et al.*, 1981(a).

APPENDIX VII(b)

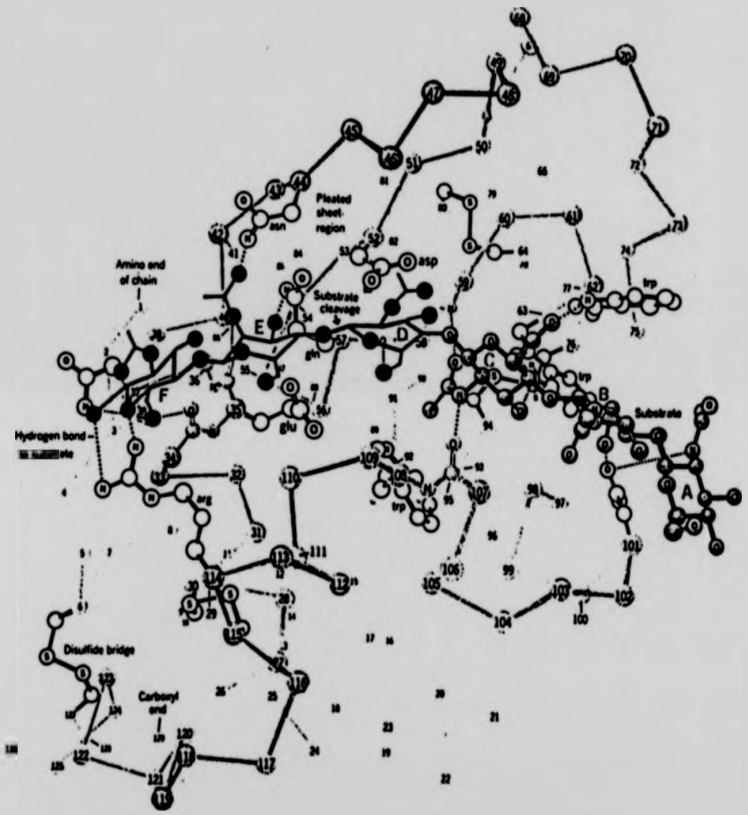

Structure of the lysozyme-substrate complex. The drawing shows the backbones of the lysozyme and substrate molecules (heavy lines) in the crystalline complex. Taken from Dickerson and Geis (1969).

APPENDIX VIII

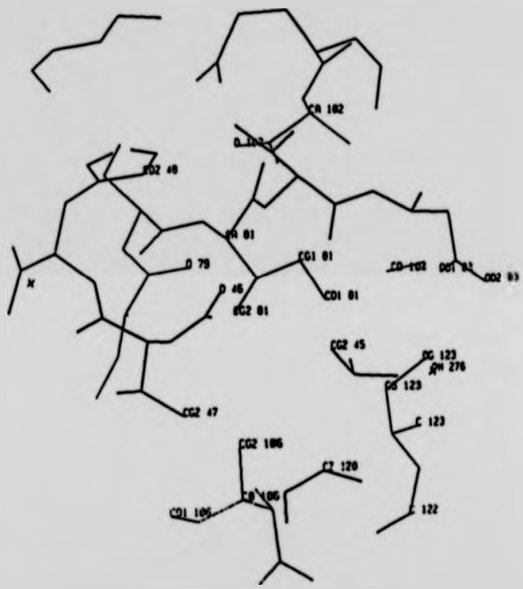

Stereoplot of part of the ribonuclease A structure showing the area around the ile-81 and ile-106 residues (Borkakoti, personal communication).

APPENDIX IX

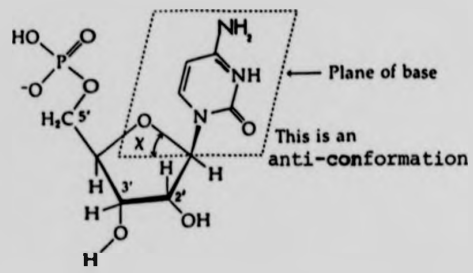

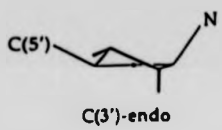

C(3')-endo

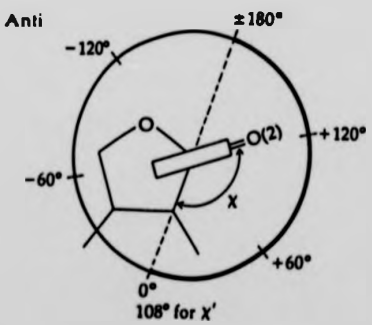

Conformation of Nucleotides (Metzler, 1977)

(a) The structure of cytidine-5'-phosphate in the anti-conformation.

(b) The C(3')-endo conformation of the ribose.

(c) View down the N-C axis joining pyrimidine base to the ribose in the nucleotide. Anti-conformations are those for which χ falls in the region of the heavy semi-circle.

APPENDIX X

MICROPROGRAMS

(a) Two-level Heteronuclear Decoupling

```
1     ZE
2     BB
3     S1
4     D1
5     S2
6     D2
7     GO   =   3
8     EXIT
```

(b) nOe Difference Spectra - Multiple Experiments using Disk

```
1     FL       FQLIST
2     IF       FQLIST
3     ZE
4     O2
5     D1
6     HG
7     D2
8     DO
9     D3
10    GO   =   5
11    NM
12    LO       4,  TIMES:  241
13    NM
14    WR       DATA
15    IF       DATA
16    IN   =   1
17    EXIT
```

(c) Inversion-Recovery T_1

```
1     ZE
2     BB
3     D1
4     P1
5     VD
6     GO   =   3
7     WR       DATA
8     IF       DATA
9     IN   =   1
10    EXIT
```

(d) Saturation Recovery T_1

```
1     ZE
2     SP
3     VD
4     GO   =   2
5     WR       DATA
6     IF       DATA
7     IN   =   1
8     PO
9     EXIT
```

(e) Gated Heteronuclear Decoupling - Decoupled Spectra with and without nOe

```
1     ZE
2     RE       DATA 1
3     D1
4     GO   =   4
5     WR       DATA 1
6     ZE
7     RE       DATA 2
8     DO
9     D2
10    BB
11    D3
12    GO   =   8
13    WR       DATA 2
14    LO  TO   1    ,      TIMES:  1000
15    PO
16    EXIT
```

(a) Two-level Heteronuclear Decoupling

(b) nOe Difference Spectra - Multiple Experiments using Disk

(c) Inversion - Recovery T_1

(d) Saturation - Recovery T_1

(e) Gated Heteronuclear Decoupling-Decoupled Spectra with and without nOe

Structuring of Denatured Ribonuclease-A

By Oliver W. Howarth* and L. Yue Lian
(*Department of Chemistry and Molecular Sciences, University of Warwick, Coventry* CV4 7AL)

Summary Denatured aqueous ribonuclease-A is shown by high-field ^{13}C n.m.r. spectroscopy to be predominantly structured even at elevated temperatures and with its disulphide bonds chemically cleaved.

Ribonuclease-A is commonly used as a paradigm of reversible protein unfolding. Although Roberts[1] and others[2,3] have noted that ribonuclease-A is not completely unfolded by heat alone, heat plus 8 M urea is considered to effect full unfolding on the basis of the ^1H n.m.r. spectra of the histidyl residues. We have investigated this further by a ^{13}C n.m.r. study at 100·6 MHz, at which frequency many of the carbon atoms in the protein give resolved resonances.

As well as noting that a few individual resonances are affected by preliminary unfolding below the main transition temperature for denaturation (to be published), we find that the resonances from the native protein are reversibly replaced as a group over the temperature interval 315 to 328 K by a new group of resonances, many of which clearly show a chemical shift heterogeneity inconsistent with that expected for a truly random-coil peptide.

For example, the upper spectrum in the Figure shows three separate resonances at δ_C *ca.* 11. From their shifts these must almost certainly arise from C-δ of the three isoleucine residues in the protein, for no other peptide resonance lies within 4 p.p.m. Each methyl group must be in a unique well-defined average environment in order to give a resolved, sharp resonance. Furthermore, this environment is probably not solvent-like, because the normal shift for this resonance in a peptide is δ 11·3—12·5 in water and 11·0 in dimethyl sulphoxide.[4] Similarly, three peaks are observed for C-γ of the three phenylalanine residues, at δ *ca.* 137.

The chemical shift heterogeneity of all identifiable groups of resonances from like carbon atoms in the denatured protein is typically 1 p.p.m., which is considerably less than that found in native proteins,[4] and simplifies the assignments. In general, hydrophobic residues such as isoleucine and phenylalanine, and including threonine, show well-resolved resonances, whereas hydrophilic residues such as glutamate, tyrosine, and histidine show single, slightly broad resonances analogous to those of lysine C-δ and C-ε in native proteins. Their linewidths are consistent with the sidechains sampling a variety of environments, and spending typically 0·01 s in each. Also, all the glutamate residues appear to have a similar pH-dependence. All these observations, together with previous T_1 measurements,[5] are consistent with the denatured protein having a relatively loosely bound, expanded structure held together by hydrophobic interactions. The expansion of molecular volume is presumably sufficient to account for the hydrodynamic behaviour[6] which is normally interpreted as that of a random coil. The general reduction in chemical shift heterogeneity may be explained by free rotation of all aromatic rings. We observed a similar spectrum for the protein at pH 1·2 and 6·0 and also in 8 M urea at 335 K, with many single carbon resonances still resolved, although broader.

In order to find out whether this structuring is merely due to the four S–S bridges we also obtained spectra where these had been cleaved either by dithiothreitol reduction[7] or by performic acid oxidation.[8] Surprisingly, the chemical shift heterogeneity is retained in both cases (see the Figure) even at elevated temperatures. The spectra show the expected changes in the cysteinyl resonances, and, following oxidation, in the methionine resonances at δ 15·2. They also differ from each other in detail, which shows that the chemical shift heterogeneity is not due to some hitherto unobserved effect of primary structure. But they all have the general features described above, with resolved resonances from hydrophobic residues and broad ones from hydrophilic.

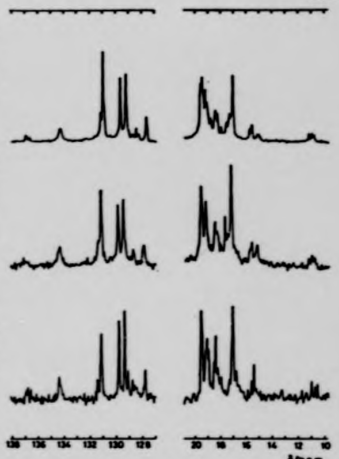

Figure. Portions of the 100·6 MHz ^{13}C n.m.r. spectrum of denatured ribonuclease-A. (Upper trace): Thermally denatured at 330 K, pH 3·3, 10 ms. The same spectrum was also obtained at 2 ms. (Middle trace): Reduced by dithiothreitol, 325 K, pH 3·3, 9·7 ms. (Lower trace): Oxidised by performic acid, 306 K, pH 4·4, 8 ms. A very similar spectrum was obtained at 325 K, but with some evidence for an additional aggregated component.

This suggests that a hydrophobically bound structure is likely to be a general feature of soluble denatured proteins, and calls into question any theoretical or kinetic study of protein folding made on the assumption that the denatured protein is a random coil.

We thank the S.R.C. for use of a Bruker WH400 spectrometer and for a research assistantship.

(*Received, 4th December* 1980; *Com.* 1293.)

[1] G. C. K. Roberts and F. W. Benz, *Ann. N.Y. Acad. Sci.*, 1973, 222, 130.
[2] C. Tanford, *Adv. Protein Chem.*, 1968, 23, 121.
[3] O. W. Howarth, *Biochim. Biophys. Acta*, 1979, 576, 162.
[4] O. W. Howarth and D. M. J. Lilley, *Prog. Nucl. Magn. Reson. Spectrosc.*, 1978, 12, 1.
[5] W. H. Konigsberg, *Methods Enzymol.*, 1972, 25, 185.
[6] C. H. W. Hirs, *Methods Enzymol.*, 1967, 11, 197.

Resolved Librational Motions of Gramicidin-S and Glutathione Dimer as studied by Nuclear Magnetic Resonance Spectroscopy

By Oliver W. Howarth * and L. Yun Lian, Department of Chemistry and Molecular Sciences, University of Warwick, Coventry CV4 7AL

A theory relating ^{13}C n.m.r. relaxation parameters to molecular motion at three levels is described, and successfully subjected to unusually rigorous experimental test. The results give information on mean conformations and on rates of internal librational motions for gramicidin-S and for glutathione dimer. They also confirm some previous conclusions regarding proteins, although in this case the model is more approximate.

THERE has been considerable progress recently in the analysis of the motions of complex molecules by ^{13}C n.m.r. relaxation and nuclear Overhauser enhancement measurements. London and Avitabile [1] have presented a general theory of the relaxation parameters for atoms in a side-chain with freely rotating links attached to a rigid core, and although this model does not give very satisfactory fits with experiment,[2] its general approach may readily be developed to allow for restricted rotation of the links,[3] and other comparable motions,[4] in a way that has been shown to fit a few experiments quite satisfactorily. Howarth [5,6] has developed a generalised version of this theory which reinterprets the restricted rotations as internal librations specified only by their average angular extent and rate and which is thus applicable to molecular loops such as in proline and in the main chains of proteins as well as to side-chains. Jardetzky [7] has also recently proposed a more abstract analysis of the same problem.

In order to explain observations on natural rubber, Howarth [8] found it necessary to assume both slow, wider and fast, small angle librations superimposed on a very slow pseudo-isotropic motion of the polyisoprene chain. The relatively tractable theoretical model that was developed for this analysis involves five motional parameters, which is about as many as one might hope to determine reliably by currently achievable experiments. The aim of the present work is to give this model as rigorous an experimental testing as reasonably possible, and thus to go on to a more detailed experimental analysis of molecular flexibility than has hitherto been possible.

Accordingly, we have tested the theory on two medium-sized molecules, gramicidin-S and glutathione dimer, for which T_1 data are available or measurable for at least three observation frequencies, together with nuclear Overhauser enhancements (n.O.e.s) at some frequencies. In the case of glutathione dimer the experiments were conducted in 50% glycerol–^2H_2O, with the aim of slowing the larger angle motions preferentially and thus improving the resolution of the theoretical analysis into underlying components of motion. Linewidths were not included in the analysis because they can often be misleadingly increased by conformational changes on the millisecond timescale.

Most of the data on these compounds cannot be convincingly reproduced by a single-libration model, but the present model fits all the data within experimental error, and even passes such severe tests as giving the same underlying overall molecular rotation rate from data for different atoms in the same molecule even when this is not assumed in advance. The one failure found so far is that the double-libration model still overestimates some n.O.e.s in proteins, albeit not as badly as does the single-libration model.

EXPERIMENTAL

T_1 Measurements were carried out at 22.6 MHz and T_1 and n.O.e. measurements at 45.2 and 100.63 MHz on Bruker WH 90, WH 180WB, and WH 400 spectrometers, respectively, at room temperature. Decoupler heating was reduced on the WH 400 spectrometer by switching of power levels and alternation of decoupler sequences during n.O.e. measurement. Measurements were repeated, with T_1s having a precision of ±10% and n.O.e.s of ±20%.

Gramicidin-S was obtained from Sigma and was used without further purification at a concentration of 0.088M in [$^2H_4$]methanol.

Glutathione dimer was prepared by the method of Rall and Lehringer,[9] and was used at 0.16M in 50% glycerol–^2H_2O for reasons described above. T_1 and n.O.e. values were assumed to be dominated by dipolar relaxation processes [10] and T_1 measurements were repeated twice.

THEORETICAL

The earlier, single-libration model [5,6] was developed from the single-rotor side-chain calculations of Woessner.[10] Its extension to double libration [6] was heuristic. However, it may be extended more rigorously by applying the same manipulations to London and Avitabile's [1] multiple-rotor model, reduced to the two-rotor case. In this way the nine components of their asymmetric matrix each become integrals involving the libration semi-angles. The resulting equations were used for the analysis described below, although their predictions are in fact experimentally indistinguishable from the simpler, heuristic theory. The underlying libration, which corresponds to the first rotation out from the rigid core in London and Avitabile's model, is assumed in all cases to be the slower one. Its jump correlation time is τ_0 and its mean semi-angle is θ. The corresponding parameters for the second, faster libration are τ_0 and X, and all these are assumed to be superimposed on an overall isotropic rotation of diffusional correlation time τ_R.

Experimental T_1 values were fitted by a least-squares programme developed from a method published by Moore.[11]

As this minimises the function $\chi^2 = [T_1(\text{expt.}) - T_1(\text{calc.})]^2/T_1(\text{expt.})$, it in effect favours the higher-field measurements, with their longer values of T_1. N.O.e.s were not fitted for the peptides, as they are frequently less sensitive to the details of the underlying motion, but they were valuable as a check against false minima, and are recorded in the Tables. The methyl group T_1 values were not considered to be experimentally reliable, because there is some suspicion of non-exponential relaxation decay; also, they would test a different theory.

Some of the calculated parameters are less sensitive to the experimental data than others. With the data and theory used, we estimate that the error limits on τ_R are $\pm 10\%$, on $\tau_s \pm 10\%$, on $\tau_0 \pm 14\%$, on $\theta \pm 8\%$, and on $X \pm 8\%$.

The overall correlation time for isotropic tumbling, τ_R, was at first allowed to vary freely for several resonances, as a test of the method of analysis. The calculated values of τ_R were found to lie within $\pm 10\%$ of a mean value, which was then fixed as the τ_R for all resonances. Any effects of anisotropic motion are likely to appear as an apparent contribution to the slow libration. We found that if the guessed starting value of τ_R was more than *ca.* 25% too small, new minima were found in some cases. These false minima could be reliably excluded because with the incorrect figures, $\Sigma\chi^2$ for all resonances was significantly larger both for values of T_1 and, independently, for values of the n.O.e.

Our method contrasts with that of Jardetzky,[7] who treats measurements at different fields independently. His resulting calculated motional parameters do not invariably harmonise, possibly because of T_1 errors, although they are generally consistent with our results.

RESULTS

The T_1 values for gramicidin-S in methanol at 15.2 and 67.5 MHz were taken from the work of Allerhand and Komoroski[10] and Komoroski *et al.*[11] The other results were obtained in the present study. The gramacidin-S results are in Table 1 and the glutathione dimer results in Table 2. Almost all the calculated T_1 values lie within 10% of the experimental ones, *i.e.* within experimental error. The calculated values of n.O.e also all lie well within the experimental error of 20%. Thus the two-libration' model gives a very satisfactory fit with one of the largest available sets of experimental data.

Gramicidin-S.—On the present analysis α-carbons show no large-angle libration, and a rapid libration of very similar mean half-range X (0.47—0.51 rad) to that found in less tightly structured main chains (typically 0.5 rad). Both these observations are entirely consistent with the known structure of gramicidin-S[13] in methanol, which is a cyclic decapeptide with four cross-ring hydrogen bonds. They confirm that the rapid X = 0.5 rad libration is a localised α-carbon libration common to many different molecules and probably not involving the entire side-chain. τ_0, the rapid jump correlation time, is 97—109 ps. This is somewhat longer than the 60 ps deduced for proteins on a single-libration model, but the difference may not be significant because of the change of models. However, the slightly faster calculated motion of Orn α-C and especially of Phe α-C may be real, because only the Orn NH and Phe NH groups remain unrestricted by cross-ring hydrogen bonding. As no apparent or real slow librational motion is detected, we may assume that the overall tumbling of gramicidin-S is effectively isotropic and that the ring does not undergo major vibrational deformations, at least at room temperature.

In contrast, the side-chain motions all have a slow, wide-angle component of libration as well as a rapid one comparable with that found for the α-carbons. These slower librations have τ_s (typically) 300 ps, so that they are not much faster than the molecular rotation in this molecule. It is convenient to consider each side-chain in turn.

TABLE 1

Gramicidin-S: nT_1 values for different resonances, motional frequencies, and amplitudes from ^{13}C relaxation data

	Resonance frequency										Motion amplitudes/frequencies				
	[illegible] MHz		[illegible] MHz		[illegible] MHz		[illegible] MHz								
	nT_1 (obs.)	nT_1 (calc.)	nT_1 (obs.)	nT_1 (calc.)	nT_1 (obs.)	nT_1 (calc.)	nT_1 (obs.)	nT_1 (calc.)	n.O.e. (obs.)	n.O.e. (calc.)	[illegible]	[illegible]	[illegible]	[illegible]	[illegible]
[illegible]	[illegible]	[illegible]	[illegible]	[illegible]	[illegible]	[illegible]	[illegible]	[illegible]	[illegible]	[illegible]	[illegible]	[illegible]	[illegible]	[illegible]	[illegible]
[illegible]	[illegible]	[illegible]	[illegible]	[illegible]	[illegible]	[illegible]	[illegible]	[illegible]	[illegible]	[illegible]	[illegible]	[illegible]	[illegible]	[illegible]	[illegible]
[illegible]	[illegible]	[illegible]	[illegible]	[illegible]	[illegible]	[illegible]	[illegible]	[illegible]	[illegible]	[illegible]	[illegible]	[illegible]	[illegible]	[illegible]	[illegible]
[illegible]	[illegible]	[illegible]	[illegible]	[illegible]	[illegible]	[illegible]	[illegible]	[illegible]	[illegible]	[illegible]	[illegible]	[illegible]	[illegible]	[illegible]	[illegible]
[illegible]	[illegible]	[illegible]	[illegible]	[illegible]	[illegible]	[illegible]	[illegible]	[illegible]	[illegible]	[illegible]	[illegible]	[illegible]	[illegible]	[illegible]	[illegible]
[illegible]															
[illegible]	[illegible]	[illegible]	[illegible]	[illegible]	[illegible]	[illegible]	[illegible]	[illegible]	[illegible]	[illegible]	[illegible]	[illegible]	[illegible]	[illegible]	[illegible]
[illegible]	[illegible]	[illegible]	[illegible]	[illegible]	[illegible]	[illegible]	[illegible]	[illegible]	[illegible]	[illegible]	[illegible]	[illegible]	[illegible]	[illegible]	[illegible]
[illegible]	[illegible]	[illegible]	[illegible]	[illegible]	[illegible]	[illegible]	[illegible]	[illegible]	[illegible]	[illegible]	[illegible]	[illegible]	[illegible]	[illegible]	[illegible]
[illegible]	[illegible]	[illegible]	[illegible]	[illegible]	[illegible]	[illegible]	[illegible]	[illegible]	[illegible]	[illegible]	[illegible]	[illegible]	[illegible]	[illegible]	[illegible]
[illegible]	[illegible]	[illegible]	[illegible]	[illegible]	[illegible]	[illegible]	[illegible]	[illegible]	[illegible]	[illegible]	[illegible]	[illegible]	[illegible]	[illegible]	[illegible]
[illegible]															
[illegible]	[illegible]	[illegible]	[illegible]	[illegible]	[illegible]	[illegible]	[illegible]	[illegible]	[illegible]	[illegible]	[illegible]	[illegible]	[illegible]	[illegible]	[illegible]
[illegible]	[illegible]	[illegible]	[illegible]	[illegible]	[illegible]	[illegible]	[illegible]	[illegible]	[illegible]	[illegible]	[illegible]	[illegible]	[illegible]	[illegible]	[illegible]
Phenylalanine															
[illegible]	[illegible]	[illegible]	[illegible]	[illegible]	[illegible]	[illegible]	[illegible]	[illegible]	[illegible]	[illegible]	[illegible]	[illegible]	[illegible]	[illegible]	[illegible]
[illegible]	[illegible]	[illegible]	[illegible]	[illegible]	[illegible]	[illegible]	[illegible]	[illegible]	[illegible]	[illegible]	[illegible]	[illegible]	[illegible]	[illegible]	[illegible]
[illegible]	[illegible]	[illegible]	[illegible]	[illegible]	[illegible]	[illegible]	[illegible]	[illegible]	[illegible]	[illegible]	[illegible]	[illegible]	[illegible]	[illegible]	[illegible]
Proline															
[illegible]	[illegible]	[illegible]	[illegible]	[illegible]	[illegible]	[illegible]	[illegible]	[illegible]	[illegible]	[illegible]	[illegible]	[illegible]	[illegible]	[illegible]	[illegible]
[illegible]	[illegible]	[illegible]	[illegible]	[illegible]	[illegible]	[illegible]	[illegible]	[illegible]	[illegible]	[illegible]	[illegible]	[illegible]	[illegible]	[illegible]	[illegible]
[illegible]	[illegible]	[illegible]	[illegible]	[illegible]	[illegible]	[illegible]	[illegible]	[illegible]	[illegible]	[illegible]	[illegible]	[illegible]	[illegible]	[illegible]	[illegible]

[illegible]

TABLE 2

Glutathione dimer[d]: nT_1 values for different resonances, motional frequencies, and amplitudes from ^{13}C relaxation data

	Resonance frequency										Motion amplitude/frequencies[c]				
	22.6 MHz		45.2 MHz				100.6 MHz								
	nT_1[a] (obs.)	nT_1 (calc.)	nT_1 (obs.)	nT_1 (calc.)	n.O.e.[b] (obs.)	n.O.e. (calc.)	nT_1 (obs.)	nT_1 (calc.)	n.O.e. (obs.)	n.O.e. (calc.)	τ_0/ps	X/rad	τ_s/ps	θ/rad	τ_R/ns
Cys-α	70	67	105	111	1.63	2.01	214	224	1.84	1.80	70	[illegible]	891	[illegible]	6.0
Cys-β	62	[illegible]	140	124	1.83	2.17	220	235	1.30	1.30	70	[illegible]	711	[illegible]	6.0
Glu-α	119	122	175	175	2.22	2.46	263	267	2.07	2.05	[illegible]	0.470	[illegible]	[illegible]	6.0
Glu-β	149	155	229	229	2.10	2.37	277	300	1.97	2.33	90	0.500	300	1.00	6.0
Glu-γ	165	170	[illegible]	249	2.22	2.16	305	300	2.02	2.09	[illegible]	0.500	304	[illegible]	6.0
Gly-α	171	165	266	279	2.13	2.05	419	470	1.93	1.97	[illegible]	[illegible]	247	[illegible]	6.0

[a] nT_1 values in ms. [b] n.O.e. values at 45.2 and 100.63 MHz were obtained from the intensity ratio between a gated decoupled spectrum and a normal decoupled spectrum. [c] See footnote *f* of Table 1. [d] Relaxation data at room temperature; sample concentration of 0.16M in 30% glycerol-^2H_2O; pH 6.4.

The ornithine side-chain shows fairly typical motional characteristics for a linear chain. The β-carbon is rather restricted in its motion, as predicted by Jones *et al.* on the basis of rotamer populations.[14] The γ- and δ-carbons show more motion, and with the δ-carbon this is on average more rapid, although not more extensive, in that a greater proportion of the motion is attributable to the rapid libration. One notable and unexpected effect of this is that the n.O.e. does not vary significantly along the chain. The ornithine side-chain appears on the above analysis to be flexible but boxed.

In contrast the phenylalanine side-chain is inflexible and boxed. The terminal ζ-carbon group has the smallest value of X in the entire molecule, presumably because the angle of the ζ-C–H bond is not affected by rotation about the β-C–γ-C bond. The T_1 differences between Phe δ-C and ε-C are probably experimentally insignificant and therefore so too are the calculated differences in librational parameters. The side-chain moves as a whole, with a rate typical for limited flexure at an α-C–β-C linkage,[5] plus some β-C–γ-C rocking.

The valine side-chain appears to be almost as motionally restricted as the ornithine side-chain at β-C. But in contrast, the leucine side-chain seems to be more flexible. It moves with about twice the angular extent and rate, consistent with the rotamer-population study.[14] This study revealed distinct preferences for single conformations of D-phenylalanine and ornithine but more extensive averaging of valine and leucine residues.

Finally, the proline ring shows motions consistent with London's detailed analysis.[15] As usual, the values of T_1 are in the order γ-C > β-C > δ-C. Our calculated variation in τ_s does, however, call into question the above authors' assumption of a single process of conformational change for the entire proline ring. It would instead seem that the Pro γ-C motion is to some extent a combination of semi-independent angular motions of β-C and δ-C.

Glutathione Dimer.—The data in Table 2 show that once again all the carbons have a fast component of motion whose semi-amplitude is *ca.* 0.5 rad. However, the motion of Cys β-C and particularly of Cys α-C is somewhat restricted, because of the S–S bridge. Also that of Gly α-C has X 0.56 which is consistent with earlier observations.[5] Evidently a side-chain partially restricts the rapid, local motions of the α-carbon of an amino-acid.

In contrast, the slow librations in glutathione dimer have a novel feature. Their maximum semi-amplitude θ is almost constant (0.96—1.07 rad) for every protonated carbon in the molecule, rather than increasing out from the molecular centre. This immediately shows that the four peptide chains extending from the Cys α-C atoms are not moving like flexible, largely unrestricted side-chains. The same conclusion is evident from the observation that one τ_R fits the entire molecule. Instead, all the slow librational motions appear to be confined within the same angular limits. One explanation of this is that the dimer molecule is cross-linked not only by the S–S bond but also by hydrogen bonds. Electrostatic interactions between the charged terminal groups may also play a limited role, although the conformation is apparently unaffected by added salt. The S–S and hydrogen bonds have a substantial but finite angular flexibility, which determines θ. Within these constraints, some atoms move more rapidly than others, particularly if they are not dynamically constrained by side-chains and associated solvent. Hence τ_s varies from 891 to 247 ps between Cys α-C and Gly α-C. Evidently the motional characteristics of a peptide molecular loop with loose links differ from those of a relatively stiff ring such as that of gramicidin-S, where no corresponding slow libration is detected.

We have studied the ^1H n.m.r. spectrum of the dimer in an attempt to identify these angular constraints more precisely. Unfortunately, anionic glutathione dimer is not readily soluble in dimethyl sulphoxide, and the solution that can be made gives the broad resonances characteristic of an aggregated product probably because of the molecular charge. This means that the standard method of identifying internal hydrogen bonds by the solvent effects on NH and CO resonances cannot be applied.

We have, however, compared the ^1H n.m.r. spectra of glutathione monomer (SH) at neutral pH in water with that of the dimer (S–S). The monomer shows no chemical shift inequivalence of the Gly α-protons, and only 0.050 p.p.m. for the Cys β-protons, whereas the dimer shows a difference of 0.054 for Gly α-H and 0.342 p.p.m. for Cys β-H. Also the coupling constants between Cys α-H and Cys β-H are 5.31 and 6.31 Hz in the monomer, but 4.41 and 9.58 Hz in the dimer. These observations are both consistent with the dimer being more conformationally restricted. For example, the approximate dihedral angles deduced from the Cys coupling constants *via* the Karplus equation, *ca.* 50 and 170°,* are consistent with the proposed cross-linked structure, but inconsistent with an open-chain, conformationally averaged molecule.

The Glu α-H–β-H coupling constants are both close to 6.2 Hz in the monomer, but 5.6 Hz in the dimer. This lower value suggests that neither β-proton is *trans* to the α-proton, which is in turn sterically consistent with the presence of some interaction between the Glu NH_3^+ and the Gly COO^- residues either as proposed above or due to steric considerations.

* 1° = (π/180) rad.

Finally, when the monomer is dissolved in H_2O and the solvent resonance is radio-frequency saturated, two amide proton resonances are observed with substantially reduced intensity due to saturation transfer by proton exchange. However, when the dimer is observed under similar conditions only the Cys-NH resonance behaves in this way. The Gly-NH resonance, which may be readily identified by its coupling patterns, is appreciably less affected, as would be expected if these protons were involved in hydrogen bonds.

Furthermore, previous studies of cyclohexapeptides[16,17] in water and dimethyl sulphoxide have shown these systems to possess a favoured conformation in which two antiparallel extended peptide segments are bridged by two transannular hydrogen bonds.

All the above observations imply that structure (A) is present.

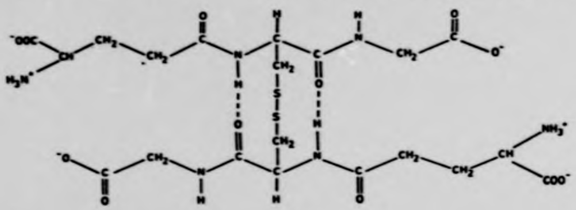

(A)

Proteins.—Earlier studies[4,5] have shown that a single-libration model can explain many observed protein T_1 values at frequencies between 14 and 68 MHz, and n.O.e values obtained at up to 45 MHz. However, two queries have since arisen. One is a suggestion by Allerhand[18] that the same results may be explained in terms of a rigid rotor with unexpectedly long α-C–H bonds. The second is that the single-libration theories predict a sharp increase in n.O.e. for resonances in small proteins at very high observation frequencies, and also for larger proteins at somewhat lower frequencies. Such measurements are now possible,[19] and we have therefore attempted them in order to test the single-libration theory more rigorously, and to compare it with the present theory.

In all these theories there is no problem in explaining how T_1 and T_2 vary with observation frequency. The crucial test lies with the values of n.O.e. Allerhand's rigid-rotor theory predicts that when the observation frequency is much greater than $\tau_R/2\pi$, the n.O.e. should be 1.15, independent of the CH bond length. Table 3 compares our experimental results for identifiable α-carbon resonance groups in various proteins with our theoretical results. It is evident that the single-libration theory predicts values of n.O.e. considerably larger than those actually observed, but also that the observed values of n.O.e. are significantly larger than those predicted for a rigid rotor. The two-libration theory gives better results than for a single-libration, because it does not artificially exclude the possibility of some internal or anisotropic rotational motions of intermediate rate, with the right correlation time to return the n.O.e. to a lower value. However, it works only by using rather large values of τ_R, from which we may conclude that in real proteins there is a still greater variety of types of slow motion than is allowed for in the present theory.

Conclusions.—The double-libration theory was devised in sufficiently general terms to be applicable to most molecules, and the above evidence shows that it withstands rigorous experimental testing better than other theories published to date. It yields sufficient detail to begin to allow some time-resolved conformation analysis of highly non-rigid molecules, although it requires further development and better experimental data before it can be used with confidence on proteins.

TABLE 3

Protein α-carbon: nT_1 and n.O.e. values, motional frequencies, and amplitudes from ^{13}C relaxation data

	Resonance frequency												Motional parameters[f]				
	[illegible] MHz				[illegible] MHz				[illegible] MHz								
	nT_1 (obs.)	nT_1 (calc.)	n.O.e. (obs.)	n.O.e. (calc.)[e]	nT_1 (obs.)	nT_1 (calc.)	n.O.e. (obs.)	n.O.e. (calc.)[e]	nT_1 (obs.)	nT_1 (calc.)	n.O.e. (obs.)	n.O.e. (calc.)[e]	[illegible]	[illegible]	[illegible]	[illegible]	[illegible]
[illegible]	[illegible]	[illegible]		[illegible]					[illegible]	[illegible]	[illegible]	[illegible]	[illegible]	[illegible]	[illegible]	[illegible]	[illegible]
[illegible]	[illegible]	[illegible]	1.3	1.4 (1.3)	72.0	72.0	1.2	1.2 (1.3)					[illegible]	[illegible]	[illegible]	[illegible]	[illegible]
[illegible]	[illegible]	[illegible]		[illegible]					[illegible]	[illegible]	[illegible]	[illegible]	[illegible]	[illegible]	[illegible]	[illegible]	[illegible]

[illegible]

We thank the S.R.C. for a research assistantship (L. Y. L.) and for use of the WH 400 spectrometer.

[1/819 Received, 21st May, 1981]

REFERENCES

[1] R. E. London and J. Avitabile, *J. Chem. Phys.*, 1976, **65**, 2443.
[2] R. E. London and J. Avitabile, *J. Am. Chem. Soc.*, 1977, **99**, 7765.
[3] R. E. London and J. Avitabile, *J. Am. Chem. Soc.*, 1978, **100**, 7159.
[4] R. J. Wittebort and A. Szabo, *J. Chem. Phys.*, 1978, **69**, 1722.
[5] O. W. Howarth, *J. Chem. Soc., Faraday Trans. 2*, 1978, 1031.
[6] O. W. Howarth, *J. Chem. Soc., Faraday Trans. 2*, 1979, 863.
[7] O. Jardetzky, A. A. Ribeiro, and R. King, *Biochem. Biophys. Res. Commun.*, 1980, **92**, 883.
[8] O. W. Howarth, *J. Chem. Soc., Faraday Trans. 2*, 1980, **76**, 1219.
[9] T. W. Rall and A. L. Lehringer, *J. Biol. Chem.*, 1952, **194**, 119.
[10] D. E. Woessner, *J. Chem. Phys.*, 1962, **36**, 1.
[11] N. W. Alcock, D. J. Benton, and P. Moore, *Trans. Faraday Soc.*, 1970, **66**, 2210.
[12] A. Allerhand and R. Komoroski, *J. Am. Chem. Soc.*, 1973, **95**, 8228.
[13] R. Komoroski, I. R. Peat, and G. C. Levy, *Biochem. Biophys. Res. Commun.*, 1975, **65**, 272.
[14] C. R. Jones, M. C. Kuo, and W. A. Gibbons, *J. Biol. Chem.*, 1979, **254**, 10307.
[15] R. E. London, *J. Am. Chem. Soc.*, 1978, **100**, 2678.
[16] K. D. Kopple, M. Ohnishi, and A. Gio, *J. Am. Chem. Soc.*, 1969, **91**, 4264.
[17] K. D. Kopple, M. Ohnishi, and A. Gio, *Biochemistry*, 1969, **8**, 4087.
[18] K. Dill and A. Allerhand, *J. Am. Chem. Soc.*, 1979, **101**, 4376.
[19] G. C. Levy, 'Topics in ^{13}C N.M.R.,' Wiley–Interscience, New York, 1976, vol. II.
[20] V. Glushko, P. J. Lawson, and F. R. N. Gurd, *J. Biol. Chem.*, 1972, **247**, 3176.
[21] R. B. Visscher and F. R. N. Gurd, *J. Biol. Chem.*, 1975, **250**, 2238.
[22] D. J. Wilbur, R. S. Norton, A. O. Clouse, R. Addleman, and A. Allerhand, *J. Am. Chem. Soc.*, 1976, **98**, 8250.

ERRATA

Page 34, Line 6	"... in the protein (*Jardetzky and Roberts, 1981*)"
Page 86, Line 15	"... the pH-dependence of the *activity of the* enzyme".
Page 88, Line 26	"... the intensities of the *ile and of the* met ..."
Page 125, Line 19	"... conformational structures. *The exchange rate is greater than* 10^3 *sec*$^{-1}$".
Page 127, Line 15	"... minimal (*Norton and Allerhand, 1977*)"
Page 153, line 3	"... are *presumed to be* non-specific ..."
Page 229	Norton, R. S. and Allerhand, A. (1977) *J. Biol. Chem.*, 252, 1795

Although in this thesis abbreviated amino acid names are given in the lower case, it is normal (in the literature) to write such names in capital letters.